POLY(N,N-DIMETHYLAMINO) ETHYL METHACRYLATE-GRAFTED SILICON:

PROTEIN RESISTANCE AND RESPONSE TO CARBON DIOXIDE

By

YIRAN REN, B.ENG.

A Thesis Submitted to the School of Graduate Studies in Partial Fulfillment of the Requirements for the Degree Master of Applied Science

McMaster University

MASTER OF APPLIED SCIENCE (2014) McMaster University
(School of Biomedical Engineering) Hamilton, ON

TITLE: Poly(N,N-dimethylamino) ethyl methacrylate-grafted silicon : protein resistance and response to carbon dioxide

AUTHOR: Yiran Ren,
B.Eng. (Nanchang University, China)

SUPERVISORS: Professor John L. Brash
Professor Shiping Zhu

NUMBER OF PAGES: xv, 101

ABSTRACT

This thesis work focused on polymer modification of silicon surface to improve its resistance to protein adsorption. Surface modification was achieved through surface-initiated atom transfer radical polymerization (SI-ATRP) grafting of poly(N,N-dimethyl amino) ethyl methacrylate (PDMAEMA). Since PDMAEMA is CO_2-responsive, CO_2 cleaning of the modified surface was also investigated.

SI-ATRP was chosen to graft PDMAEMA brushes on silicon surface for high graft densities and its good control of polymer molecular weight and polydispersity.

Surface characterization of PDMAEMA-modified silicon surfaces included hydrophilicity, layer thickness and surface chemical elemental composition.

Protein adsorption experiments were carried out to evaluate the protein resistance of the modified surfaces. Albumin adsorption from single protein solution, as well as from human plasma, decreased significantly after PDMAEMA grafting, and the adsorbed amount decreased with increasing polymer chain length. The maximum decrease in adsorption of 90% relative to the unmodified silicon, was reached at a graft layer thickness of 40 nm (measured in the dry state). Protein resistance in plasma showed PDMAEMA -modified silicon provided significant resistance to most of the tested proteins. Compared to the PEO-modified surface, the PDMAEMA surface showed much greater resistance to albumin adsorption, but, surprisingly, it adsorbed relatively large amounts of vitronectin and prothrombin. Vitronectin may have been degraded in contact with PDMAEMA-modified surface. Also, it was the only surface out of the four, which adsorbed significant amounts of prothrombin. These unexpected observations

indicate further investigation will be required to fully assess the protein-resistant properties of these PDMAEMA surfaces.

CO_2-induced protein desorption was also studied. Cleaning experiments were performed by bubbling CO_2 into vials containing the protein-adsorbed PDMAEMA-modified surface after 2 h protein solution exposure. Radiolabelling of albumin showed that the CO_2 cleaning effectiveness was related with the PDMAEMA thickness. It was found that a surface with graft thickness 20 nm (dry) responded more strongly to CO_2 than one with 15 nm thickness. Western blotting results confirmed that CO_2 contributed to protein desorption from the PDMAEMA surface.

ACKNOWLEDGEMENTS

I would like to take this opportunity to thank many people for their support and guidance throughout my project at McMaster.

First, I would like to express my sincerest appreciations to my supervisors, Dr. John L. Brash and Dr. Shiping Zhu, for letting me be a part of your research group. I feel very fortunate for this has allowed me to work with and learn from such accomplished experts in biomedical and polymer areas. Your passions and dedications to research are truly admirable, and I am indebted to you for your continuous guidance, caring, and endless patience through all these years. Thank you Dr. Brash, I'm very grateful for you've been such a supportive supervisor, giving me all the excellent guidance in research and writing. I've learned a lot from you, especially about protein works, and special thanks to your patience and carefulness in correcting my poor writing. Thank you Dr. Zhu, I truly appreciated that you've provided me with a very inspiring research atmosphere and your patience and support in giving me practical advices. I've learned many things from your polymer lectures.

Second, I would like to thank all the group members. Special thanks to Rena Cornelius, for your warm and caring attitudes, along with all your valuable suggestions on my research, I've learned numerous laboratory skills from you. To members of Dr. Brash's group, Jennifer and Kyla, thank you for your friendship and guidance, especially to Jennifer for your help and guidance in both my life and research, and also Kyla for travelling all the way back to McMaster after you had graduated to teach me how to use ellipsometry. To members of Dr. Zhu's group, Erlita, Ali, Chad, Hermes, Hongyu, Lily, Lei, Sharon, Dan, Darko, Yong, Dr. Liu, Dr. Zhang and many other visiting students and profs. I really enjoyed working with you all. I've got lots of

suggestions and shared lots of happy times, especially to Erlita and Ali, for our discussions on ATRP.

Lastly, I would like to thank my parents and friends. Mom and Dad, I can’t express my gratitude enough for your love and continuous supports. To many friends who are unmentioned but loved, thank you very much for your encouragements.

TABLE OF CONTENTS

List of Figures

List of Tables

List of Abbreviations

AFM	Atomic force microscopy
ATRP	Atom transfer radical polymerization
APOA1	Apolipoprotein-A1
BSA	Bovine serum albumin
CLRP	Controlled/living radical polymerization
CTA	Chain transfer agent
HEMA	Poly(hydroxyethyl methacrylate)
HMWK	High molecular weight kininogen
HSA	Human serum albumin
IgG	Immunogammaglobulin
LCST	Lower critical solution temperature
MEA	2-methoxyethylacrylate
MEO_2MA	2-(2-methoxyethoxy)ethyl methacrylate
MPC	2-methacryloyloxyethyl phosphorylcholine
NMP	Nitroxide mediated polymerization
NMR	Nuclear magnetic resonance
OEGMA	Oligo(ethylene glycol)ethyl ether methacrylate
PAI-1	Plasminogen activator inhibitor-1
PDEAEMA	Poly(N,N- diethylamino ethyl methacrylate)
PDMAEMA	Poly(N,N-dimethylaminoethyl methacrylate)
PEO	Polyethylene oxide
PEG	Polyethylene glycol

pI	Isoelectric point
PU	Polyurethane
PVP	Polyvinylpyrrolidone
RAFT	Reversible addition-fragmentation chain transfer
SDS	Sodium dodecyl sulfate
SDS-PAGE	Sodium dodecyl sulfate - polyacrylamide gel elecrophoresis
SFRP	Stable free radical polymerization
SI-ATRP	Surface-initiated atom transfer radical polymerization (ATRP)
SIF	Surface initiator fraction
XPS	X-ray photoelectron spectrometry

CHAPTER ONE

INTRODUCTION AND THESIS OUTLINE

1.1 Introduction and Objectives

Silicon-based materials are widely used in biomedical devices. Modification of silicon to improve biocompatibility and addition of bio-functionality to the material are often required in many applications such as biosensors, implants, etc. Preventing nonspecific protein adsorption from biofluids to the surface is a key concern for biocompatibility. Protein adsorption may cause further fouling in vitro, and cell adhesion and activation and immune reactions in vivo.

Minimal protein fouling has been associated with hydrophilic, electrically neutral, and hydrogen bond-rich surfaces. Modification with polymer coatings is a common approach to achieve these properties. Graft polymerization from the surface via SI-ATRP is a powerful method. It has the advantages of good control over polymer molecular weight and polydispersity, high tolerance for solvent and monomer, and higher grafting density compared to "grafting to" of preformed polymer chains.

PDMAEMA has been considered as a hydrophilic and biocompatible polymer. Numerous studies on PDMAEMA-based biomaterials have been reported over the past decades. A typical interest was in gene delivery. Protein resistance was also a focus. In addition to its good biocompatibility, PDMAEMA is a multi-stimuli responsive polymer: it is sensitive to both temperature and pH change. Based on its responsiveness to pH, decreasing the environmental pH

by bubbling CO_2 through the contacting fluid, thereby causing the chains to auto-repel and stretch, may have promise as a way of cleaning a protein-fouled surface. Such a process is simple of low cost and low toxicity, and does not involve salt accumulation.

With the above background in mind, the objectives of this thesis research are:

1) to provide new information on the protein resistance of PDMAEMA-modified surfaces, including the effect of PDMAEMA graft layer thickness. A more severe test of resistance to a broader range of proteins will be achieved using adsorption experiments with human plasma as opposed to the single protein solutions used in most previous research,

2) to explore the potential of removing residual protein by treatment with CO_2.

1.2 Thesis outline

This thesis has five chapters. Chapter one provides an introduction and an objective statement. Chapter two gives research background on protein adsorption mechanisms, surface modification methods and stimuli-responsive polymers. Chapter three summarizes the materials and experimental procedures used in this research. Chapter four presents the results and discussion related to the protein resistance of PDMAEMA-grafted surfaces, as well as the surface "cleaning" effect triggered by CO_2 bubbling. Chapter five presents conclusions and recommends future work.

CHAPTER TWO

LITERATURE REVIEW

Biomaterials, loosely defined as any material that interacts with a biological environment, are widely used in tissue engineering, gene therapy, drug delivery, biosensors and biomedical implants. In all applications, biocompatibility, which requires minimizing unwanted interactions between material and environment, is a central concern. The definition of biocompatibility may differ depending on the application. However, the inevitability of protein adsorption from biological fluid to solid is a major concern in all applications of biomaterials [1][2]. It is the initial event in contact of the biomaterial with the bio-environment, and determines subsequent events including cell adhesion, thrombus formation, foreign body reaction and other unwanted responses [3]–[6]. Therefore, preventing protein adsorption on biomaterial surfaces is of great importance. The problem has been studied for many years, but no solution has been found thus far, although progress has been made.

The following sections provide background pertaining to protein-surface interactions and protein-resistant surfaces, as well as preparation methods for such surfaces.

2.1 Protein Adsorption

Proteins are polypeptides formed by the linking of various amino acids. The chains are folded in specific patterns, driven by non-covalent interactions such as hydrogen bonding,

hydrophobic packing, ionic interactions, and Van der Waals forces. Among these driving forces, hydrophobic interactions are the major contributor.

In the presence of an interface, proteins have a tendency to adsorb due to their amphiphilic nature (presence of distinct polar and non-polar regions) and generally high molecular weight. Protein adsorption at the solid-liquid interface is a complex process, and depends on both the protein and the surface. Diversity in the structure and molecular mass of proteins results in different adsorption behavior; differences in size and shape add more complexity. In addition results from different laboratories can be contradictory due to different surface preparation or experimental conditions [7].

The surface properties of biomaterials, both physical and chemical, also affect protein adsorption. These properties include surface chemical composition, surface morphology and topography, hydrophilicity/hydrophobicity, and surface energy [8].

2.1.1 Protein properties that influence adsorption

As mentioned above, protein properties are thought be responsible for their tendency to reside at interfaces. Possible influencing properties are summarized in Table 2.1

Size is an important determinant of adsorption. Clearly the larger the protein molecule is, the greater the number of potential binding sites. Therefore bigger proteins can bind with higher "valency".

Protein structure is the key determinant of adsorption behavior. All proteins have three levels of structure: primary, secondary and tertiary. Some proteins have a quaternary structure.

The primary structure of a protein refers to the linear sequence of amino acids which is held together by peptide bonds to form polypeptide chains. Differences in surface activity among proteins arise from variations in their primary structure. Secondary structure refers to local stereochemical sequences which determine the shape of the sequences. Alpha helix and beta sheet are the two main types of secondary structure first suggested by Pauling and coworkers in 1951 [9]. Secondary structures are defined by patterns of hydrogen bonds between peptide residues. Tertiary structure refers to the overall geometric shape of a protein molecule into a compact globular structure determined by chain folding. Quaternary structure is present in proteins which contain more than one polypeptide or subunit. It refers to the spatial arrangement of the subunits [10].

Protein properties related to structure that influence protein adsorption include stability, unfolding rate, cross-linking and complexity in the subunits. Proteins which unfold faster or which have lower stability in contact with the surface are considered to be more easily adsorbed, because configurational entropy gain favors the adsorption process. Proteins with large numbers of disulfide bonds are less likely to unfold because of the strong covalent bonds which cross-link the subunits and therefore are less likely to adsorb. For proteins with large numbers of non-covalently bonded subunits, adsorption may be favored due to rearrangement of inter-subunit contacts leading to more contact of each subunit with the surface [11].

Charge and charge distribution of proteins also impact the adsorption process. Proteins at their isoelectric point are electrically neutral. Thus electrostatic interactions are disfavoured, and hydrophobic interactions are favoured.

Table 2. 1. Protein properties that influence adsorption. (Adapted from [11])

Size :	Larger molecules have more contact points
Charge:	Molecules nearer their isoelectric point may adsorb more easily
Structure:	
a. Stability:	Less stable proteins may adsorption more easily
b. Unfolding rates:	More rapid unfolding may favour adsorption
c. Cross-linking:	Disulfide bonds may reduce adsorption
d. Subunits:	Proteins with multiple subunits may adsorb more easily
Other properties:	
a. Amphipathicity:	Adsorption depends on amino acid composition
b. Hydrophobicity:	More hydrophobic proteins tend to adsorb more easily
c. Solubility:	Less soluble proteins tend to adsorb more easily

Chemical differences in amino acid residues among proteins are also important for adsorption. The amphipathic nature of proteins (with hydrophobic, hydrophilic, negatively charged and positively charged amino acid side chains) along with the folding patterns of the peptide chains, determine the hydrophobicity and charge at the periphery of the protein, which in turn influences adsorption behaviour. Lastly, the solubility of a protein is essentially determined by its chemical composition. Protein adsorption to an interface can be thought of as insolubilization or phase separation. Therefore, less soluble proteins may adsorb more readily.

2.1.2 Driving forces for protein adsorption

Interactions between proteins and solid surfaces are mostly non-covalent. These include hydration, hydrophobic interactions, Coulomb and Van der Waals interactions. The major interactions involved in protein adsorption at the solid solution interface are summarized in Table 2.2.

Hydration Effect

Hydrogen bonds occur frequently between amide and carbonyl groups of the polypeptide backbone in proteins and contribute to the stability of the protein structures. Formation of hydrogen bonds appears not to be the main driving force for protein adsorption. It is a strong force only at short-range (1 – 2 nm) and with an exponential decay length of 0.1 – 0.3 nm [12].

Hydrophobic Interaction

Hydrophobic interaction is a strong attraction between nonpolar molecules and surfaces in water. In a protein adsorption process, dehydration of nonpolar parts of the protein surface in water is favourable because it increases the entropy and decreases the Gibbs energy of the system, causing protein aggregation and internalization of hydrophobic residues. Hydrophobic interactions are long-range (< 50 nm) attractive interactions, decaying exponentially with a decay length of 1 - 2 nm within the range of 0 - 10 nm, and then more moderately at longer distance [12]. Therefore, hydrophobic interactions are very strong at a short separation distance.

Coulomb Interaction

Coulomb interaction refers to the electrostatic force between charges, which is a very important driving force for protein adsorption, as shown in many investigations [13][14]. Since

most charged amino acid residues in a protein molecule are located at the aqueous periphery, this leads to a strong electrostatic interaction with charged surfaces. By varying the pH of the environment, the charges of surface and protein can be changed. Generally speaking, close to the isoelectric point (pI), the net charge will be approximately zero, and electrostatic interactions less important. Interactions may then be attractive. Remote from the pI, the interaction will be repulsive due to electrostatic interactions.

Van der Waals Forces

Van der Waals interactions refer to interactions between induced dipoles. They are long range interactions (> 10 nm). In an aqueous system, the interaction energy is usually negative, that is, the interaction is attractive [12]. Experimentally, Van der Waals interactions can be calculated from contact angle measurements on a flat surface [7].

Table 2. 2. Attractive and repulsive interactions involved in protein adsorption at the solid-solution interface.

Attractive Interactions	**Repulsive Interactions**
Electrostatic Interactions	Electrostatic Interactions
Hydrophobic Interactions	Hydration Effect
Van der Waals Forces	Steric Repulsion
Specific Interactions (i.e., covalent bonds)	

2.1.3 Thermodynamics of protein adsorption

Protein adsorption occurs spontaneously only when the change in Gibbs energy of the system, ΔG, is negative:

$$\Delta G = \Delta H - T\Delta S < 0 \qquad (1.1)$$

where H , T and S are the enthalpy, absolute temperature and entropy, respectively. Therefore, the adsorption process must have a sufficient gain of entropy be sufficiently exothermic. Previous research has shown that protein adsorption can be either enthalpically driven or entropically driven [13][14].

Enthalpic Contributions

Enthalpic contributions could come from Van der Waals forces and hydration forces as discussed in Section 2.1.2 , such as proton transfer, transfer of ions other than protons, overlap of electric fields, changes in hydration state of surface, and structural rearrangement of protein. On the other hand, hydrophobic interaction is mainly an entropic phenomenon.

Entropic Contributions

In protein adsorption from solution to solid, entropy increases when protein approaches surface as a result of the reduction of ordered structures in water molecules in the vicinity of the protein and the surface [15]. Although the entropy of the protein may decrease because it tends to be configurationally more ordered, the gain in entropy by release of ordered water molecules from the protein is greater. Hydrophobic interactions more generally and protein denaturation also contribute to the entropy increase. Hydrophobic interactions results in dehydration of the adsorbing surface as well as the protein surface; the system entropy increases due to disruption

of the ordered water layers [16]. Protein denaturation refers to unfolding of its structure and loss of quaternary, tertiary and secondary structures, leading to loss of function. Denaturation can be induced by heat, by chemical denaturants or by contact with a surface. The 3D structure of a protein can be easily perturbed in the presence of a solid-fluid interface, resulting in decreased ordering (loss of secondary structure), and increased configurational entropy [17] .

2.1.4 Kinetics of protein adsorption

Several models have been used to describe the kinetics of protein adsorption (Fig. 2.1). The equilibrium between protein adsorption and desorption can be written as:

$$P + S \underset{k_d}{\overset{k_a}{\rightleftharpoons}} PS \qquad (1.2)$$

Where P indicates protein, S indicates surface, k_a is the adsorption rate constant, k_d is the desorption rate constant.

The Langmuir model has been widely used. This model considers only reversible adsorption as shown on the left portion of Fig 2.1. However it is known that proteins can undergo configurational rearrangement upon adsorption as depicted schematically on the right, and that adsorption is effectively irreversible in a practical sense. However although it has limitations from a fundamental point of view, the Langmuir model has been found to fit well for many systems. It is usually used to describe single component adsorption and is based on the following assumptions: 1) protein adsorption is reversible; 2) the surface is energetically uniform

and the heat of adsorption ΔHa is independent of coverage; 3) adsorption is restricted to a monolayer; 4) adsorption sites are independent of each other [18].

The rate of adsorption $d\theta/dt$ in a Langmuir model is calculated as:

$$\frac{d\theta}{dt} = k_a C_0 (1-\theta) - k_d \theta \tag{1.3}$$

where θ is the fractional surface coverage, t is the adsorption time, C_0 is the bulk protein concentration.

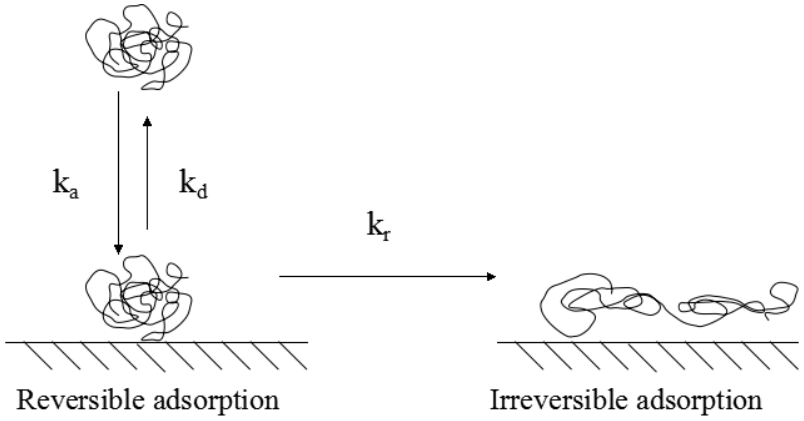

Figure 2. 1. Kinetic models of reversible and irreversible adsorptions. ka is the rate constant of adsorption, kd is the rate constant of desorption, kr is the rate constant of rearrangement.

The Langmuir model can be written as:

$$\theta = \frac{K C_p}{1+K C_P} = \frac{\Gamma}{\Gamma_{max}} \tag{1.4}$$

where $K=k_a/k_d$ is the equilibrium constant of adsorption, C_p is the protein solution concentration at equilibrium. As a function of solution concentration, the adsorption increases

linearly at low concentrations (KC_p<<1; θ~KC_p) and reaches a plateau at higher concentrations (KC_p>>1; θ~1). The plateau is interpreted as monolayer coverage Γ_{max}.

For a heterogeneous surface with sites of different energy, the Freundlich isotherm may be seen as more applicable to protein adsorption [18][19]. This model may be written as:

$$\theta = kC_p^{\frac{1}{n}} \tag{1.5}$$

where k and n are empirical constants: k is related to adsorption capacity and $1/n$ to adsorption energy. This model assumes that ΔHa decreases exponentially with surface coverage and predicts that adsorption increases indefinitely with increasing solution concentration.

Multiple states of adsorbed protein

Protein adsorbed on surfaces will exhibit multiple-state adsorptions, impacting the final surface coverage and the kinetics of adsorption and desorption. All of the protein properties discussed in Section 2.1.1 can contribute to more than one state of an adsorbed protein. Possible mechanisms of forming multiple states are depicted in Fig 2.2.

Site occupancy (coverage) can vary depending on the surface properties, protein size and concentration, and it is strongly influenced by repulsive interactions between protein molecules. Fig. 2.2 (a) depicts different occupancies.

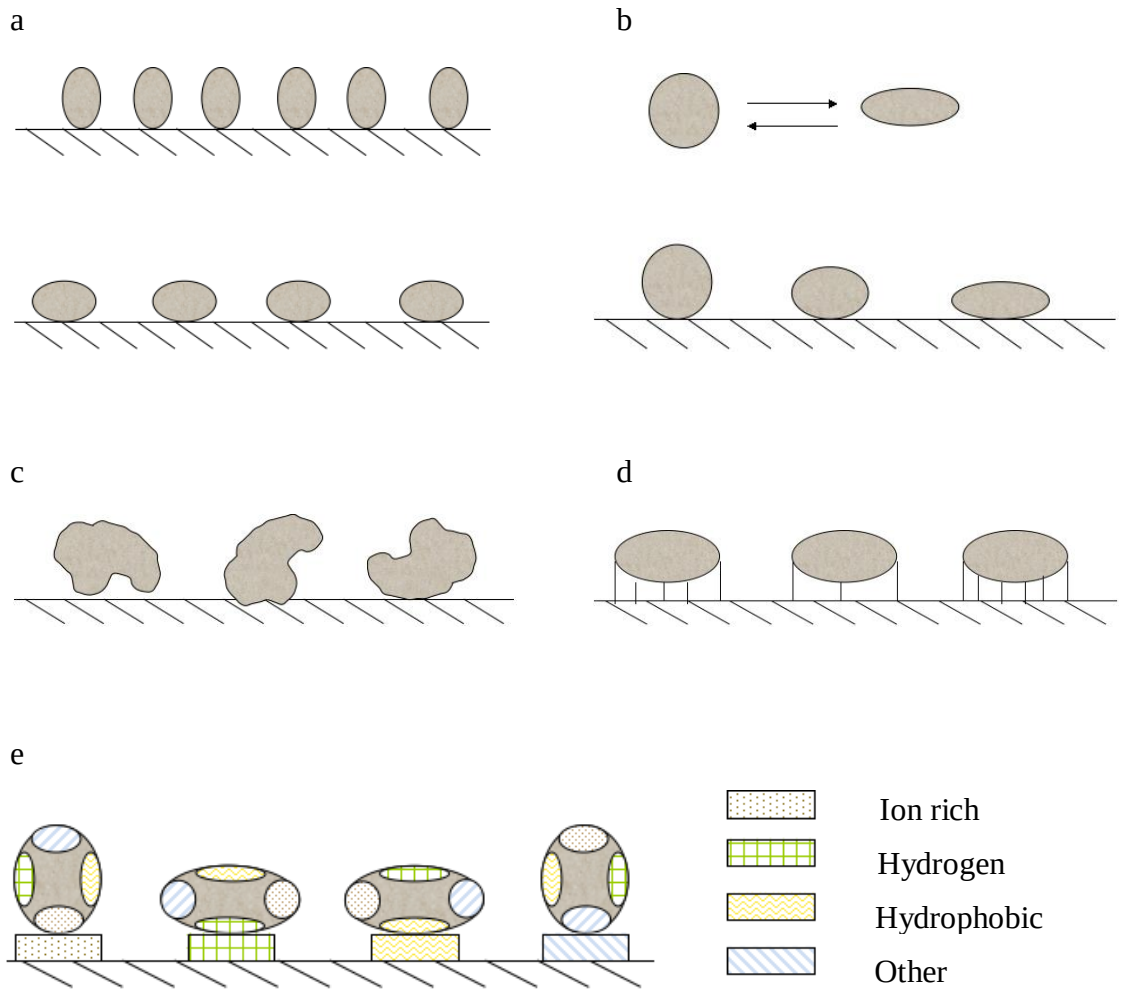

Figure 2. 2. Multiple states of adsorbed proteins: a) occupancy effects: 1) site size less than molecular size; 2) site size greater than molecular size, b) structural alternation, c) orientational effect, d) statistical distribution of bonds per molecule, e) multiple binding modes. (adapted from [11])

Protein molecules may assume different conformations. Conformational transitions may occur before adsorption, or rapidly immediately upon adsorption or slowly after adsorption. Fig 2.2 (b), upper panel, illustrates conformational change. In the lower panel, the three differently conformed adsorbed protein molecules represent adsorption without transition, adsorption with

slow transition and adsorption with rapid transition (or pre-transition before adsorption) respectively from left to right.

Certain orientations of the molecule approaching the surface might be favoured due to the higher binding affinity of certain amino acids in "patches" at the surface of the protein. Fig 2.2 (c) illustrates orientational effects. Fig 2.2 (d) illustrates the possibility of multiple adsorption states due to different numbers of protein-surface "bonds" per molecule. Lastly, Fig 2.2 (e) demonstrates multiple adsorption states caused by the mixed site nature of a real interface. A perfectly homogeneous surface is difficult, if not impossible, to produce. The attractive interactions between protein and surface could possibly be electrostatic, hydrophobic, hydrogen bonding, and others.

Vroman effect (Competitive adsorption behavior of proteins)

The adsorption of proteins from systems of many components such as blood plasma is a competitive process. In the initial phase it is strongly affected by protein transport. Proteins of higher concentration and higher mobility (diffusivity) dominate the interface in the early stages. But protein affinity for the surface soon becomes critical and initially adsorbed proteins can be replaced by lower concentration, higher affinity proteins in a dynamic process. This phenomenon is known as the "Vroman effect" [20][21], in recognition of the pioneering work of Leo Vroman [22][23]. It has been shown that the process depends strongly on material surface properties, with hydrophilic surfaces being generally more "dynamic" than hydrophobic ones.

2.1.5 Four human plasma proteins involved in this research

In this work, albumin was chosen as a model protein for radiolabelling experiments, and the adsorbed amount of albumin was used as an indicator of the protein resistance of the modified surfaces. Vitronectin, complement C3 and prothrombin were found to be prominent in the interactions of the PDMAEMA-modified surfaces with plasma as shown by immunoblotting data. Some background information on these four proteins is given below.

Albumin

Albumin is the most abundant protein in human plasma and serum. The normal concentration of HSA in serum is in the range of 35~50 mg/mL [24], i.e about 50% of the total. Albumin is unique among the plasma proteins in that it is not glycosylated. It functions mainly as a carrier to transport molecules of low water solubility in the circulation such as hormones, fatty acids, and other compounds [25]. Another important function of serum albumin is to maintain the colloid osmotic pressure of blood [26]. As a negative acute-phase protein, it is down-regulated in inflammatory conditions. The shape of albumin has long been presented as a prolate ellipsoid protein with a dimension of 140 Å × 40 Å and axial ratio of ~ 3.5 [27]. More recently, in 1999, Sugio presented a new X-ray based structure of albumin as a heart shape of 80 Å × 80 Å × 30 Å [28]. Human albumin contains about 600 amino acid residues and has a molecular weight of around 67 kDa [25][27]. It has only one peptide chain, and hence does not break down when treated with detergents or reducing agents. Its isoelectric point (pI) is around pH 4.7 [29]. When the pH varies over the range from 7 to 5, the α-helix content increases, and the net charge

changes from negative to neutral. Further decrease in pH past the pI leads to decreasing α-helix content and a net positive charge [30][7].

Plasma albumin is easy to prepare in highly purified form with retention of the native state; thus it has been used extensively as a model protein in a wide variety of research including adsorption.

Complement C3

The complement system is responsible for non-specific immune responses of the body, helping antibodies and phagocytic cells in defending against invasion by pathogenic organisms. There are two main complement activation pathways (classical and alternative) and three mechanisms to kill pathogens via the complement system (membrane attack, inflammation and opsonization). The system contains over 30 proteins; the major ones are designated C1, C4, C2, C3, C5, C6, C7, C8, C9, in order of their sequential reactions during activation [31]. The activation pathways are shown in Fig 2.3.

The classical pathway is initiated via C1 activation by antibodies. In the alternative pathway, activation bypasses C1, C4 and C2, and starts with the attachment of the C3 fragment C3b to a cell surface. C3b is formed by spontaneous cleavage of C3. It is clear that C3 activation plays an essential role in activation. It is the most abundant (1.2 mg / mL in plasma) component of the complement system and its structural features allow it to interact specifically with many different proteins [32]. C3 consists of two subunits: an α-chain with a molecular weight of 110 kDa and a 70 kDa β-chain. The two chains are connected covalently by a single disulfide bond. C3 can attach covalently to acceptor molecules on cell surfaces by ester or amide

linkages [33]. C3b is considered to have a strong preference for hydroxylated targets because the majority of C3b is linked via ester bonds.

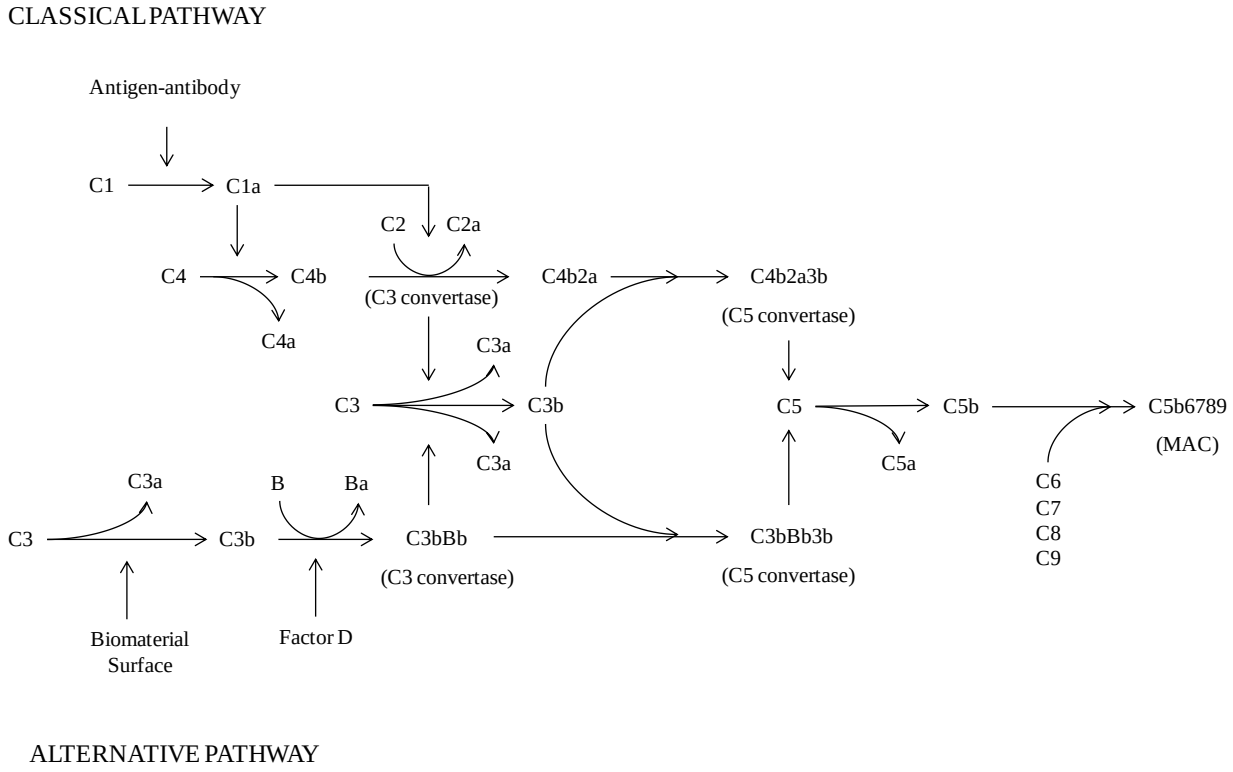

Figure 2. 3. Complement activation pathways (Adapted from [34]).

Vitronectin

Vitronectin is a liver-secreted glycoprotein, existing abundantly(0.2 - 0.4 mg/mL) in serum and in the extracellular matrix [35]. It is a multifunctional adhesive protein which promotes cell adhesion and spreading [35][36]. Two forms of vitronectin have been found, a single chain (75 kDa) form or a clipped, two chain (65 kDa, 10 kDa) form held together by a disulfide bond [37][38]

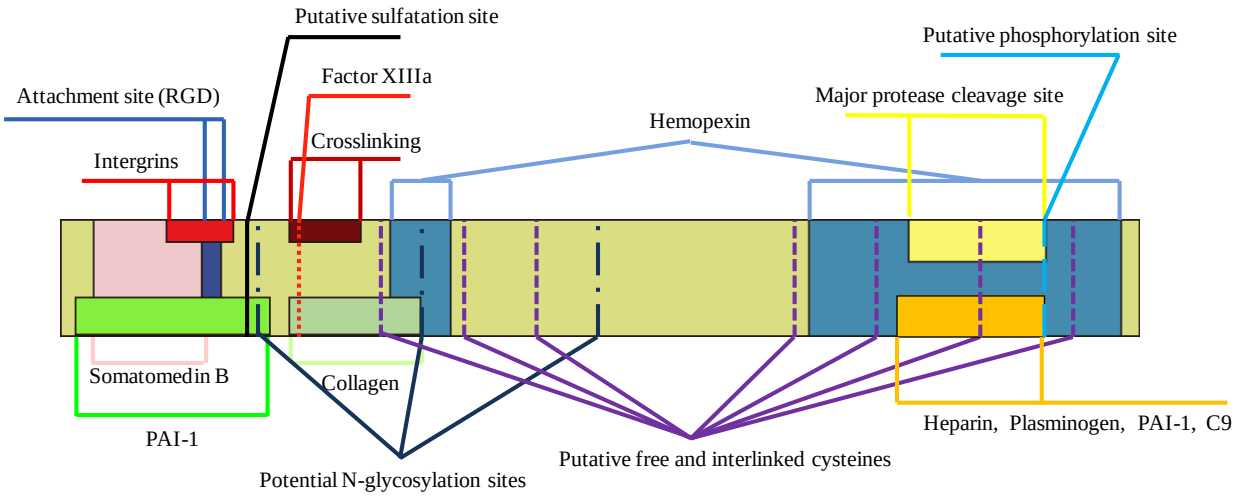

Figure 2. 4. Schematic of vitronectin structure showing binding sites (Adapted from [37])

Vitronectin has a positively charged C-terminal and a negatively charged N-terminal, and is stabilized by an ionic interaction between its polyanionic and polycationic segments. A schematic structure of vitronectin including its numerous binding domains is shown in Fig 2.4. The somatomedin B domain binds to plasminogen activator inhibitor-1 (PAI-1), thus regulating proteolysis initiated by plasminogen [38][39]. The heparin binding domain is located near the C-terminal, and cell attachment sites near the somatomedin B domain [38]. It has 3 potential N-glycosylation sites, one putative phosphorylation site, two putative sulfatation sites, one factor XIIIa/transglutaminase crosslinking site, and domains containing integrin and collagen binding sites [37].

Proteolytic cleavage and phosphorylation sites are depicted in Fig 2.5. Research on the protease degradation of vitronectin shows that it has sites for cleavage by thrombin, elastase and plasmin [40]. Vitronectin also contains sequences for phosphorylation by various protein kinases. Phosphorylation by cAMP-dependent protein kinase at Ser 378 could modulate the conformation

and function of vitronectin, reducing its ability to bind PAI-1. Phosphorylation by protein kinase C at Ser 362 attenuates the cleavage of vitronectin by plasmin. Phosphorylation by casein kinase II occurs at a cell attachment domain and thus promotes cell adhesion and spreading [41].

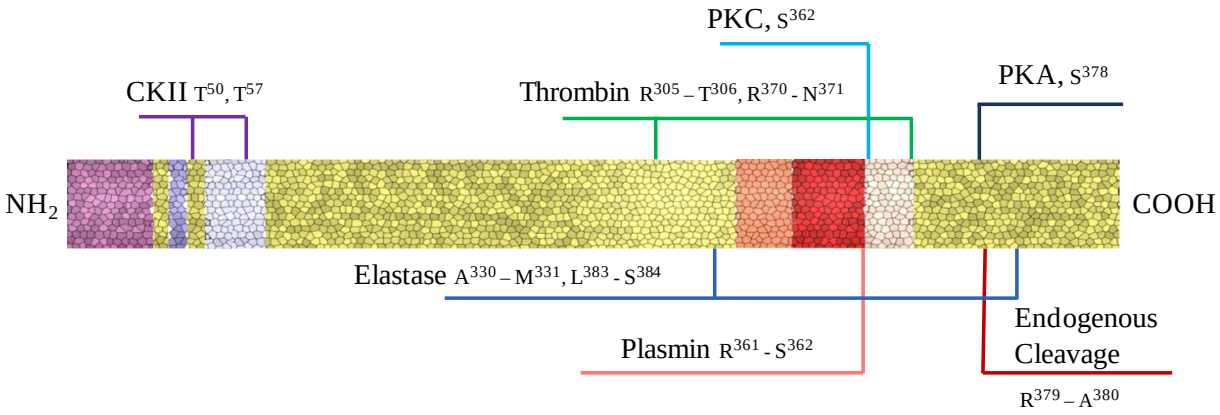

Figure 2. 5. Phosphorylation and proteolytic cleavage sites on vitronectin. Phosphorylation by casein kinase II (CKII) (threonine50, threonine57), by protein kinase C (PKC) (serine362), and by cAMP-dependent protein kinase (PKA) (serine378). At least in vitro, vitronectin is susceptible to proteolysis by thrombin (arginine 305-threonine 306, arginine 370-asparagine 371), elastase (alanine 330-methionine 331, leucine 383-serine 384) and plasmin (asparagine 361-serine 362). (Adapted from [42])

Prothrombin

Plasma prothrombin plays an essential role in blood clotting. It is the precursor of thrombin, a key proteolytic enzyme in the blood coagulation pathways which converts fibrinogen to fibrin, the material of the clot. The isoelectric point of prothrombin is around pH 4.2 [43] . The molecular weight of prothrombin is 68 kDa. Lamy and Waugh described it as an ellipsoid of 119 Å length and 34 Å diameter [44]. The plasma concentration of prothrombin is relatively low at ~0.12 mg/mL. It is inherently unstable, and is vulnerable to heat, acid and alkali environments.

Inactivation occurs at pH ≥ 10 and ≤ pH 4.2. Aggregation occurs on heating at T ≥ 80 °C. It is highly soluble in water at high pH but is easily precipitated at pH 4.2 - 4.5 [44].

2.2 Protein-Resistant Surfaces

Proteins are in general highly surface active. Thus the realization of a surface that does not adsorb proteins is a difficult goal that has so far not been achieved. In general to prevent or minimize nonspecific protein adsorption the surface should be hydrated and/or should be grafted with suitable polymer chains of high flexibility [45][46]. More specifically, all surface properties including hydrophilicity/hydrophobicity, surface charge, topography and chemical composition, as summarized in Table 2.3, play principal roles.

Table 2. 3. Surface properties that affect protein adsorption. (Adapted from [47])

Surface Property	**Description**
Hydrophilicity/Hydrophobility	Hydrophobic surfaces favours protein adsorption
Charge	Electrostatic repulsion decreases protein adsorption
Topography	Rough surfaces favour protein adsorption
Chemistry	Chemical composition of the surface determines the types of bonds between adsorbed proteins and the surface.

Hydration is considered to be favorable for protein resistance since a hydration layer that is relatively tightly bound can be viewed as a barrier to the approach of the protein. This idea is supported by a considerable body of work showing that the attachment of hydrophilic polymers such as polyethylene oxide (PEO), polyvinylpyrrolidone (PVP), poly(hydroxyethyl methacrylate)

(PHEMA), and polysaccharides such as dextran gives surfaces that are protein resistant in some degree. These materials are discussed in more detail below.

The presence of polymer chains of high flexibility relates to the idea of steric repulsion or steric exclusion whereby access of the protein to the surface is inhibited by the loss of entropy when the chains are compressed as the protein approaches. At the present time it appears that the hydration barrier idea is the more plausible of the two.

Surface charge is also very important for protein adsorption [48]. As commonly known, opposite charges attract each other. A surface with charge the same as the protein would be more protein resistant. In reality the situation is more complicated because of the complexity of protein structures. Even if the net charge of a protein molecule is negative, it contains positively charged domains. Tran and co-workers measured lysozyme and fibrinogen adsorption to anionic poly(styrene sulfonic acid) brushes [49]. These brushes adsorbed both negatively charged lysozyme and positively charged fibrinogen. Similarly, Wittemann and co-workers observed anionic poly(acrylic acid) adsorbed net negatively charged bovine serum albumin (BSA) [50].

Increased surface roughness leads to increased protein adsorption. Uniformity in topography decreases the area for protein adsorption [51].

The chemical composition of the surface can strongly impact protein adsorption. For example, it has been shown that methyl, nonpolar and hydrophobic groups bind fibrinogen and IgG, while hydroxyl groups reduce protein adsorption enhancing surface hydrophilicity [52].

2.2.1 Surface modification strategies for preventing nonspecific protein adsorption.

Biomaterials can be either natural or synthetic. Natural biomaterials are usually based on proteins and polysaccharides. Synthetic biomaterials include polymers, ceramics and metals. Currently available biomaterials generally have good bulk properties but poor biocompatibility. To improve biocompatibility, or more specifically related to this project, to improve protein resistance, surface modification of biomaterials becomes essential.

Table 2. 4. Examples of surface modification strategies.

Physicochemical Modification	chemical: oxidation, reduction, silanization, acetylation.
	physical: etching, mechanical roughening/polishing/ patterning.
Surface Coating	grafting, non-covalent/covalent coating, thin film deposition.

Surface modification methods can be classified into two broad categories: 1) physicochemical modification including alteration to surface chemical composition or reforming of physical shape; 2) surface coating involving adding a layer of a different material but without changing the nature of the supporting substrate. Examples of these strategies are listed in Table 2.4.

For the purpose of preparing protein-resistant biomaterials, surface coating is widely used [53][54] and has advantages over physicochemical modification, the main one being that it does

not affect the bulk properties of the supporting substrate and the surface can be made multi-functional by using multi-layer coatings [46][55].

Polymers are used extensively in surface coating for a variety of applications including adhesion promotion, lubrication, nonfouling surfaces, environmentally responsive materials and others [56]–[59]. They have several advantages as coatings including 1) tailorable mechanical properties, 2) ability to form thick films which can provide numerous functional groups; 3) they can be used as combinations of two or more polymers, thus providing a variety of functionalities.

Polymers used for protein resistant coatings are generally hydrophilic and include poly(ethylene glycol) [PEG] and its derivatives [60]–[64], poly(2-hydroxyethyl methacrylate) [poly(HEMA)] [65], (poly(2-methoxyethylacrylate) [poly(MEA)] [66]–[68], poly(vinyl pyrrolidone) [PVP] [69][70], poly(2-methacryloyloxyethyl phosphorylcholine) [poly(MPC)] and its copolymers [71][72], poly(sulfobetaine methacrylate) (poly SBMA) and poly(carboxybetaine methacrylate) [poly(CBMA)] [73]. The most widely used polymer is PEG, which is water-soluble and strongly hydrophilic. In addition, PEG chains are highly flexible and thus may repel proteins by steric repulsion/exclusion as well as by "erecting" a water barrier.

Spin coating and Langmuir-Blodgett deposition are popular polymer coating techniques. However, although they are simple to implement, these methods have the inherent weakness that the coating is easily detached. To obtain coatings with greater stability, grafting methods involving covalent attachment of the polymer chains to the substrates, are preferable.

2.2.1.1 Surface grafting methods

Surface grafting methods fall into two general categories: i.e. “grafting from” and “grafting to” [46][74][75]. “Grafting to” refers to tethering pre-synthesized polymer chains, which contain reactive moieties on the chain ends or side chains, to surface sites by chemical reaction. In the “grafting from” method polymer chains are grown from surface-immobilized initiators.

Compared to “grafting to”, the “grafting from” technique has the following advantages [76]: 1) higher graft density can be achieved since small monomer molecules can access surface sites more easily than large polymer chains; 2) a wider range of monomers can be used with different polymerization methods. However, the technique is more complicated and characterization of the grafted layers is more difficult for the “grafting from” method.

The configuration and conformation of the grafted chains is important and is determined largely by the graft density. Three conformations are depicted in Fig. 2.6, adapted from [77]. When the graft density is low, the polymer chains can retain the random coil conformation, resulting in the so-called mushroom layer configuration. As the density increases, the grafted chains begin to interact with each other, inducing a change of conformation from coil to fully stretched. At intermediate density (transition stage) the chains are compact and somewhat constricted and the layer coverage is high. Storm et.al have suggested that the transition stage is the best for protein resistance, since both “mushroom” and “brush” form have disadvantages in reducing protein adsorption. Surface with a “mushroom” arrangement of coated polymers is more vulnerable to smaller macromolecules, while in a “brush” form, high lateral pressure between polymer chains allows exposure of hydrophobic sites [78].

In this research, the "grafting from" method was chosen since it can potentially generate surfaces with high graft density and high coverage for protein resistance. Controlled/living polymerization, with the potential to optimize homogeneity of the grafted polymer layer, was used.

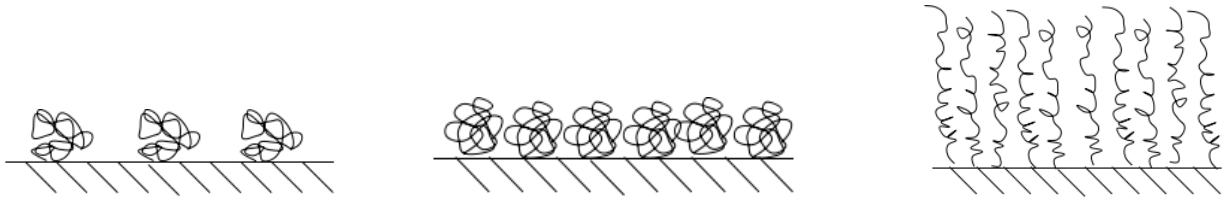

Figure 2. 6. Conformation of polymer chains at different graft densities.

2.2.1.2 Controlled/living radical polymerization

Controlled/living radical polymerization (CLRP) eliminates chain termination and chain transfer reactions [79]. It overcomes the rapidity of free radical polymerization, producing polymers with well-defined molecular weight, polydispersity, functionality, chain conformation and composition [80]. The controlled/living feature of CLRP is achieved by a reversible activation/deactivation cycle of a propagating radical, $Pn^{\bullet}$, with a capping agent X, as shown in Fig.2.7. k_{act} is the rate constant of activation and k_{deact} is the rate constant of deactivation. k_{deact} is usually six orders of magnitude higher than k_{act}. Therefore, the equilibrium between propagating radicals and dormant species Pn-X, which are unable to terminate or propagate, greatly favours deactivation, and prolongs the lifetime of the propagating chain from seconds to hours. Thus, for each activation/deactivation cycle, only a few monomers can be added to the growing chain, and

all chains in the system have the same possibility of propagating during the entire reaction, resulting in a low polydispersity (narrow molecular weight distribution) of the final product.

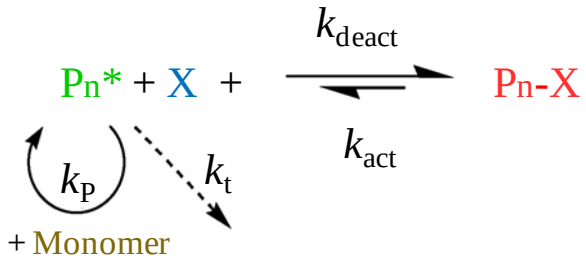

Figure 2. 7. Mechanism of controlled/living radical polymerization.

Many CLRP approaches with different capping techniques have been developed. The three most promising ones are: 1) stable free radical polymerization (SFRP); 2) transition metal-catalyzed atom transfer radical polymerization (ATRP); 3) reversible addition-fragmentation chain transfer (RAFT) radical polymerization.

Nitroxide mediated polymerization (NMP) is the most common example of the SFRP method. The propagating radicals are reversibly capped by 2, 2, 6, 6-tetramethyl-l-piperidinoxyl. However, this method is limited in the monomer type that can be used.

Chain growth in RAFT polymerization is controlled by addition of chain transfer agent (CTA). The CTA forms an intermediate radical by reaction with a propagating radical, which is fragmented into a new radical and a polymeric-CTA compound. The reversible addition and fragmentation ensures livingness of the polymerization. Compared to NMP and ATRP, RAFT can be used with a wider range of monomers to produce high molecular weight, but still narrowly distributed polymers [81]. However, the synthesis of an effective RAFT agent is very

challenging, and the final product usually has undesirable odors and colors because of the presence of a large amount of dithioester groups introduced by CTA as discussed in many reviews [79][82].

In an ATRP system, the activation/deactivation cycles are modulated by a transition metal salt, *Mt*, in complex with a ligand *L*. The mechanism is shown in Fig. 2.8. The propagating radicals are reversibly capped by the transition metal salt through a redox reaction. Compared to other CLRP methods, ATRP has many advantages: a greater range of monomer type can be polymerized, it can be carried out in either organic or aqueous media, it can employ a large range of temperature, and its initiators are usually commercially available. The limitation of ATRP is mainly related to the requirement of the removal of the transistion metal complex [79].

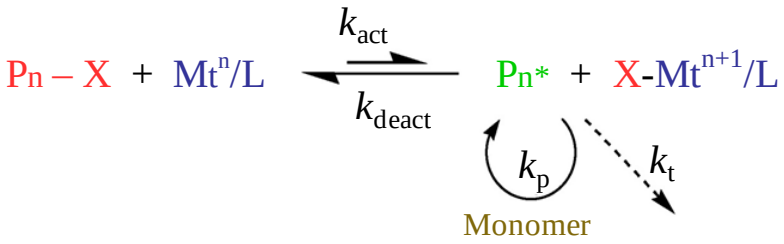

Figure 2. 8. Mechanism of atom transfer radical polymerization

Surface-initiated atom transfer radical polymerization (SI-ATRP)

Although NMP and RAFT have been used to graft polymers on a number of surfaces, most CLRP grafting work is based on ATRP. The major advantage of using ATRP as a surface grafting method is the relative ease of synthesis of SI-ATRP initiators compared to NMP or RAFT.

Ejaz et al. first reported the use of ATRP to graft dense polymer brushes from silicon surface in 1998 [83]. Since then, ATRP has been used in numerous studies on surface modification with a variety of polymers of well-defined architecture and functionality from a number of materials [84]–[90]. The use of SI-ATRP to prepare surfaces that are resistant to nonspecific protein adsorption has been reported by a number of labs [71], [91]–[94].

Three major factors of grafted polymers which affect surface properties are monomer properties, graft density (chains per unit area) and graft layer thickness. The graft density of polymer chains is dependent on the density of initiator sites on the substrate [95]. Surface-immobilized ATRP initiators are usually bromo-esters, thiols and silanes. One end of the initiator is covalently bonded to the substrate, and the other end, containing the bromine atom initiates chain growth. The thickness of the grafted polymer layer is influenced both by polymerization time and initiator density. Ma et al. found that the thickness of grafted poly(OEGMA) layers increased rapidly as the surface initiator fraction (SIF, initiator coverage on the surface, varied by mixing with an analogue molecule that does not have a bromine moiety) increased from 0 to 25%. For SIF > 25%, the thickness increased more slowly [91].

It has been shown by several groups that a surface initiated polymerization is similar to the same polymerization in solution [96][97][98]. Although the initiator density (coverage) on the surface is generally high, the total amount is extremely low; thus, it does not affect reactions in solution. In the presence of free initiator in solution, chains grow simultaneously both from the surface and in solution. Therefore, it is generally assumed that the polymer properties (e.g. chain length) on the surface are the same as in the solution. However, it has been pointed out that chain termination could occur on surface. The chain lengths could then be different because termination reactions could occur between radicals on the surface (surface/surface) radicals in

solution and on the surface (surface/solution), and radicals in solution (solution/solution). Surface/surface termination will play an important role in determining the grafted chain length, and could be caused by "rolling migration" of surface radicals in RAFT polymerization as proposed by Fukuda [99] or by "hopping migration" in ATRP and RAFT as suggested by Zhu [100]. Depending on the relative importance of surface/surface, surface/solution, and solution/solution termination, the chain length of grafted polymers could be lower or higher than in solution.

2.3 Stimuli-responsive Polymers

Stimuli-responsive polymers, also known as "smart" polymers, have attracted great interest for various applications in the past few decades. "Smart" implies that the polymer can undergo a rapid, reversible transition in physicochemical properties in response to an external stimulus such as a change in solvent composition, temperature, pH, radiation, ionic strength, electric field, magnetic field, or mechanical stress. Applications of smart polymers include drug delivery, tissue engineering, bioseparation and cell culture [101]. The use of smart polymers for the preparation of "switchable" surfaces (i.e. surfaces that can change rapidly, or "switch", between distinct states by sequential application and removal of a stimulus) has been extensively studied as well.

A number of approaches to protein resistant surfaces have been based on smart polymers [58], [101]–[105]. Some of the polymers used were based on their ability to undergo a phase transition causing desorption of the previously adsorbed protein [106][107]. These surfaces are not protein resistant before the transition occurs, and thus are not suitable for implants and other

biomedical devices which require inherent resistance to nonspecific protein adsorption. They are applied in drug delivery where onset of the transition causes release of the drug as stated in many reviews [108].

With respect to protein interactions, smart polymers are better adapted to the removal of adsorbed protein, i.e. surface cleaning. Cleaning is essential in the re-use of medical devices and for equipment used in the biotechnology industry (e.g. food processing). The work described in this thesis is focused on the development of a surface that is: (1) inherently protein resistant, and (2) recognizing that complete resistance is probably not possible, is responsive to an external stimulus that removes the small amounts protein that are inevitably adsorbed.

2.3.1 CO_2 -Responsive Polymers

In the context described above, our interest was drawn to polymers that are responsive to carbon dioxide. CO_2-responsive polymers are a class of smart polymers which undergo reversible conformational change upon introduction of CO_2 due to interactions between the CO_2 and functional groups such as amidine, amine, and carboxyl on the polymer chains. Compared to other stimuli, CO_2 has the following advantages: environmentally friendly, low cost, low toxicity and easy manipulation. In addition there is no accumulation of unwanted reagent with repeated cycles. pH-responsive polymers, for example, require exposure to salts which accumulate, contaminate the system, weaken switchability, and can increase protein adsorption by salting out effects [109][110]. Compared to temperature-responsive polymers, CO_2-responsive polymers reduce energy consumption and avoid thermal damage to biological materials. For UV-responsive polymers, the depth of penetration is limited and damage to biological materials can

occur. CO_2-responsive polymers eliminate all of these shortcomings. Moreover, CO_2 is a key metabolite in biological systems and is not toxic. Hence, CO_2 is a promising environmental stimulus for smart biomaterials.

For a long period in the last century, CO_2 responsive materials used traditional aqueous amine solutions to capture CO_2. More recently, researchers have expanded the range of CO_2 responsive materials to include metal oxides, organic solids, ionic liquids, carbonaceous adsorbents and many more materials. Lately, interest has been drawn to introducing CO_2 responsive groups used in CO_2 responsive solvents onto polymer chains to explore further applications. Details are given below.

CO_2-responsive polymers can be divided into three categories based on different response mechanisms [111][112]: 1) Polymers containing responsive groups which are strongly nucleophilic (electron donors) or basic: e.g. amidine or guanidine which can form amidinium bicarbonates, zwitterionic adducts, or ammonium carbamates on reaction with CO_2, 2) Polymers containing responsive groups, e.g. tertiary amine, that switch from a neutral to a positively charged state by protonation caused by CO_2; 3) Polymers containing responsive groups, e.g. primary amino groups, which can form ammonium carbamate salt bridges with CO_2 and consequently cause cross-linking.

Examples of CO_2 responsive polymers in the first category are: Endo et al. and co-workers [113] used an amidine-containing polymer to capture CO_2 from air. Yuan's group synthesized an amidine-containg polymer, poly(N-amidino) dodecyl acrylamide (PAD) that was copolymerized with PEO to make a CO_2 switchable vesicle [114]. Zhu's group employed a

N_2/CO_2-switchable acyclic amidine-containing comonomer as surfactant in emulsion polymerization [115].

Examples under the second category are: Zhao's group investigated the deformation of a triblock copolymer (poly(ethylene oxide)-b-polystyrene-b-poly((2-diethylamino)ethyl methacrylate)) assembly in ways that mimic the shape regulation of organelles when triggered with CO_2. They found by controlling the CO_2 stimulation levels, that the size, shape, and morphology of the polymer aggregates can be modulated [116]. The same group developed a CO_2 responsive block copolymer vesicle (poly(ethylene oxide)-b- poly(N,N'-diethylamino ethyl methacrylate)) which exhibits very good gas stimuli responsiveness [117]. They also developed an ABA type triblock copolymer P(MEO_2MA-co-DMAEMA)-b-PEO455-b-P(MEO_2MA-co-DMAEMA) which undergoes a gel-to-sol transition by introducing CO_2. The tertiary amino group on DMAEMA chains functioned as the CO_2 responsive group [118]. Miura et al reported that an aqueous solution of microgel and nanogel particles consisting of N-isopropylacrylamide (NIPAm) and N-[3-(dimethylamino)propyl]methacrylamide (DMAPM) reversibly absorbs and desorbs CO_2 via a phase transition induced by a thermal trigger [119].

As examples under the third category, Nagai et al. showed that an aqueous solution of polyallylamine (PAA) undergoes chain association/dissociation via CO_2 responsive crosslinking/de-crosslinking [120]; and Wang et al. reported that porous polyamine particles could be used to absorb CO_2 [121].

Overall, amine containing monomers are considered to be better candidates in the preparation of CO_2 responsive polymers than amidine-containing ones. Because the amidine group has limited stability in water, it is generally more difficult to synthesize.

2.3.1 .1 Poly(N,N-dimethyl amino)ethyl methacrylate (PDMAEMA)

Poly(N,N- dimethyl amino)ethyl methacrylate (PDMAEMA) is well known for its responsiveness to both pH and temperature. The chemical structure of PDMAEMA is shown in Fig.2.9.

In aqueous solution PDMAEMA shows a thermal transition at the lower critical solution temperature (LCST) (about 40 to 50 °, depending on molecular weight [122]–[124]). At temperatures below the LCST the PDMAEMA chains are hydrated and stretched. Above the LCST they dehydrate and collapse into compact shapes. The ionizable tertiary amine moieties on the polymer backbone make PDMAEMA a weak polyelectrolyte responsive to pH. The pKa (defined as the pH at which 50% of the amino groups in the polymer chains are protonated) of PDMAEMA is in the range of 7 to 7.5 [124]–[126]. It is protonated (positive) at pH<7, and deprotonated (uncharged) at pH>8.

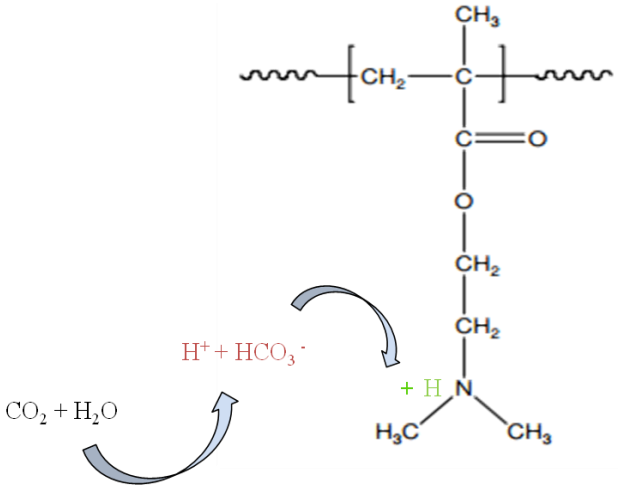

Figure 2. 9. PDMAEMA response to CO_2.

Based on their responsiveness to temperature and pH, surfaces modified with PDMAEMA and its copolymers have been used in various applications, including bioseparations[127][128], antibacterial surfaces [129]–[131], and biosensors [132]. In recent years, PDMAEMA has been widely used as a nonviral vector for gene transfection since it can bind to DNA via electrostatic interactions [133]–[135]. PDMAEMA surfaces associated with controllable protein uptake have also reported [136][137].

More recently, PDMAEMA has been shown to be effective as a CO_2-responsive polymer. The first study on CO_2 responsiveness of PDMAEMA was reported by Zhao et al. in 2012 [138]. They copolymerized PDMAEMA with poly(N-isopropylacrylamide) (PNIPAM) or poly[2-(2-methoxyethoxy)ethyl methacrylate] ($PMEO_2MA$), showing that by triggering with CO_2, the LCST of the copolymer changes. Later, these workers developed a hydrophobic, PDMAEMA analogue, poly(N,N- diethylamino ethyl methacrylate) (PDEAEMA) as a CO_2-responsive reversible protein uptake system. BSA adsorption on PDEAEMA-grafted Au surface was shown to decrease by 95% after CO_2 treatment [106]. Unlike PDEAEMA, PDMAEMA is soluble in aqueous solution, thus it may be assumed to have a certain degree of protein resistance in its uncharged state. With the introduction of CO_2 into the system, tertiary amine groups on PDMAEMA chains are protonated, causing further chain extension and additional protein resistance due to increased repulsion. Su et al. reported increased hydrophilicity of a PDMAEMA modified surface as the ionic strength increased [139]

The interaction of PDMAEMA with CO_2 is illustrated in Fig.2.9. When CO_2 is dissolved in water, it generates hydrogen ions and bicarbonate ions. The tertiary amino groups on the PDMAEMA chains capture the hydrogen ions and become protonated. Electrical repulsion between monomer residues increases and causes extension of the polymer chains. An illustration

of the expected protein repelling mechanism of PDMAEMA grafted surface is shown in Fig. 2.10.

Although data for change in thickness of PDMAEMA graft layers by CO_2 treatment are not available, it was shown by Sanjuan et al. that the thickness of a PDMAEMA brush layer increased significantly with pH change from neutral to acidic [140]. They investigated three batches of surface with initial thickness of 30, 40 and 45 nm, respectively. With pH change from 7 to 2, the thickness increase in the different batches was different, but all increased by approximately 1/3, indicating the effect of pH on chain extension was proportional to initial thickness. The pH of aqueous solution saturated with CO_2 is reported to be 4.9 [106]. Within the range of pH 5-7, PDMAEMA chains extended 1.3 fold as found by Sanjuan eta al [140]. In the present thesis work this number is used to simulate the chain extension and to estimate protein desorption caused by CO_2 (Section 4.3).

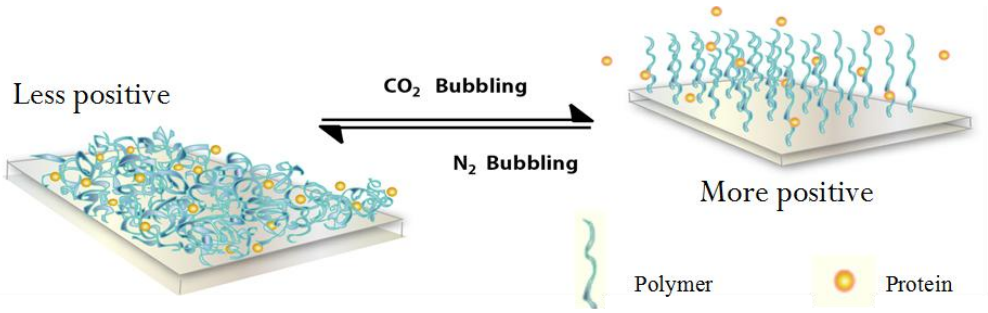

Figure 2. 10. Protein repelling mechanism of PDMAEMA surface upon CO_2 treatment. The effect is reversed by treatment with N_2.

CHAPTER THREE

MATERIALS AND METHODS

3.1 Materials

Silicon wafers of thickness 0.56 mm were purchased from University Wafer Company (Boston, MA). Milli-Q water (Ω=18.2 ohm cm) was prepared by EMD Millipore purification system (Billerica, MA). Hydrofluoric Acid (48%) was purchased from EMD Chemicals (Gibbstown, NJ). Nitrogen gas (99.999%) and carbon dioxide gas (99%) were purchased from Air Liquide (Hamilton, ON). $Na^{125}I$ was purchased from the McMaster Nuclear Reactor (Hamilton, ON). Pooled human plasma was collected from multiple healthy donors; it was aliquoted and stored at -70 ℃. Human serum Albumin was purchased from Enzyme Research Laboratories (South Bend, IN). Ready Gel® (Tris-HCl gel, 4–15%; 10 well, 30 μL) was purchased from Bio-Rad (Richmond, CA).

The following materials were all purchased from Sigma-Aldrich: CuBr (99.999%), $CuBr_2$ (99%), 4,4'-dinonyl 2-2'-dipyridyl (98%), (2-dimethylamino) ethyl methacrylate (98%), tetrahydrofuran (anhydrous, >99.9%), methanol (>99.9%), acetone (>99.9%), toluene (anhydrous, 99.8%), 5-hexen-1-ol (98%), α-bromoisobutyryl bromide(>98%), tert-butyl α-bromoisobutyrate(>98%), ethyl α-bromoisobutyrate (98%), trichlorosilane(99%), triethylamine (99%), Karstedt's platinum catalyst (2–3 wt% in xylene), n-hexane (anhydrous, 95%), dichloromethane (98%), inhibitor remover (for removing hydroquinone and monomethyl ether

hydroquinone, Product number: 306312), aluminum oxide (neutral), isopropanol (anhydrous, >99%).

3.2 Surface Preparation

3.2.1 Surface pre-cleaning

Silicon wafer was cut into 5 mm × 5 mm square pieces by Microace 3 dicing saw (Centre of Emerging Device Technologies, McMaster University). Wafers were ultrasonically washed subsequently in methanol, DI water and acetone for 1 min each and dried by airflow. The following steps were all done in a Class 10000 clean room (Centre of Emerging Device Technologies, McMaster University). The wafers were exposed under UV/OZONE for 10 min for each side of the wafer to remove any organic residues on the surface. Wafers were immersed in 49% hydrofluoric acid solution for 5 min to remove the original silicon dioxide layer and hence to reveal a bare silicon layer [141]. Subsequently, wafers were rinsed with Mill-Q water and dried by nitrogen stream. Wafers were then exposed to UV/OZONE for 30 min for each side to form contamination-free silicon oxide layer and active silicon-oxygen bonds on the surface. Lastly, wafers were rinsed with DI water for 5 min to form a new, clean layer of Si-OH groups on the surface, and dried by N_2 flow.

3.2.2 Initiator synthesis

6-(2-Bromo-2-methyl) propionyloxy hexyl trichlorosilane was synthesized in two steps as depicted in Fig 3.1, involving bromination and hydrosilylation, respectively, according to the methods reported [84][85][142] with minor alternations. In brief, intermediate compound pent-4'-enyl-2-bromo-2-methyl propionate was synthesized by bromination of α-bromoisobutyryl bromide and 5-hexen-1-ol in dry dichloromethane as solvent and triethylamine as catalyst. Into a stirred solution of 5-hexen-1-ol (5.0 g, 50 mmol), dry dichloromethane (30 mL) and trethylamine (6.0 g, 30 mmol) under nitrogen at 0 ℃, α-bromoisobutyryl bromide (11.5 g, 50 mmol) were added dropwise over 20 min. After 1 h reaction, the mixture was warmed to room temperature and stirred for another 2 h. The precipitate of triethylamine hydrochloride formed was removed by vacuum filtration; it was then purified by extraction in saturated NH_4Cl and water sequentially, and the oil phase collected. Dichloromethane was removed by vacuum distillation (78 ℃/10 mm Hg).

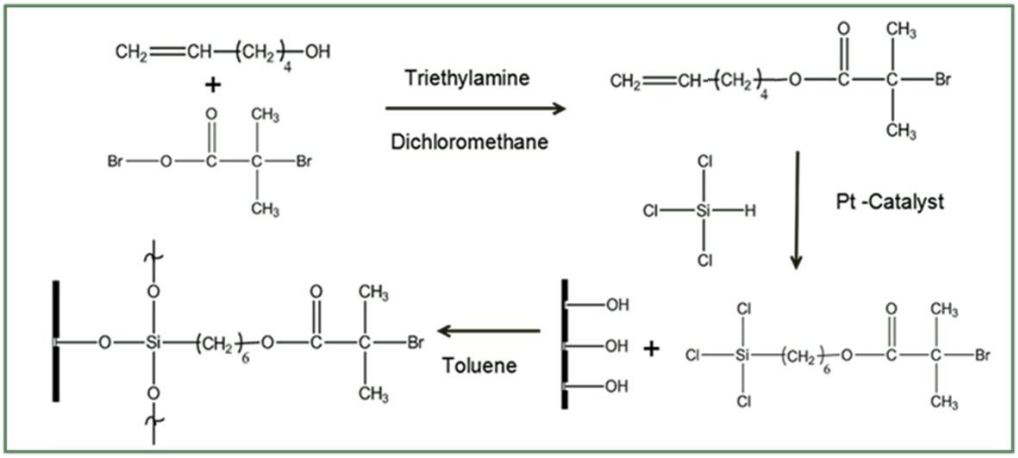

Figure 3. 1. Reaction scheme for initiator synthesis.

Final product, 6-(2-Bromo-2-methyl) propionyloxy hexyl trichlorosilane was synthesized by hydrosilylation of trichlorosilane and the intermediate compound. To a solution of 15 mL (149mmol) trichlorosilane and 0.75 g (3. 2 mmol) 4'-enyl-2-bromo-2-methyl propionate, 500 uL Karstedt catalyst was then added. The reaction mixture was stirred overnight at room temperature under nitrogen in dark. Dry toluene was added afterwards, and the excess trichlorosilane was removed under reduced pressure. The product was characterized by NMR. The initiator was stored in solution in dry toluene and kept in an inert atmosphere.

3.2.3 Initiator attachment to silicon substrate.

Twenty freshly cleaned silicon wafers were placed in a glass jar. N_2 gas was flowed through the container for 30 min. Then 10 mL anhydrous toluene and 500 µL (5-trichlorosilylpentyl) 2-bromo-2-methylpropionate were added. The reaction was carried out at room temperature overnight. A monolayer of initiator molecules was self-assembled on the surface by reaction between -OH groups on the silicon and -H group from the initiator. The initiator-anchored wafers were rinsed with toluene, acetone, water, acetone in sequence and were dried by N_2 flow immediately before use. Wafers were stored in dry toluene under nitrogen.

3.2.4 PDMAEMA grafting by surface-initiated ATRP.

Inhibitors (hydroquinone and monomethyl ether hydroquinone) were removed from the monomer by passing through a column packed with inhibitor remover. Monomer (3.15 g, 200 mmol) and THF (**1**:1,v:v ratio) were placed in a flask. CuBr (14.4 mg, 1 mmol) as the catalyst

and dNbpy (81.7 mg, 2 mmol) as the ligand were placed in a second flask. $CuBr_2$ (1.87 mg, 0.1 mmol) was added to assure good control of the polymerization rate [143]. Initiator-anchored wafers were placed in a glass jar. All apparatus was degassed for 30 min.

When the mixture of monomer and solvent was added to the catalyst and ligand mixture, the color turned dark brown. The mixture was stirred for 30 min to assure homogeneity. The mixture was then cannulated through a double-tip needle to the wafer jar. EBIB (5 μL, 5 mmol) as free initiator was added to assist polymerization control which is difficult with a low overall concentration of dormant species immobilized on a flat substrate [83][144] . Polymerization was initiated both on the surface and in the solution. The reaction was stopped by opening the jar to air or by adding $CuBr_2$ to the solution to convert CuBr into $CuBr_2$.

Polymer-grafted wafers were rinsed several times in THF, DI water, and isopropanol, and then dried by air flow. Additional THF was added to the solution (containing the polymer formed in solution) which was then passed through an alumina column to remove residual catalyst and ligand. The column was washed extensively with THF. All column effluents were collected. Most of the THF was evaporated and the remaining solution was added drop by drop to a reservoir of n-hexane at -20 ℃. The polymer precipitated and was dried in a vacuum oven at room temperature overnight.

3.3 Surface characterization

A general overview of the surface characterization techniques used in this research is shown in table 3.1.

Table 3. 1. Surface analysis techniques used in this project.

	Principle	Operating environment	Spatial resolution	Surface sensitivity
Contact angle	Liquid wetting of surface	Air/Liquid	NA	3-20 Å
XPS	X-rays cause emission of photoelectrons with characteristic energies	Vacuum	10 μm	10 - 150 Å
Imaging Ellipsometry	Analysis of polarized light after reflection	Air/Liquid	NA	1 nm - 50 μm
AFM	Measures interatomic forces between tip and sample	Air/Liquid	Atomic	NA

3.3.1 Contact angle

Static water contact angles were measured with a Model 200 Ramé-Hart goniometer (Mountain Lakes, NJ) using the sessile drop method with Milli-Q water. Samples were freshly cleaned with solvent and dried under an air stream before use.

3.3.2 X-ray photoelectron spectrometry (XPS)

XPS spectra are obtained by irradiating the sample with an X-ray beam under vacuum. The kinetic energy and the number of electrons escaping from the top ~10 nm of the sample are measured and analyzed. In this work XPS spectra were obtained with a Physical Electronics PHI Quantera II spectrometer (Physical Electronics, MN, USA) in the Biointerfaces Institute at

McMaster. Low resolution scans for C, O, N, Br, and Si were carried out at take-off angles of 20 ° and 90 °.

3.3.3 Imaging Ellipsometry

The dry polymer layer thickness was determined with a Nanofilm ep3sw Imaging Ellipsometry (Accurion Inc., Germany). EP4 modeling software was used for data processing. Samples were cleaned with solvent and dried in an air stream before use. Data were collected from both sides of the samples, with at least 9 randomly selected spots on each side. The optical constants (refractive index, extinction coefficient) of Si (n=3.865, k=0.020) and values of n=1.500 and k=0 were used to calculate the thickness of the initiator-immobilized and polymer-grafted substrates.

3.3.4 Atomic Force Microscopy (AFM)

Layer thicknesses of anchored initiator and grafted polymer were investigated by Tapping Mode AFM using a BioScope Catalyst microscope (Bruker, MA, USA). A SCANASYST-AIR AFM probe (Bruker, MA, USA) was used for the measurements both in air and in liquid.

3.4 Protein Adsorption Measurements

3.4.1 Quantification of protein adsorption by I-125 radiolabelling

Proteins were radiolabelled with I-125 and the quantity of protein adsorbed was determined by measuring surface radioactivity. Common I-125 radiolabelling methods include the iodine monochloride (ICl) method and the Iodogen® method [145]. The ICl method was chosen for this work.

3.4.1.1 ICl radioiodination method

Human serum albumin was radioiodinated using $Na^{125}I$. A first vial was charged with 200 mL of protein stock solution (20 mg/mL) and 40 µl of glycine buffer (2M, pH=8.8). A second vial was charged with 18 µl of ICl reagent and 5 µl of $Na^{125}I$ and mixed for 1 min. Vial 1 contents were then added to vial 2, and mixed for 2 min during which iodide attached to the protein through tyrosine residues. The mixture was then passed through an AG1X4 anion exchange resin column to remove unbound radioiodide. The column was washed with 4 mL of citrate buffer. The collected solution contained the radiolabelled protein. The concentration of the radiolabelled protein was measured by UV-Vis spectrometry at a wavelength of 280 nm.

3.4.1.2 Determination of free radioiodide

Free radioiodide refers to the radioactive iodide in the protein solution that is not bound to the protein. To determine free iodide, the protein is precipitated from the solution after labelling using trichloroacetic acid (20% w/v in water). Unbound iodide is then present in the supernatant. In this work the radioactivity of the supernatant was measured using a Wizard

Automatic Gamma Counter (PerkinElmer, Waltham, MA). Free radioiodide in the radiolabelled albumin solutions was found to be consistently less than 1% of the total.

3.4.2 Protein adsorption experiments

Surfaces were in the form of 5mm × 5mm squares. Samples were incubated in buffer overnight in the wells of 96-well plates before the adsorption experiment. The surfaces were then transferred to wells containing 1 mg/mL protein solution (10% radiolabelled, 90% unlabelled) or plasma (radiolabelled protein added to give a concentration corresponding to 10% of the normal level in plasma) and incubated for 2 h. The surfaces were then rinsed with buffer 3 times, 5 min each time. The radioactivity on the surface, giving a measure of protein adsorption, was measured using a Wizard Automatic Gamma Counter (PerkinElmer, Waltham, MA). When the surfaces needed to be used subsequently in desorption experiments, they were placed in 500 mL of pH 7.4 buffer solution to maintain hydration. The time used in the quantification step was controlled at the same level for each group.

3.4.3 Protein desorption experiments

These experiments were carried out to investigate the possible effect of CO_2 in removing adsorbed protein from the surfaces. Surfaces with adsorbed protein (i.e. following adsorption experiments) were exposed to three different "desorption" solutions: (1) buffer at pH 7.4, i.e. the same as for adsorption; (2) buffer at pH 5.0, to investigate the effect of acid pH; (3) water into which CO_2 was bubbled.

After measuring protein adsorption, the surfaces were transferred to the "desorption" solution and incubated for 30 min. The surfaces were then rinsed and the remaining radioactivity was determined.

3.4.4 Protein adsorption from plasma: analysis by gel electrophoresis (separation) and Western-blotting (identification).

The interactions of the surfaces prepared in this project with plasma were also investigated. Plasma exposure gives a more severe test of protein resistance than exposure to a single protein in buffer. In addition it is important to investigate the behavior of the surface in a "real" biofluid.

Specific protein types adsorbed on the surfaces were identified by immunoblotting. Proteins were eluted from the surface after plasma contact, denatured and separated by their molecular weights by gel electrophoresis. The proteins were then transferred from the gels to a membrane, where they were stained with antibodies specific to the target protein. The procedure is depicted in Fig. 3.2

3.4.4.1 Plasma exposure and protein elution.

Procedures for plasma exposure were the same as described in section 3.4.2. Protein elution was carried out by incubating surfaces in 2% SDS overnight to elute the adsorbed proteins (250 µL for 8 surfaces.)

3.4.4.2 Separation of eluted proteins by gel electrophoresis

Elutes were then loaded on sodium dodecyl sulfate - polyacrylamide gel elecrophoresis (SDS-PAGE) gels, run for 1 h at the constant voltage of 220V to separate the proteins.

3.4.4.3 Identification of eluted proteins by immunoblotting

The proteins were transferred from SDS-PAGE gels to polyvinylidene fluoride (PVDF) membranes by the semi-dry method using the iBlot® 7-Minute Blotting System (Invitrogen, Israel, WV). The membranes were incubated in a skim milk solution to block unbound sites. After 2 h exposure to blocking solution, primary antibodies were added (1:1000 (v:v) ratio). After 1 h primary antibody incubation the surfaces were rinsed three times to remove unbound antibody. The surfaces were then exposed to alkaline phosphatase-linked secondary antibodies (1:1000 (v:v) ratio), rinsed and treated with color development solution. The intensity of the gel/blot bands was determined by Chemidoc MP Imaging System (Bio-Rad, Inc.).

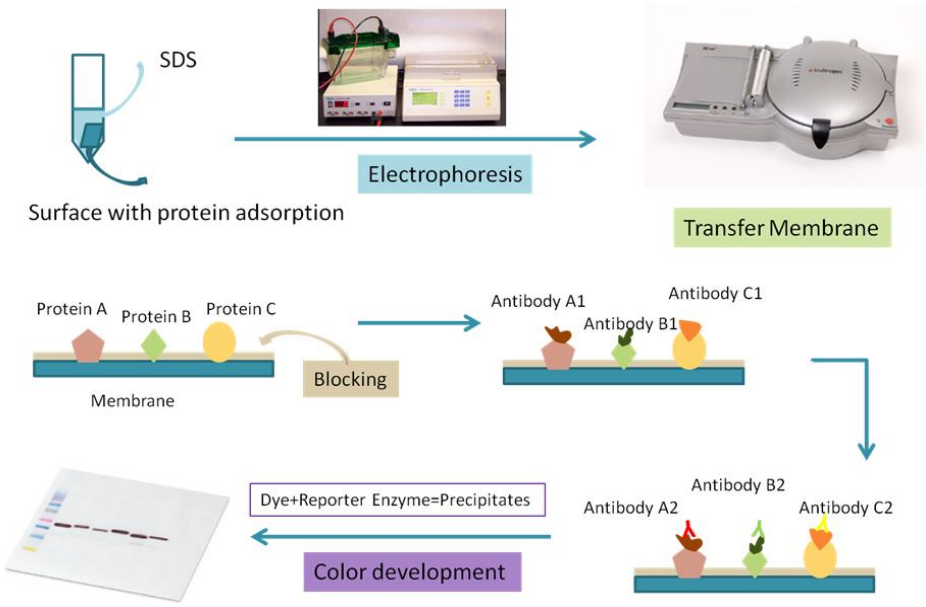

Figure 3. 2. Scheme of western-blotting protocols

CHAPTER FOUR

RESULTS AND DISCUSSION

4.1 PDMAEMA-Modified Surfaces: preparation and characterization

In this chapter, some aspects of the preparation and characterization of the PDMAEMA-modified surfaces are discussed. NMR was used to determine the chemical structure of the ATRP initiator used for grafting to the silicon surface. Water contact angles were used as a measure of surface hydrphilicity. The thickness of the initiator and polymer layers was measured using ellipsometry (dry state) and AFM (hydrated state). XPS provided data on the elemental composition of the surfaces.

4.1.1 Initiator synthesis

The ATRP surface initiator (5'-trichlorosilylpentyl) 2-bromo-2-methylpropionate, and its intermediate product, pent-4'-enyl 2-bromo-2-methylpropionate, were characterized by NMR. The ^{1}H and ^{13}C spectra are shown in Figure 4.1 and 4.2, respectively. The chemical shifts (ppm) of the intermediate product pent-4'-enyl 2-bromo-2-methylpropionate are listed below:

^{1}H NMR ($CDCl_3$): δ 1.37 (quintet, 2H, CH_2), 1.56 (quartet, 2H, CH_2), 1.80 (s, 3H, CH_3), 2.00 (q, 2H, CH_2), 4.04 (t, 2H, CH_2), 4.83-4.93 (complex m, 2H, alkene=CH_2), and 5.56-5.78 (complex m, 1H, alkene=CH);

^{13}C NMR ($CDCl_3$): δ 24.98, 27.71, 30.65, 33.16, 56.83, 65.70, 114.81, 138.11, and 171.27

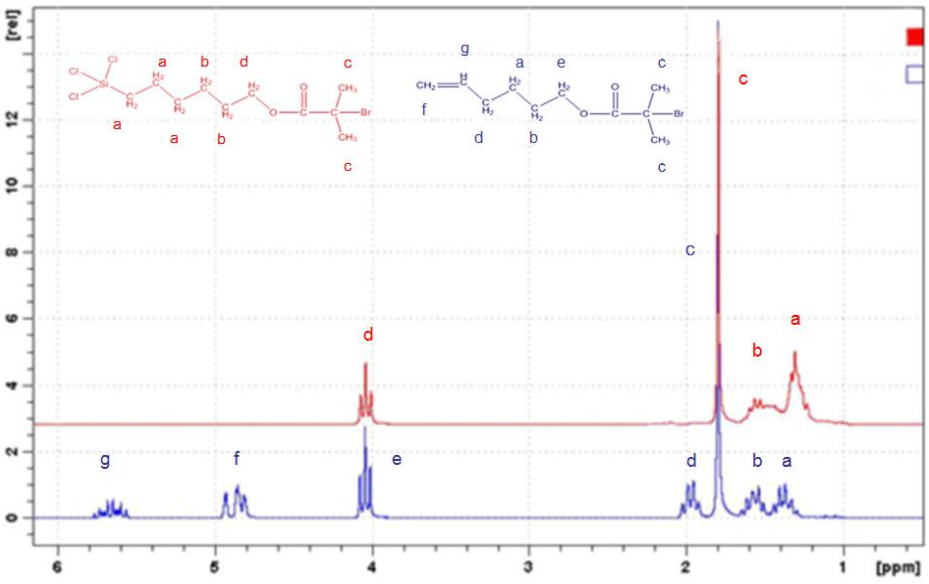

Figure 4. 1. Proton NMR spectra of (blue) pent-4'-enyl 2-bromo-2-methylpropionate and (red) (5'-trichlorosilylpentyl) 2-bromo-2-methylpropionate.

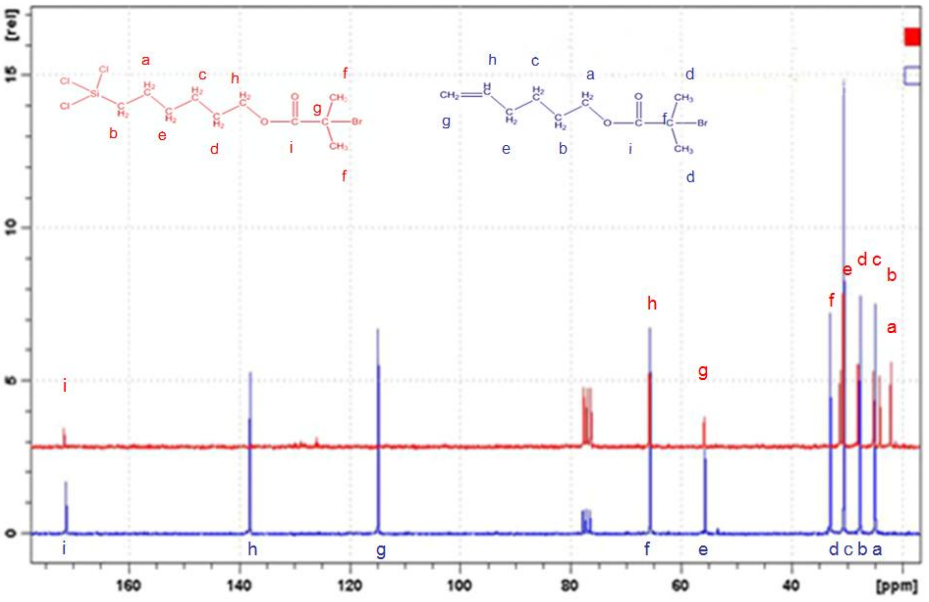

Figure 4. 2. 13-C NMR spectra of (blue) pent-4'-enyl 2-bromo-2-methylpropionate and (red) (5'-trichlorosilylpentyl) 2-bromo-2-methylpropionate.

The chemical shifts (ppm) of the final initiator product (5'-trichlorosilylpentyl) 2-bromo-2-methylpropionate are listed below:

^{1}H NMR ($CDCl_3$):

δ 1.37-1.49 (complex m, 3H, CH_2), 1.57-1.77 (complex m, 2H, CH_2), 1.94 (s, 3H, CH_3), 4.18 (t, 2H, CH_2);

^{13}C NMR ($CDCl_3$)

δ 22.17, 24.20, 25.36, 28.12, 30.72, 31.45, 55.94, 65.80, and 171.74

The obtained data agree with those reported in the literature [84], suggesting successful synthesis and purification of the initiator.

4.1.2 Water Contact Angle Measurements

Water contact angles give a measure of surface hydrophobicity/hydrophilicity. The images in Fig 4.3 show the evolution of the contact angle at each step of the PDMAEMA-grafted silicon surface preparation. Table 4.1 shows the contact angle data.

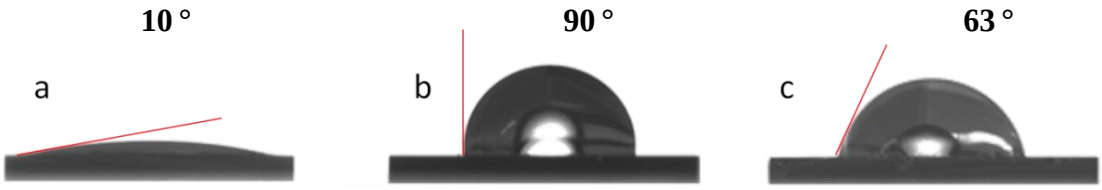

Figure 4. 3 Images of advancing water contact angle on: (a) unmodified silicon surface after UV/OZONE treatment, (b) initiator-anchored silicon surface, (c) PDMAEMA-grafted silicon surface.

The silicon substrate surfaces after UV/OZONE treatment were strongly hydrophilic, with a contact angle less than 10 °. This value reflects the large number of Si-OH groups formed on the surface by UV/OZONE. These Si-OH groups do not remain permanently on the surface, but disappear over time on exposure to air. The hydrophobicity of the bare silicon surfaces increased with time as a result. The water contact angle after initiator attachment increased significantly to 90 ° due to the hydrophobic nature of the initiator. This sharp increase in the water contact angle indicated that the initiator was successfully attached.

Table 4. 1. Water contact angles. Data are mean ± SD, n=6.

	Unmodified Silicon(UV/OZONE)	**Unmodified Silicon**	**Initiator-attached Silicon**	**PDMAEMA modified surfaces of varying thickness (nm)**					
				15	20	25	35	40	45
θ_{adv}(°)	<10	50 ±3	90 ±2	63 ±3	63 ±2	63 ±2	63 ±1	63 ±1	63 ±1

Water contact angles on the PDMAEMA-grafted surfaces were ~63 ° independent of graft layer thickness, suggesting that polymer coverage was complete in the thickness range studied (15 to 45 nm). Although changes in water contact angle do not confirm the grafting of polymer, they are suggestive. Moreover the angles are consistent with those reported in the literature for similar materials. Reported water contact angle values of PDMAEMA grafted surfaces vary considerably, ranging from 40 ° to 75 ° [137][139][146] depending on the substrate material. This variation may be due to variable graft density or to the different methods used to clean the surface prior to the measurement, or to differences in substrate.

4.1.3 Thickness of grafted PDMAEMA layers and anchored initiator layer

4.1.3.1 Thickness measurements by ellipsometry

Ellipsometry was used to determine the thickness of the initiator and polymer layers in the dry state. Data were collected from at least 6 spots on each sample, 3 spots each side. Ellipsometric images of the polymer-grafted surfaces are shown in Fig. 4.4. In these images, darker areas indicate lower thickness. Clear changes can be seen in the PDMAEMA-grafted surfaces compared to the unmodified silicon. PDMAEMA-grafted surface appears more inhomogeneity. The patterns appeared on the surface may caused by residues of cleaning solvent. The scratch was made for thickness determination with AFM is clearly seen in Figure 4.6 (d). And the same surface was used to compare the thickness data measured by ellipsometry and AFM.

The polymer layer thickness depends on polymer chain length which in turn is determined by polymerization time. Thickness data as a function of polymerization time are shown in Table 4.2. and Fig. 4.5. The layer thickness increased linearly with the polymerization time initially, then more slowly. This decelerating growth was probably due to the loss of active chain ends which would caused by termination or limited monomer diffusion to the surface.

As shown in table 4.2, the dry thickness of the initiator layer was found to be 2.4 nm , consistent with three dimensions of the initiator molecule and with data reported in literature [147].

Table 4. 2. PDMAEMA layer thickness versus polymerization time, data are mean ± SD, n=4

Time (h)	0(initiator)	4	6	8	16	20	24
Thickness (nm)	2.4 ±0.2	15 ±2	20 ±1	25 ±1	35 ±1	40 ±1	45 ±1

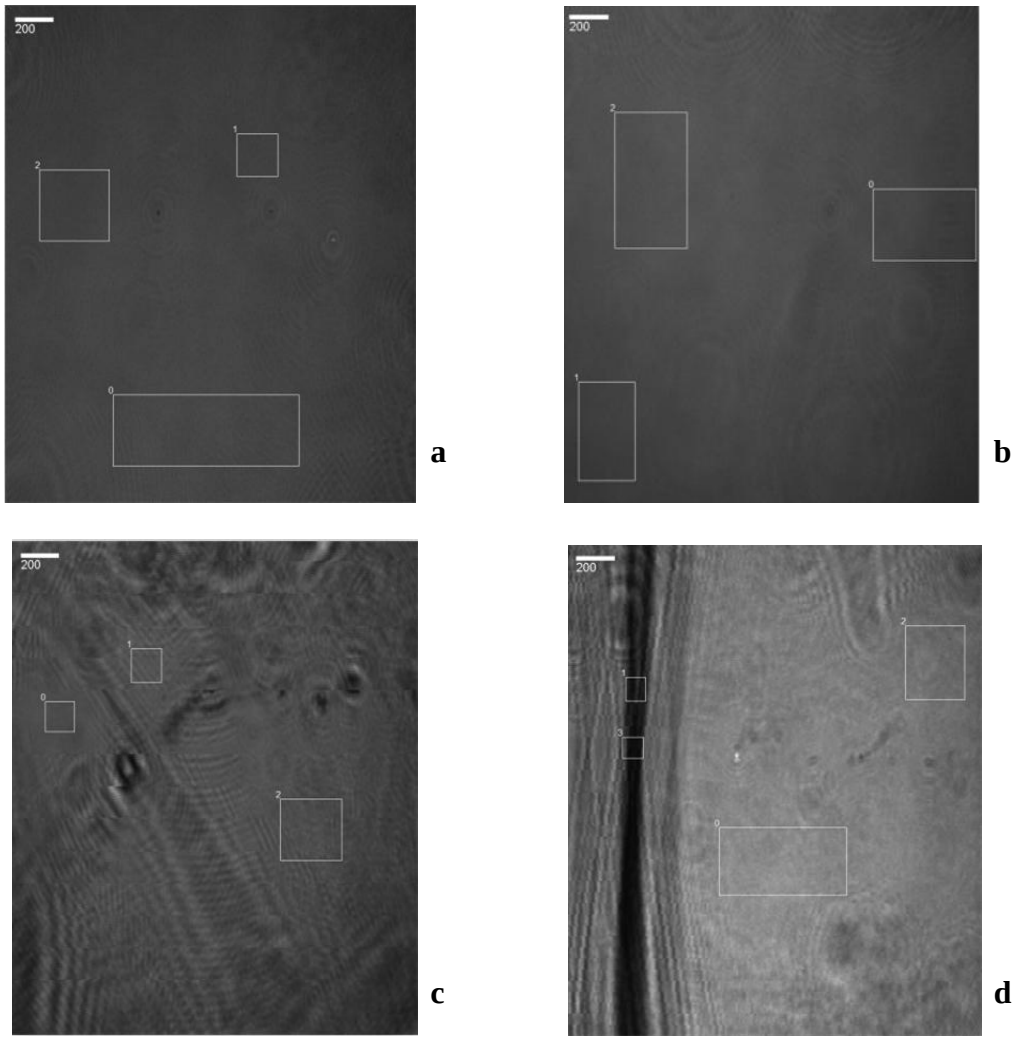

Figure 4. 4. Ellipsometric images of: (a) unmodified silicon surface, (b) initiator-anchored surface, (c) PDMAEMA grafted surface, (d) PDMAEMA-grafted surface with a scratch. Squares and rectangles indicate specific data collection areas.

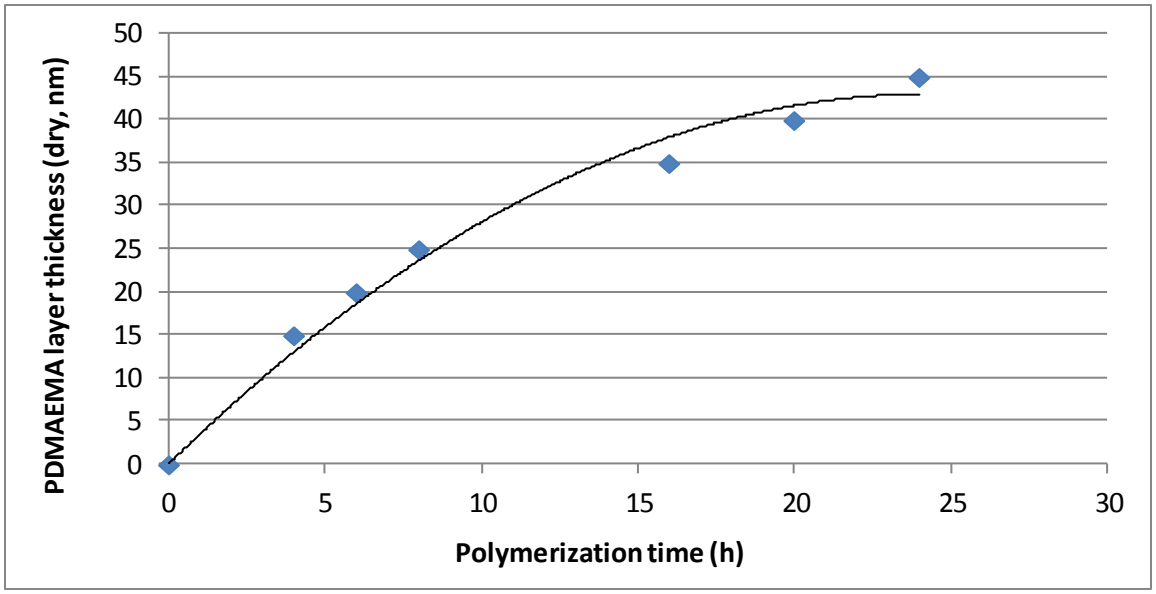

Figure 4. 5. PDMAEMA layer thickness versus polymerization time. Data are mean, n=4.

4.1.3.2 Thickness measurements by atomic force microscopy (AFM)

Both dry and hydrated layer thicknesses were investigated by AFM in tapping mode. The polymer layer thickness in the dry state was determined by measuring the height difference between a scratch area and the polymer covered area as shown in Fig. 4.6 (A). Thickness in the hydrated state was determined using a fluid cell with a SCANASYST-AIR AFM probe. Images of dry and hydrated samples are shown in Fig. 4.6 (E) and (F)

The effects of CO_2 on grafted polymer thickness were also investigated by AFM. Different environments including pure water and water bubbled with CO_2 were used in these experiments. Surfaces were incubated in the solutions for 2 h prior to AFM measurement. Typical thickness data are listed in Table 4.3 for a polymer layer formed after 20 h polymerization.

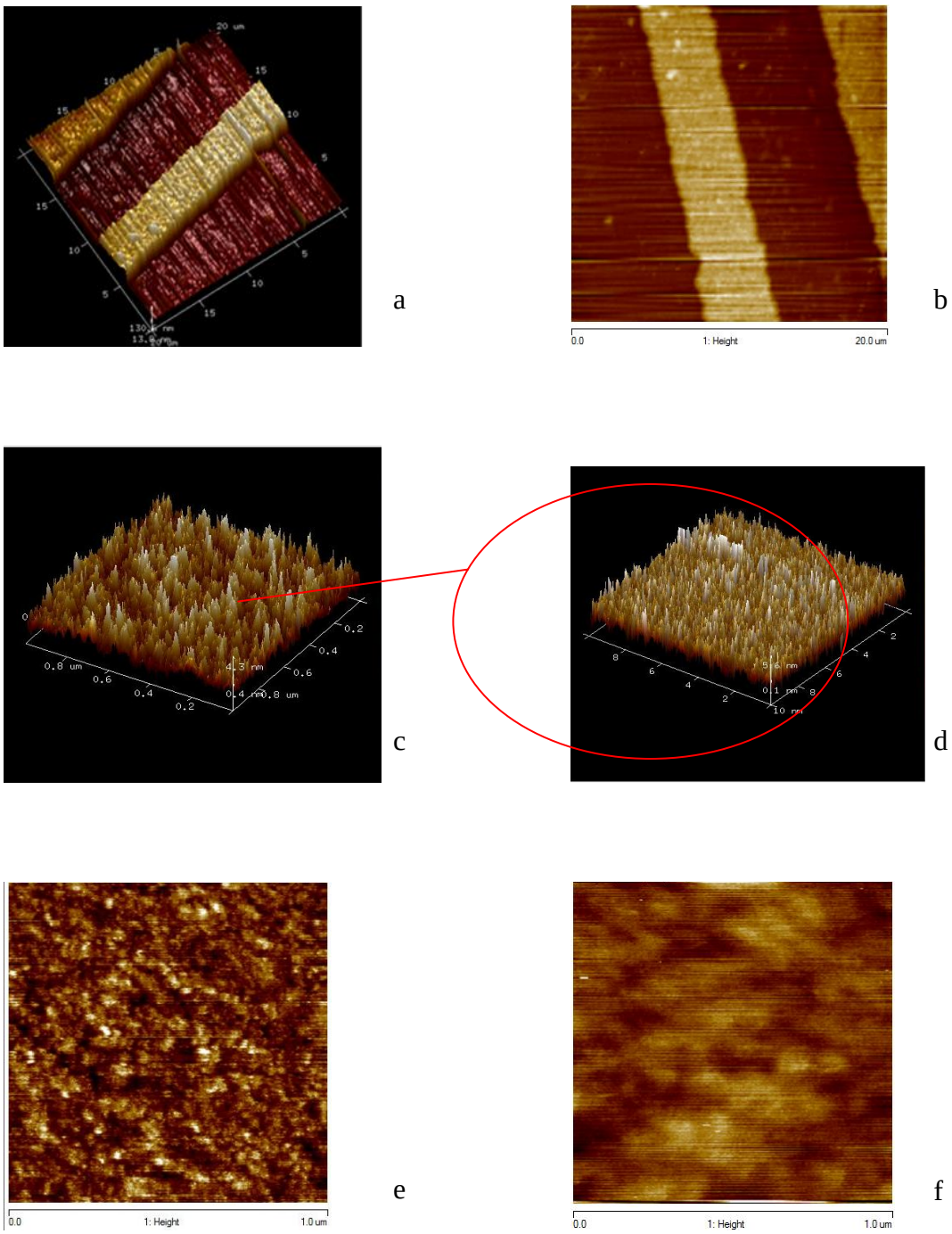

Figure 4. 6. AFM images of PDMAEMA-grafted surfaces with a dry thickness of 40 nm: a) 3D image of a PDMAEMA-grafted surface with scratches for measuring thickness. b) 2D version of image A, c) 3D image of an area with full coverage of polymer, 1 µm × 1 µm, d) image of an area with full coverage of polymer, 10 nm × 10 nm. e) PDMAEMA surface in hydrated state. f) PDMAEMA surface in dry state.

Surface roughness is also important for protein adsorption. First, depending on the scale of the roughness, rough surfaces have a greater true area per nominal unit area compared to smooth surfaces and thus may show greater apparent adsorbed quantities. Second, roughness can influence the geometrical arrangement of protein on surface and therefore affect protein adsorption [47][51]. Roughness data are shown in Fig.4.7 and Table 4.4.

Table 4. 3. Thickness of PDMAEMA grafted surface measured by AFM (polymerization time 20h)

State	Dry	Hydrated	CO_2 treated
Thickness (nm)	40	70	70

As seen in table 4.3 the dry thickness data from AFM were consistent with those obtained by ellipsometry. In the hydrated state, the polymer layer thickness was a factor of 1.75 greater than in the dry state. This relatively low swelling ratio (swollen thickness/dry thickness) is possibly due to the high graft density. Bao et.al. reported different aqueous swelling ratios for poly(HEMA) grafted from Au substrate at different initiator density [148]. The graft density was not reported, but the swelling ratio of poly(HEMA) as a function of surface initiator fraction (SIF) was investigated. It is normally considered that the higher the surface initiator fraction, the higher the graft density. When the SIF was 100% (initiator density = 4 initiator/nm^2), the percentage increase in thickness was only 1.77, similar to the swelling ratio found in this work. While SIF is lowered to 0.1((initiator density = 0.04 initiator/nm^2), the swelling ratio was 1600. Therefore, this PDMAEMA grafted layer could be considered to be in a dense brush configuration.

The PDMAEMA layers were expected to show different thickness in the different solution environments due to protonation/deprotonation caused by pH differences. On this basis

the polymer layers incubated in CO_2-bubbled H_2O were expected to be thicker than in pure water due to chain stretching caused by inter-chain electrostatic repulsion. However, the AFM data do not support this hypothesis. Technical issues may be responsible for this apparent discrepancy. The test was done in air and the layer of solution covering the surfaces was thin. Escape of CO_2 gas from the fluid could be the most likely reason. Since the responsiveness of polymer to pH is instantaneous, the polymer chains could return to their neutral state rapidly and faster than the time required for set-up of the measurement.

As shown in Figure 4.7 and Table 4.4 the roughness of the dry samples was less than 1 nm, while that of the hydrated samples was less than 0.5 nm. These data suggest that the PDMAEMA-grafted surfaces were relatively smooth, and that complications in the interpretation of adsorption data due to differences in roughness should not be an issue.

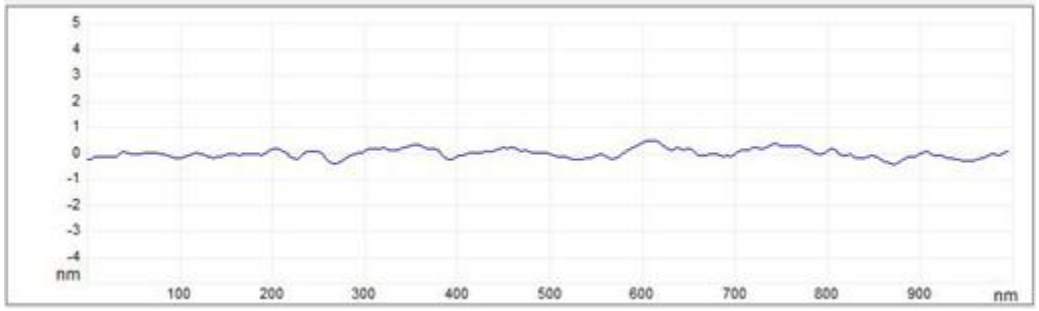

a

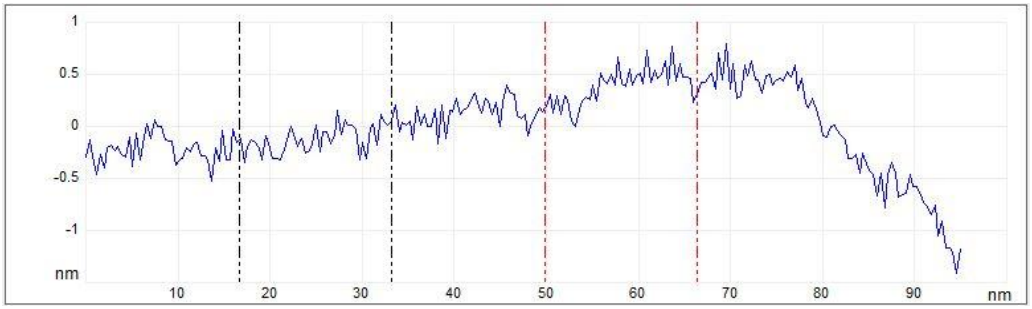

b

Figure 4. 7. Roughness profiles from AFM for PDMAEMA-grafted surface: a) data collected from a 1 μm × 1 μm area, and b) data collected from a 100 nm × 100 nm area.

Table 4. 4. Roughness parameters of PDMAEMA-grafted surfaces. Measurement over 1 μm × 1 μm area

Sample #	Ra (nm)	Rq (nm)
1	0.428	0.555
2	0.625	0.802
3	0.852	1.09

Ra is the arithmetic average roughness. Rq is the root-mean-square roughness.

Unfortunately, it was not possible to obtain the molecular weight of the grafted PDMAEMA chains and the graft densities of the polymer layers are unknown. However, the initiator immobilization conditions for each batch were the same so the graft densities should be the same or very similar for all surfaces.

4.1.4 Surface elemental composition

Low resolution XPS was used as a qualitative indicator of initiator anchoring and polymer grafting to the silicon substrate. The surface contents of C, O, N, Br and Si were determined; Br, specific to the initiator, and nitrogen, specific to the polymer, were given special attention. In this work the take-off angle at 90 º and 20 º were taken as the angle between the surface and the line of emitted electrons to the detector as shown in Fig.4.8. Smaller angles indicate the detector is "closer" to the surface. Observation at different take off angles effectively varies the depth from which the observed photoelectrons come, and thus gives

information on surface composition at different depths. A depth of about 12 nm is the maximum the machine can detect. Theoretically, the larger the take-off angle is (as defined above), the greater the sampling depth.

Three samples were tested for each type of surface, and three areas were examined on each sample. A summary of the XPS data is shown in Table 4.5. Fig 4.9 (a) and (b) show the low resolution XPS spectra of initiator-anchored surface and PDMAEMA-grafted surface respectively at a 20 °take-off angle.

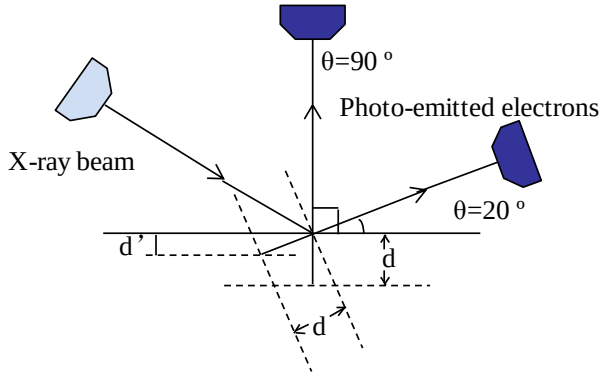

Figure 4. 8. Illustration of take-off angle in XPS.

On the initiator-anchored surface, the presence of bromine suggests successful formation of the initiator layer. With a thickness of 2.3 nm, the change of take-off angle from 20 to 90 °is expected to affect the contents of Si and O. As the take-off angle increased, the proportion of oxygen increased; this is expected if, for example, the material sampled at the higher take off angle, i.e. greater sampling depth, includes a layer of SiO_2 present on the silicon. Theoretically, the ratio of C:Br should remain the same as in the initiator structure independent of take off angle. It is seen from table 4.5, however, that the ratio was greater at 20 than at 90 °because the bromine content was smaller at 90 than at 20 °, suggesting that the bromine content was greater near the surface. This is expected for an overlayer of initiator. The rather large difference

between the surface atomic composition and that of the initiator molecule at both take off angles is undoubtedly due to sampling of the underlying Si/SiO_2. The much higher silicon content in the grafted layers supports this explanation.

Table 4. 5. Low resolution XPS data (atom %) for silicon surfaces at 20 °and 90 °take-off angle.

	Initiator Anchored Surface			**PDMAEMA Grafted Surface (dry thickness of 40 nm)**		
	20 °	90 °	Theoretical	20 °	90 °	Theoretical
C (%)	45.4	39.9	71.5	65.2	64.2	72.7
O (%)	37.0	39.4	14.3	21.5	23.0	18.2
N (%)	——	——	——	8.2	7.3	9.1
Si (%)	15.8	19.6	7.1	4.9	5.2	——
Br (%)	1.8	1.1	7.1	0.2	0.4	——

* Data precision: ±5%. * Theoretical values estimated from molecular structures.

For the polymer-grafted surfaces, the material of layer thickness 40 nm was investigated. Change of take-off angle affected the elemental composition only slightly. The silicon content decreased while C, O, and N increased at the higher take-off angle. Trace amounts of bromine detected on this surface could be due to catalyst residue. At both take off angles the ratio of C:N was the same in the grafted layers as in the polymer molecule itself suggesting that very little of the underlying substrate was sampled, as would be expected for a 40 nm thick layer.

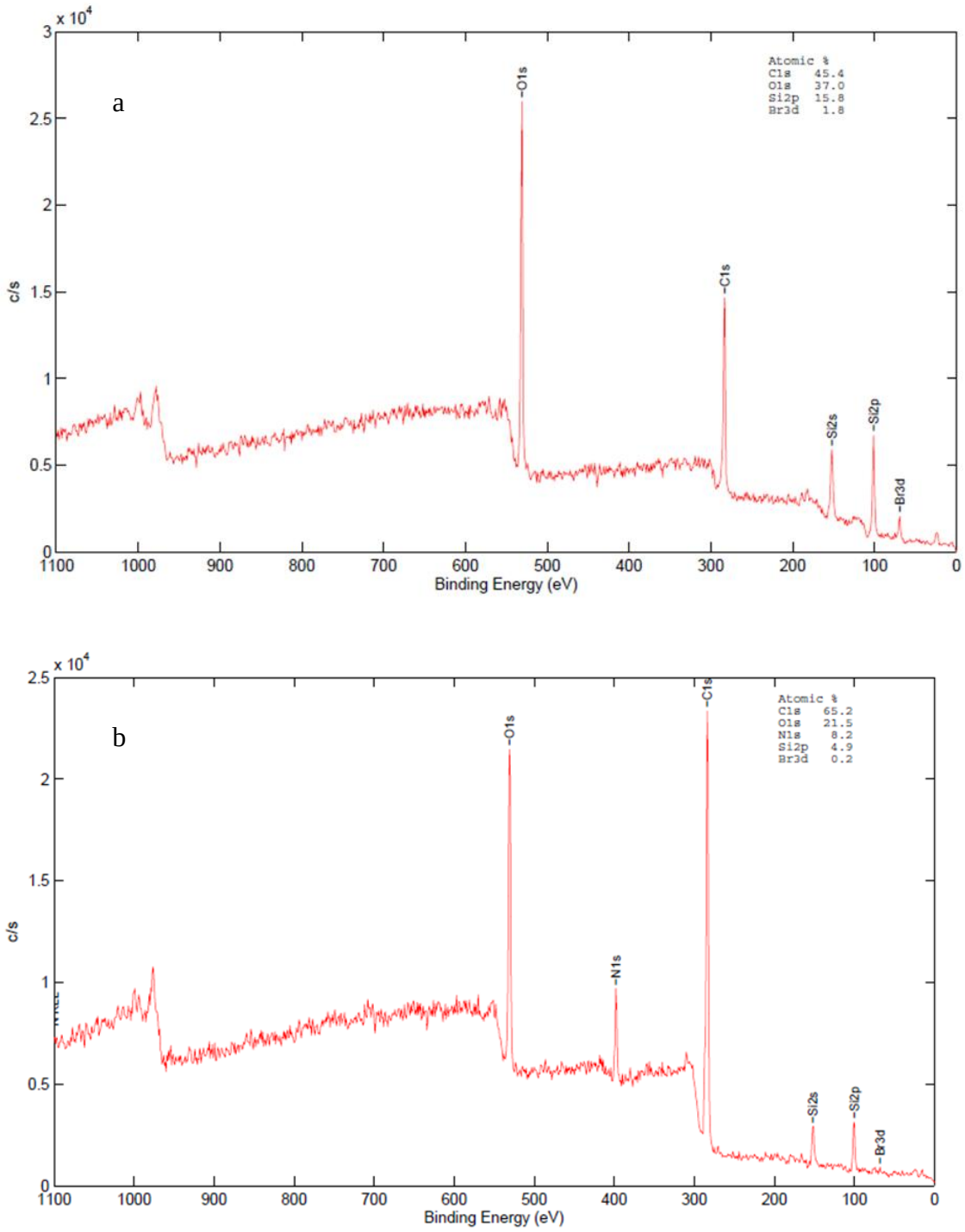

Figure 4. 9. (a) XPS spectrum of initiator-anchored surface. Take-off angle 20 °. (b) XPS spectrum of PDMAEMA-grafted surface (PDMAEMA dry thickness 40 nm). Take-off angle 20 °.

4.1.5 Conclusions

The chemical structures of the intermediate and final products of the initiator were determined by NMR. The chemical shifts and integration of each peak obtained from the spectra were consistent with the literature. Surface pre-cleaning with HF and UV/OZONE generated a high concentration of –OH groups on the silicon surface, resulting in super hydrophilicity of the surface, as confirmed by water contact angle measurements. The self assembly of an initiator monolayer on the silicon surface was confirmed by water contact angle measurements and XPS. The water contact angle increased to 90 °and the bromine was detected by XPS.

The thickness of the grafted PDMAEMA layer on surface was found to increase linearly with the polymerization time. The collapsed polymer layer thickness (dry state) was measured by ellipsometry. AFM provided information on the polymer layer thickness layer in water, where the chains are hydrated and stretched. The hydrated thickness was a factor of 1.75 greater than the dry state thickness. The elemental composition of the dry PDMAEMA-grafted surfaces was also determined by XPS. In a 40 nm thick layer the the ratio of carbon to nitrogen was consistent with the chemical structure of the polymer suggesting high coverage of the grafted polymer.

The thickness of hydrated PDMAEMA layers after CO_2 treatment could not be measured reliably with the AFM technique. Therefore the effect of CO_2 on removal of adsorbed protein from the surface (surface cleaning) could not be measured reliably with this method.

4.2 Protein Adsorption on PDMAEMA-Grafted Silicon

In this research albumin, as the most abundant protein in human plasma and serum, was chosen as a model for the study of a single protein in buffer using radiolabelling for quantification. In plasma experiments several other proteins were investigated using immunoblotting methods. The plasma experiments gave information on competitive adsorption and on the effects of molecular weight, shape and pI of the protein on the ability of the PDMAEMA-modified surface to resist adsorption.

4.2.1 I-125-labelled albumin in buffer

4.2.1.1 Adsorption isotherms

Adsorption as a function of protein concentration in buffer (citrate phosphate pH 7.4) was determined for a series of 5 concentrations up to 2 mg/mL. Four replicates were measured at each concentration. Solution concentration was determined by UV absorbance at 280 nm using an extinction coefficient of 0.454. As shown in Fig. 4.10, adsorption increased with concentration for both surfaces. For the unmodified surface, adsorption increased continuously over the entire concentration range. For the PDMAEMA-modified surface, adsorption levelled off at a concentration of 1 mg/mL. pH 7.4 is very close to the pKa (pH=7.5) of PDMAEMA, so the surface should be close to net electrically neutral. At this pH, albumin molecules are net negatively charged, with approximately 7 charges per molecule. At low coverage of protein, adsorption is mainly determined by interactions between protein and surface, with minimal effect of protein-protein interactions. In this case, the protein resistance of the polymer-modified

surface is expected to be mainly due to hydration of the protein and surface creating a "water barrier" to protein adsorption as discussed earlier.

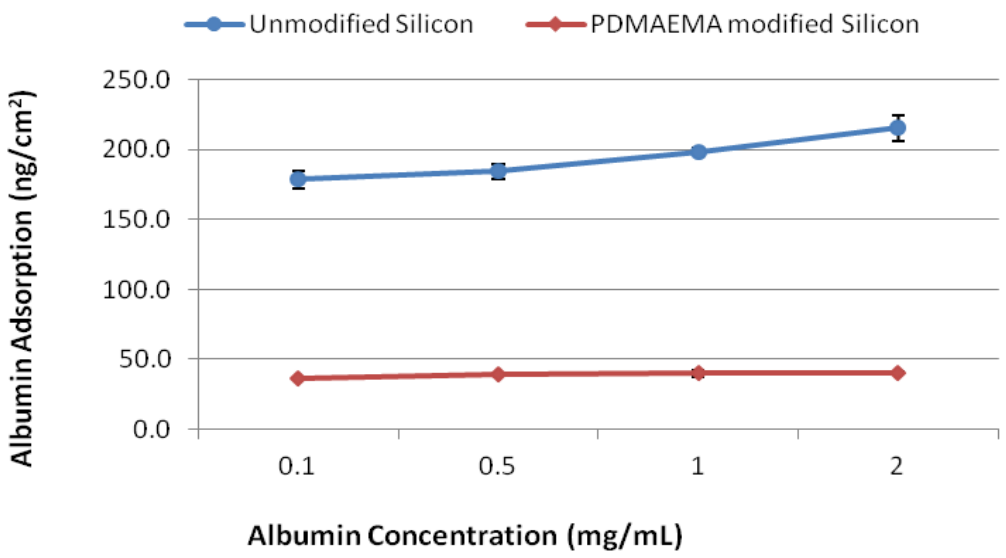

Figure 4. 10. Albumin adsorption from citrate phosphate buffer, pH 7.4: (●,blue) unmodified silicon; (♦, red) PDMAEMA-modified silicon (polymerization time, 20 h). Adsorption time, 2 h. Error bars are ±SD, n=4; the bars not visible are smaller than the symbols.

4.2.1.2 Protein adsorption versus polymer layer thickness

Optimal nonfouling performance should be achieved when surface hydration and steric repulsion/exclusion are both active. Steric repulsion is affected by polymer chain conformation, with flexible chains (longer chains) being more effective than stiff ones on reducing protein adsorption [149]–[154]. Thus, at a fixed grafting density, PDMAEMA layer thickness should be a major contributor to protein resistance.

The albumin adsorption data at a concentration of 1 mg/mL are shown in Fig. 4.11 as a function of polymer layer thickness. The surface with a layer of 15 nm thickness reduced adsorption by 50% compared to unmodified silicon. As the layer thickness increased, albumin adsorption decreased, with the effect levelling off at about 40 nm. For surfaces in this thickness range albumin adsorption was of the order of 25 ng/cm^2, much less than the 200-400 ng/cm^2 expected for a monolayer of albumin (200-400 ng/cm^2). A reduction in adsorption of the order of 90 to 95% compared to the unmodified silicon, as seen here, indicates a surface that is strongly protein resistant.

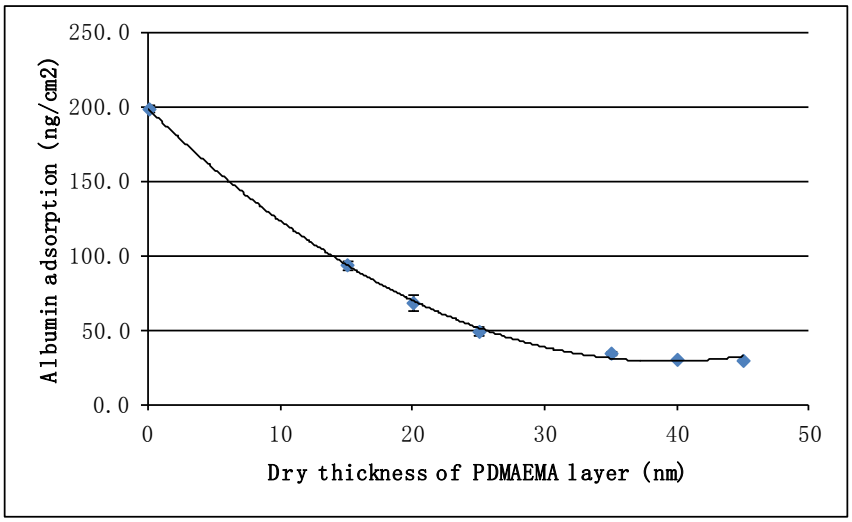

Figure 4. 11. Albumin adsorption from citrate phosphate buffer, pH 7.4 on PDMAEMA-grafted surfaces versus graft layer thickness. Albumin concentration, 1 mg/mL. Adsorption time, 2 h. Data are mean±SD, n=4

4.2.1.3 Albumin adsorption from plasma

In the plasma adsorption experiments PDMAEMA-modified silicon surfaces were compared to unmodified silicon surfaces, and to a polyurethane (PU) and the PU blended with a PEO-containing copolymer. The blend material was shown in previous work to be strongly protein resistant [155]. The data are shown in Fig. 4.12.

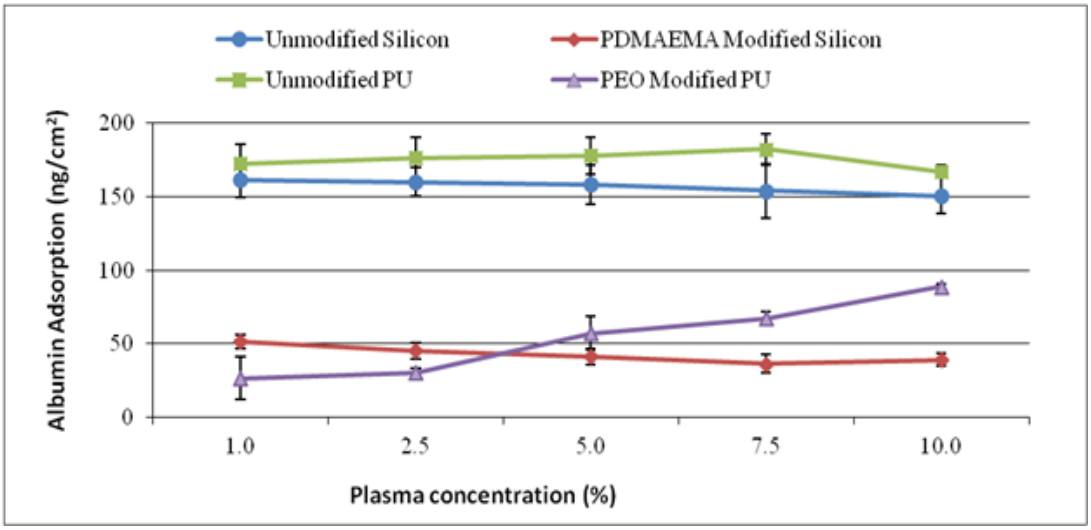

Figure 4. 12. Albumin adsorption from plasma diluted serially with citrate phosphate buffer, pH 7.4. Green (squares) represents unmodified PU, blue (circles) unmodified silicon, purple (diamonds) PEO-modified PU, and red (triangles) PDMAEMA-modified silicon. Adsorption time, 2 h. Data are mean ±SD, n=4.

Albumin adsorption on the modified surfaces was much lower than on the unmodified ones over the entire plasma concentration range. At the lowest concentration, adsorption on the PDMAEMA-modified surface was low, with ~70 % reduction compared to unmodified silicon and unmodified PU. The PEO-modified PU adsorbed about half as much as the PDMAEMA. However, adsorption on the PEO-modified PU surface increased significantly as the plasma concentration increased whereas on the PDMAEMA-modified surface adsorption decreased

slightly. The increase on the PEO surface may reflect adsorption to “bare” areas not covered by PEO. The fact that no increase with plasma concentration was seen on the PDMAEMA surface suggests that coverage was sufficient to prevent further adsorption even at the highest concentration. It may be concluded that the PDMAEMA surface is significantly protein resistant even in plasma at high concentration. As far as we are aware these (and the results presented in section 4.2.2) are the first data to be obtained on the interactions of PDMAEMA with plasma.

4.2.2 Western blotting of eluted proteins after plasma contact.

Experiments were also carried out in which the surfaces were contacted with plasma and the adsorbed proteins were eluted and identified by Western blotting (immunoblotting). These experiments allowed investigation of a relatively wide range of proteins. The properties of the nineteen proteins investigated are listed in Table 4.6. Typical blots for four surfaces: unmodified silicon, unmodified PU, PDMAEMA modified silicon, and PEO modified PU, are shown in Fig 4.13. The blots were optically scanned and the normalized band intensities are shown in Table 4.7.

Densitometer results are listed in Table 4.7. The data for unmodified silicon were used as the basis for normalizing the data for the modified surfaces. Two things must be pointed out with respect to these numbers. First, they do not necessarily correlate linearly with quantity adsorbed, although they may do so within a certain limited range. The standard curves of single protein concentration versus stain density could not be used under our lab conditions, and thus the linear range was not known. Second, the values for different proteins on the same surface cannot be

compared on an absolute basis. Lastly, the SDS elutabilities of the different proteins may be different. All these variables contribute to the complexity in comparing the adsorption of different proteins on different surfaces. The data do give, however, a qualitative indication of the adsorption (and protein resistance) of the different proteins for each surface.

Table 4. 6. Proteins tested for by Western blot.

Lane	Protein	MW (kDa)	Isoelectric Point	Concentration in Human plasma (ug/mL)
1	Factor XI	160	8.9 - 9.1	5
2	Factor XII	80	6.8	15 - 45
3	Prekallikrein	85	8.7	35 - 45
4	HMWK	120	4.7	30 - 90
5	Fibrinogen	340	5.8	3000 - 4000
6	Plasminogen	94	6.7 - 8.3	200
7	Antithrombin	58	4.9 - 5.3	150
8	Complement C3	186	6.3	1100
9	Transferrin	80	5.6	2000 - 3200
10	α-1-antitrypsin	57	4.0	2900
11	Fibronectin	450	5.5 - 6.0	300
12	Albumin	67	4.7	45000 - 80000
13	IgG	160	6.4 - 9.0	8000
14	Vitronectin	75	4.7 - 5.2	200 - 400
15	Prothrombin	68	4.2	120
16	Factor B	93	6.7	200
17	Factor H	150	6	500
18	Factor I	88	7.7	34
19	Apolipoprotein AI	28	5.7	NA

Table 4. 7. Integrated band intensities normalized to unmodified silicon.

Surfaces / Proteins	Unmodified Silicon	PDMAEMA Modified Silicon	Unmodified PU	PEO Modified PU
HMWK	1(2.1×10^6) *	0	0	0
Fibrinogen	1(2.7×10^7)	0.03	0.37	0.08
Plasminogen	1(5.5×10^6)	0	0	0
C3	1(1.2×10^6)	0.44	0.67	0.25
Albumin	1(7.3×10^6)	0.25	0.67	1.44
IgG	1(9.6×10^6)	0.50	0.77	0.24
Vitronectin	1(1.1×10^7)	2.08	0.74	0.13
Prothrombin	0	(7.0×10^6) **	0	0
Factor B	1 (8.3×10^5)	0	0	0
Factor I	1 (2.6×10^6)	0.62	1.01	0
ApoAI	1 (1.2×10^7)	0.48	1.06	0.04

* Numbers in bracket are the original band intensities (arbitrary units).

**Prothrombin intensity was not normalized.

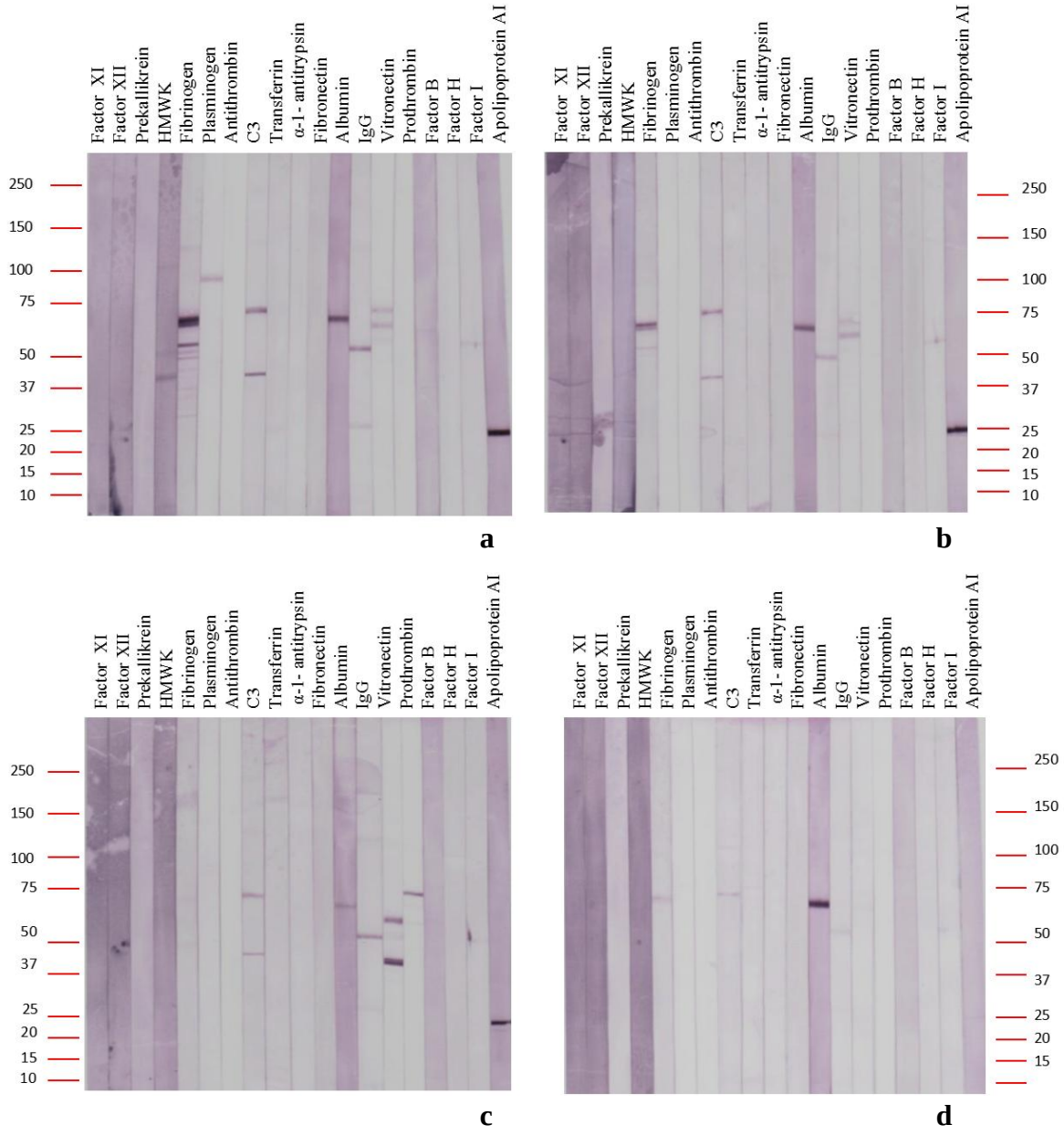

Figure 4. 13. Western-blots of 19 proteins eluted from surfaces after contact with plasma. (a) unmodified silicon, (b) unmodified PU, (c) PDMAEMA-modified silicon, (d) PEO-modified PU.

Based on the blots it appears that the unmodified silicon surface adsorbed 10 of the 19 proteins probed for. Moreover, the adsorption of most of these proteins was greater than on the other surfaces. The unmodified PU surface adsorbed 7 of the 19 proteins. Both of the modified

surfaces adsorbed fewer protein s than the unmodified ones. The PEO-modified PU was the most resistant of the two; only 6 of 19 proteins appeared to be adsorbed on this surface : fibrinogen, C3, IgG, vitronectin, albumin and ApoAI. Only albumin was adsorbed in significant quantity, and indeed albumin adsorption was higher on this surface than on any of the others, consistent with the data from the experiments with labelled albumin (Section 4.2.1.3).

Eight proteins were detected in the eluate from the PDMAEMA-modified silicon surface: fibrinogen, complement C3, IgG, vitronectin, albumin, prothrombin, factor I and ApoAI. Adsorbed proteins varied a lot in basic properties (MW 28-340 kDa, pI 4.2-7.7). Relative to proteins that were not found, there is no simple explanation for the protein selectivity exhibited by this surface. In the uncharged state this surface showed quite strong resistance to fibrinogen and albumin. Resistance to complement C3, IgG, Factor I and ApoA1 appeared to be less strong. However, quite unexpectedly, very considerable quantities of vitronectin and prothrombin appeared to be adsorbed to this surface.

The PDMAEMA-grafted surface was the only one of the four which adsorbed prothrombin. It may be that the tertiary amino groups on the PDMAEMA side chains may have affinity to a specific site on the prothrombin molecule.

The adsorption of vitronectin on the PDMAEMA surface was significantly greater than on unmodified silicon. The reason for this observation remains unknown. Specific chemical interactions may be responsible. Another possible explanation may be that the charges on the PDMAEMA surface interfere with ionic interactions between polyanionic and polycationic segments of vitronectin, causing significant adsorption.

As shown in Fig. 4.13, the bands for vitronectin were in unusual positions; three bands at 60, 50, and 40 kDa respectively were observed, whereas the expected bands for vitronectin in

SDS-PAGE are at 75 and 65 kDa as seen for the other three surfaces. This observation suggests the possibility of degradation occurring in the interactions between vitronectin and the PDMAEMA surface. Bale et al. reported that adsorbed vitronectin showed two fragments of molecular weight 56 and 48 kDa on polymer surfaces with carboxylic acid groups [156].

Unfortunately, the mechanism of cleavage of vitronectin remains unknown. Cleavage at the 3 glycosylation sites might be a reasonable assumption. Another possibility might be cleavage by thrombin or plasmin present in the plasma. This suggestion is based on the existence of thrombin and plasmin cleavage sites in the vitronectin structure (Fig.2.4). The blot data show that the PDMAEMA surface did not adsorb plasminogen, the precursor of plasmin, while prothrombin appeared to be extensively adsorbed as described.

Determination of the amino acid sequence of the vitronectin fragments adsorbed on the PDMAEMA surface could help to determine the location of the fragments in the vitronectin structure and thereby clarify the mechanism of the apparent surface degradation of the protein. Studies of cell attachment and heparin binding might give further insights into the interactions between vitronectin and PDMAEMA.

In summary, PDMAEMA surfaces showed good resistance to a group of 19 plasma proteins, especially to fibrinogen and albumin. However, significant adsorption of vitronectin and prothrombin gave rise to doubts as to whether this type of surface is universally protein resistant. Further investigation is required to fully understand the interactions between PDMAEMA modified surface and these two proteins.

4.2.3 Conclusions

Protein adsorption on PDMAEMA-modified surfaces was found to be dependent on the polymer layer thickness. Albumin adsorption from single protein solution in buffer as a function of thickness decreased sharply initially and then reached a plateau at around 40 nm thickness. Adsorption decreased by ~90% on PDMAEMA-modified surface with a thickness of 40 nm relative to unmodified silicon. Albumin adsorption from plasma to the PDMAEMA surface as measured by radiolabelling was reduced by ~70% in concentrated as well as dilute plasma. Western blotting analysis of proteins eluted from the surface after plasma contact gave further evidence of the protein resistant properties of the PDMAEMA surface. This surface, surprisingly, showed relatively high adsorption of vitronectin and prothrombin. The reasons for and significance of these observations are unknown; further investigation would be required to provide explanations.

4.3 Effect of CO_2 on Protein Desorption from PDMAEMA-Grafted Surfaces

When CO_2 is dissolved in water, the pH decreases from 7 to 5, and properties of the whole system change, including the ionic strength of solvent, the charge on PDMAEMA surface and on the proteins. The PDMAEMA surface is expected to become positively charged due to protonation of tertiary amino groups on the polymer chains. Degree of protonation, α can be calculated as $([H^+]/Ka)/(1 + [H^+]/Ka)$. Using a pKa of 7.5, the protonation degree of PDMAEMA

should increase from to 0.76 to 0.98 as pH decreases from 7 to 5, meaning that almost every monomer unit on the PDMAEMA chains is positively charged at this pH. The surface will become more hydrophilic and chain-chain repulsion due to the positive charges will cause the chains to extend away from the surface and reveal more hydrophilic groups. It is expected that any adsorbed protein will therefore tend to be released. Charges on protein surfaces differ from protein to protein, depending on the presence of ionizable amino acids on the surface, i.e. aspartic and glutamic acids, arginine and lysine.

In this work, desorption of albumin (adsorbed as a single protein from buffer) in response to CO_2 was studied using the ^{125}I radiolabelled protein. The effect of PDMAEMA layer thickness on desorption was studied. In addition, Western blotting was used to investigate the desorption of albumin, complement C3, vitronectin, and prothrombin by CO_2 treatment.

4.3.1 CO_2 induced desorption of albumin assessed by radiolabelling

4.3.1.1 Effect of graft layer thickness on CO_2 responsiveness

Based on the data presented in Section 4.2.1.2, it was hypothesized that desorption from PDMAEMA surfaces would be dependent on the graft layer thickness. Since the polymer layer thickness in the CO_2-bubbled water system could not be measured, this hypothesis could not be tested experimentally. Instead, a qualitative simulation of the expected trend of desorption is used (Fig 4.14). The assumed value of the increased thickness was based on Sanjuan's work [140]: the PDMAEMA thickness in a CO_2 bubbled system (pH 5) is approximately 1.3 times that at pH=7. The swollen thickness at pH 7 was calculated as 1.75 times the dry thickness based on the AFM data obtained in Section 4.1.3.2. The swollen thickness data are shown in Fig. 4.14(b).

The simulated swollen thicknesses in the CO_2 system were fitted to the regression curve (Fig. 4.14(a)), derived from the data presented in Section 4.2.1.2. The equation was developed based on an exponential decay. The simulated adsorption data of CO_2-treated PDMAEMA-modified surfaces are shown in Fig.4.14(c). The estimated desorption quantities caused by PDMAEMA as a function of thickness are shown in Fig.4.14(d).

a

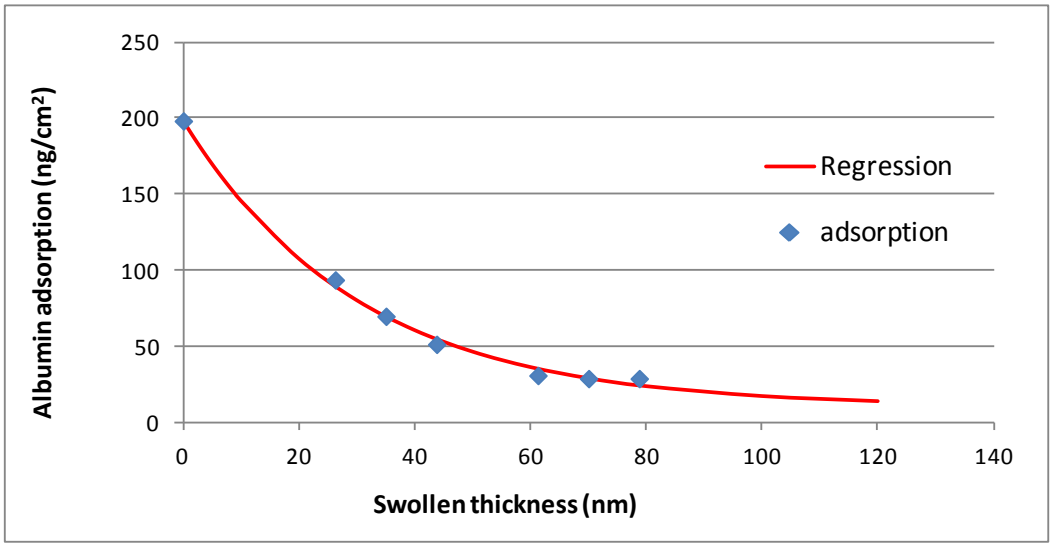

b

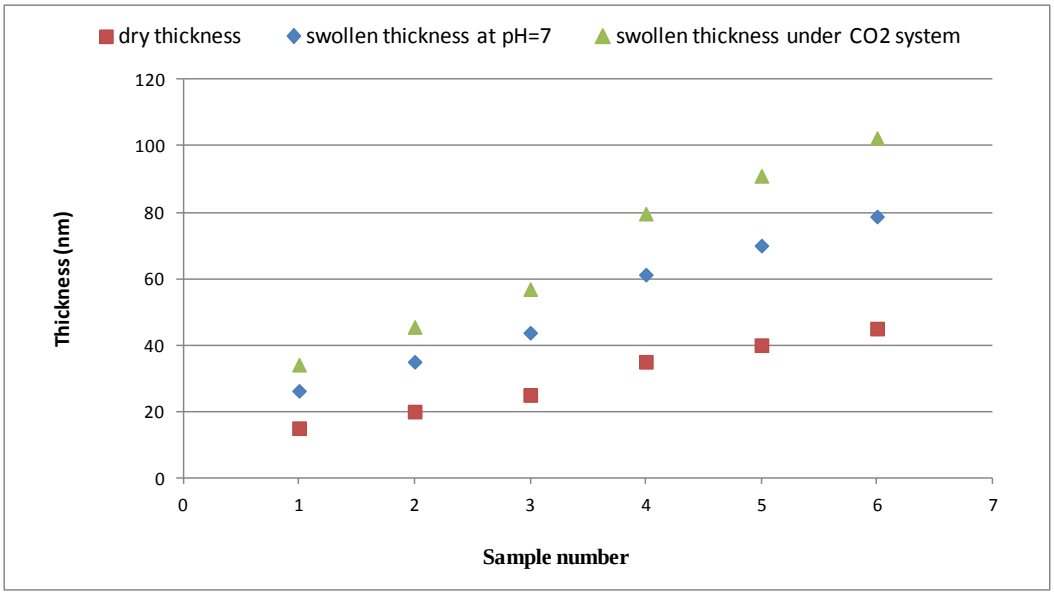

c

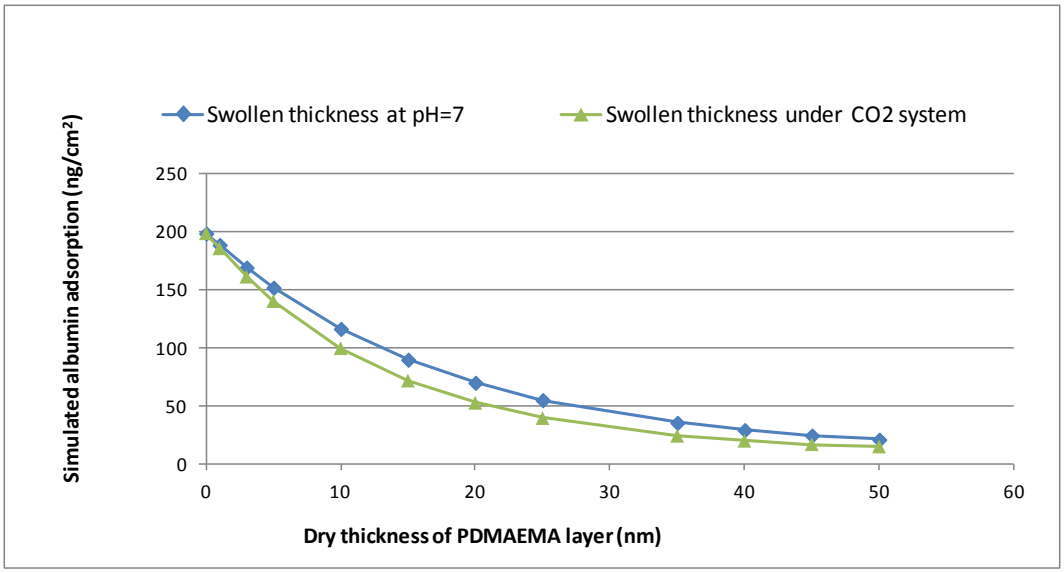

d

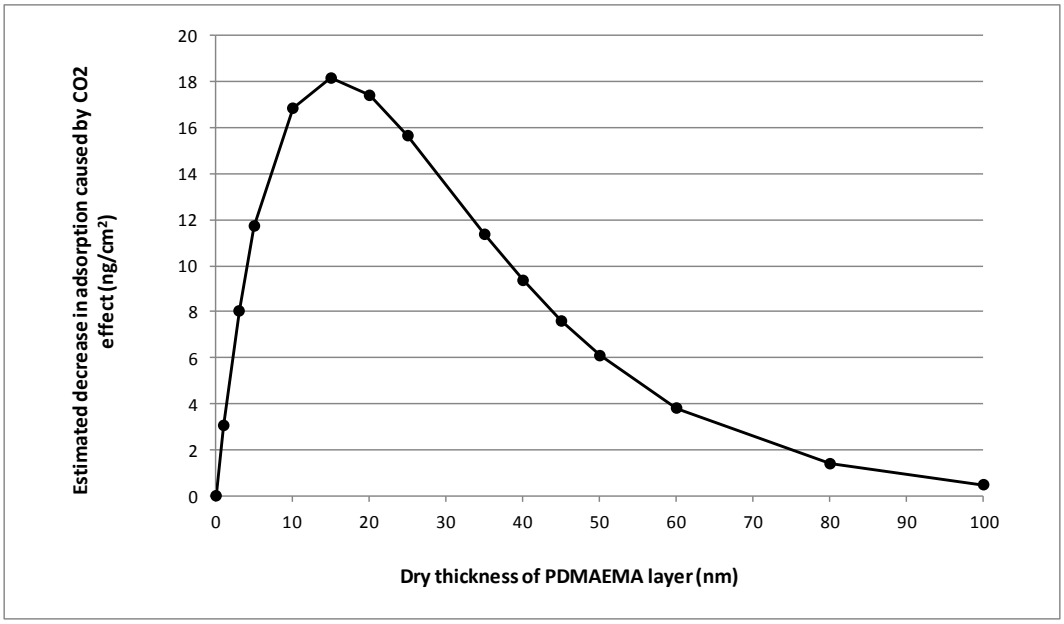

Figure 4. 14. Simulations of desorption induced by CO_2. a) Experimental data and regression fit for albumin adsorption on PDMAEMA surface with increasing swollen thickness (data fitted to exponential decay), b) estimated thickness under CO_2 conditions (green, triangle), experimental thickness in swollen state at pH 7 (blue, diamond) and dry state (red, square), c) estimated albumin adsorption on PDMAEMA surface (under CO_2 (green, triangle)) with increasing thickness versus PDMAEMA surface without CO_2 (blue, diamond), d) estimated desorption caused by chain extension from CO_2 effect.

According to this model, desorption caused by CO_2 would increase first, then pass through a maximum, and finally decrease as the polymer thickness increases. At high thickness, desorption becomes close to zero. The simulation predicts that the maximum desorption occurs between 10 nm and 20 nm dry polymer thickness.

Based on the above analysis, the intermediate values of PDMAEMA thickness are expected to give surfaces that are most responsive to CO_2 cleaning. Accordingly, the surfaces of dry thickness 15 nm and 20 nm were chosen for experiment. However, this model only considered chain extension caused by the CO_2 effect, the effect of how charges changed electrostatic interactions between PDMAEMA and protein could not be estimated. Radiolabelling data are shown in Fig 4.15 and Table 4.8. Table 4.8 gives quantities of protein (ng/cm^2) desorbed after 30 min exposure to either buffer or CO_2-bubbled buffer. These data may give some indications of how electrostatic interactions changed by CO_2 would affect protein desorption.

For the unmodified silicon surface, desorption was minimal. The CO_2 treated surface showed greater desorption than the "control" (adsorbed surface incubated 30 min in starting buffer, no CO_2) but with bigger error bars possibly due to physical forces caused by the gas bubbling. In the case of the PDMAEMA-modified surfaces, different extents of desorption were observed. The surfaces of 20 nm thickness lost almost 20 ng/cm^2 of the protein after CO_2 treatment (decrease of 26.3%), while those of 15 nm thickness lost 14 ng/cm^2 (decrease of 10.3%).

The differences between experimental and simulated data for the dry thicknesses of 15 nm and 20 nm were 20% and 11%, respectively. Based on the experimental data, more protein desorbed from surfaces of 20 nm thickness than from 15 nm. A possible reason for the difference

could be that the actual chain extension volume is different from the simulated volume. Also desorption should be influenced by changes in electrostatic interactions. As CO_2 is bubbled into the system, the solution pH changes from 7 to 5, close to the pI of albumin (~4.7), causing a change in net charge from -7.5 per molecule to zero. However, the polymer surface is more positively charged; this will inevitably affect the surface-protein interactions.

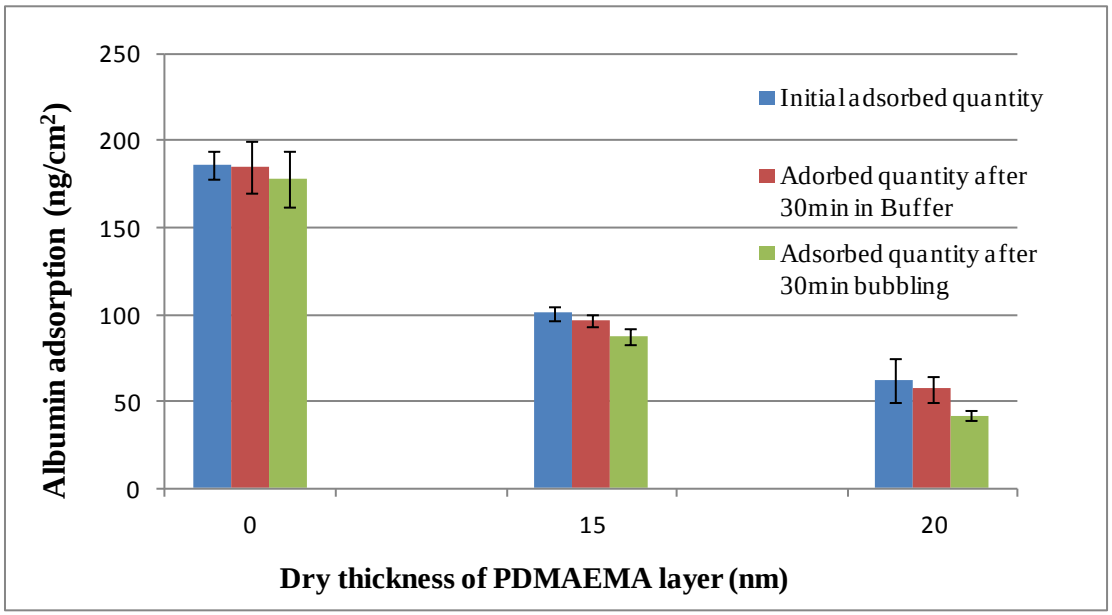

Figure 4. 15. Albumin adsorption to and desorption from PDMAEMA surfaces in response to CO_2: effect of graft layer thickness. Blue, adsorption after 2 h exposure to 1 mg/mL albumin in buffer, pH 7.4; Red, adsorption after additional 0.5 h treatment in protein-free buffer; Green, adsorption after additional 0.5 h treatment in CO_2-bubbled water. Data are mean ±SD, n=6.

In summary, the desorption of albumin from PDMAEMA-modified surface caused by CO_2 is not as significant as expected. The small CO_2 effect is possibly due to the low internal stability of albumin leading to a conformational change as the pH changes. Therefore, it may be less affected by electrostatic interactions because it can alter its conformation to adapt to the

changing environment. It was reported that "soft" proteins (albumin, IgG, hemoglobin, etc) adsorb even on an electrostatically repelling surface, while the adsorption of "hard" proteins (α-chymotrypsin, ribonuclease, lysozyme, etc) reaches a "valley" due to electrostatic repulsion [1]. It is difficult to draw definitive conclusions on the effect of layer thickness from these data based on only two thicknesses. Clearly, additional experiments will be required for a more complete understanding.

Table 4. 8. Albumin desorption by buffer and CO_2 treatment. Data are mean ±SD, n=6

	Decrease of Adsorption (ng/cm^2)		
	Buffer	CO_2	
		Experimental	Simulated
Unmodified Surface	1 ± 3	8 ± 5	0
PDMAEMA Surface (15 nm)	4 ±1	14 ± 2	18.1
PDMAEMA Surface (20 nm)	5 ± 7	20 ± 5	17.4

4.3.2 CO_2 induced desorption of proteins adsorbed from plasma assessed by Western blotting of eluates

Although the CO_2 effect on albumin desorption appeared not to be very significant on PDMAEMA- modified surface as indicated above, it was of interest to investigate the CO_2 effect for other proteins. Based on the results in Section 4.2.2, albumin, complement C3, vitronectin and prothrombin were chosen as proteins to be investigated for CO_2 desorption after exposure of

surfaces to plasma. As stated previously blotting gives only qualitative indications of adsorption and desorption.

The effect of CO_2 on protein desorption is expected to be two-fold, stemming both from effects on the polymer and effects on the protein. The decrease in pH caused by CO_2 will affect the surface hydrophilicity and chain conformation. At pH higher than pI, proteins have a net negative charge and at pH lower than pI they are net positive. Therefore for a given protein interactions with a charged surface such as grafted PDMAEMA will depend on pI relative to the pH. The molecular weights of bands on reduced gels and the isoelectric points of the four proteins used in these experiments are listed in Table 4.9.

Table 4. 9. Isoelectric point and molecular weights (kDa) of gel bands for albumin, complement C3, prothrombin and vitronectin.

	Albumin	**C3**	**prothrombin**	**vitronectin**
pI	4.7	6.3	4.2	4.8
Normal MW bands on Western Blots	67	110, 75	68	75, 65

Experiments on the CO_2 desorption effect after plasma exposure were carried out using the PDMAEMA-modified surface of dry thickness of 20 nm, and unmodified silicon. All samples were exposed to plasma for 2 h, and divided into 2 groups: (1) treatment with buffer for 30 min (control group); (2) CO_2 bubbling into buffer for 30 min (test group). Each group consisted of 6 unmodified silicon surfaces and 6 PDMAEMA modified surfaces. After treatment, proteins adsorbed on the surfaces were eluted by SDS, separated by gel electrophoresis and identified by immunoblotting. The loading volume for each lane in the gels was 100 μL

compared to 30 µL/lane for the data shown in Fig. 4.13. The blots are shown in Fig.4.16, and the normalized intensities of the bands in the blots are listed in Table 4.10.

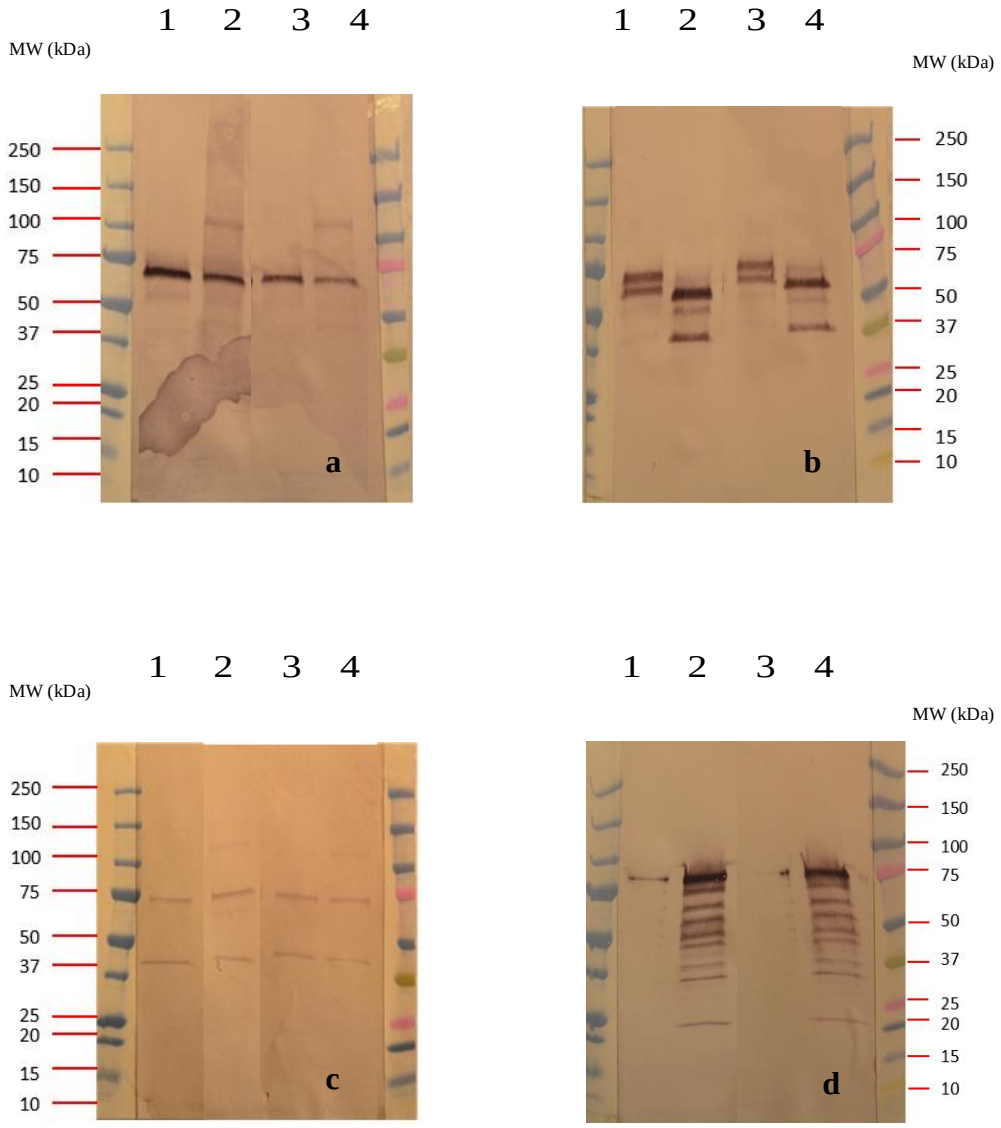

Figure 4. 16. Western blots of four proteins eluted from surfaces after 2 h contact with plasma. Panel (a) albumin, (b) vitronectin, (c) complement C3, (d) prothrombin. Lanes 1 to 2 lanes are SDS eluates from control group; lanes 3 and 4 show SDS eluates from CO_2 test group.

The SDS eluates from the control group on each surface (lanes 1 and 2, reflecting adsorption) were consistent with those seen in Fig 4.13. In the test group, CO_2-induced desorption of albumin was observed on both unmodified silicon surface and PDMAEMA-modified surface, PDMAEMA surface exhibiting greater desorption by percentage. CO_2-induced desorption of vitronectin and complement C3 from the unmodified silicon surface was minimal (lanes 3), while desorption from the PDMAEMA-modified surface (lanes 4) was significant. The prothrombin bands appeared to be "saturated" so that the values before and after CO_2 treatment did not show any difference. However, the blots in Fig.4.13 (d) clearly showed an obvious reduction in intensity after CO_2 treatment of the PDMAEMA surface showing that some CO_2-induced desorption of prothrombin occurred as well. In addition, multiple bands are seen for prothrombin in Fig 4.14 which were not seen in Fig 4.13, possibly due to overloading of the gel in the former.

Table 4. 10. Normalized band intensities in blots of eluates after plasma exposure.

Surface	**Unmodified Si**	**PDMAEMA modified Si**	**Unmodified Si**	**PDMAEMA modified Si**
CO_2 treatment	-	-	+	+
Albumin	1 (9.2×10^7) *	0.24	0.67	0.12
Vitronectin	1 (1.3×10^8)	2.12	0.99	1.51
C3	1 (1.3×10^7)	1.26	0.9	0.85
Prothrombin	——	1 (1.6×10^8)	——	0.99♦

* Numbers in bracket are the measured band intensities (arbitrary units).

♦ Intensity of prothrombin adsorption on PDMAEMA modified surface after CO_2 treatment is over the linear range.

The reason of why the desorption behavior of vitronectin, complement C3 and prothrombin is so different from that of albumin remains unknown. All four proteins can be considered as "big" with the molecular weights of vitronectin, complement C3, and prothrombin are higher than that of albumin. Prothrombin and vitronectin have isoelectric points similar to albumin. The pI of complement C3 is the highest; it is the only protein the four that would change its net charge from negative to positive after CO_2 treatment. Overall, the internal stability of the adsorbed protein molecules might be responsible for their response to CO_2. Information on how charge/pH affects the structures of vitronectin, complement C3 and prothrombin would be required to test this hypothesis.

4.3.3 Conclusions

Based on the results from the radiolabelling and Western blotting experiments, it is concluded that CO_2 did cause protein desorption from the PDMAEMA surfaces. The effect was different for the different proteins. It was minimal for albumin. For vitronectin, C3 and prothrombin, the CO_2 cleaning effect appeared to be significant. The minimal desorption of albumin may be due to its "soft" character which allows easy conformational change and greater binding affinity, possibly through multiple contacts. But information of this "soft"/ "hard" character of vitronectin, C3 and prothrombin is lacking. Thus, it is difficult to draw any definitive conclusion regarding the CO_2 cleaning effect on the PDMAEMA surfaces based on the results obtained so far. Further investigation of the interactions between proteins, between proteins and surfaces will be necessary. In addition, changes in surface properties and protein structures induced by CO_2 should be investigated further.

CHAPTER FIVE

SUMMARY & RECOMMENDATIONS FOR FUTURE WORK

5.1 Summary

The objectives of this research were to study the ability of PDMAEMA-modified surfaces to resist protein fouling and to evaluate the potential of CO_2 treatment to remove adsorbed protein from these surfaces. PDMAEMA grafts were formed on silicon substrate via surface-initiated atom transfer radical polymerization (SI-ATRP). SI-ATRP was employed in order to obtain high-graft-density surfaces with grafted chains of uniform length. The initiator, 6-(2-bromo-2-methyl) propionyloxy hexenyl trichlorosilane, was synthesized by bromination of hexen-1-ol, followed by reaction with trichlorosilane. The initiator structure was confirmed by NMR. The initiator was covalently self-assembled onto silicon surface by silylation. The attachment of initiator was confirmed by XPS and water contact angle measurements. The Advancing contact angle on silicon surface increased from <10 ° to about 90 °, and bromine was detected on the initiator-anchored surface. DMAEMA was graft polymerized from the initiator-immobilized surface in THF as solvent at room temperature. The chain length of the grafted polymer was varied by varying the polymerization time. XPS spectra of the grafted surfaces showed the presence of nitrogen, and the ratio of nitrogen to carbon corresponded to that of the expected polymer structure. Water contact angle measurements indicated increased to be more hydrophilicity after polymer grafting. Measurements of the grafted layer thickness were carried

out using ellipsometry in the dry state and AFM for both the dry and hydrated states. The hydrated thickness was found to be a factor of 1.75 greater than that of the dry state.

Protein adsorption and desorption were investigated using radiolabelling (albumin in buffer) and Western-blotting (proteins eluted after plasma contact) methods. The adsorption of human serum albumin from buffer to the PDMAEMA surfaces decreased with increasing PDMAEMA layer thickness, and levelled off at a thickness of 40 nm. Adsorption on these surfaces was reduced by ~90% compared to the unmodified silicon surface. This decrease was presumably due to the transition from hydrophobic to hydrophilic, and more specifically to the water barrier created by abundant and tightly bound water molecules on the surface. The adsorption of albumin on PDMAEMA-modified surfaces from plasma at various plasma concentrations (plasma diluted serially with buffer), was compared to that on unmodified silicon, unmodified polyurethane (PU) and PEO-modified PU. The PDMAEMA surface was the most albumin-resistant of the four. Western blots of proteins eluted from these four surfaces after contact with undiluted plasma, showed that the PDMAEMA surface was much more resistant to albumin than the other surfaces. However, the blots also showed that this surface adsorbed significant quantities of vitronectin and prothrombin from. The interactions of these proteins with the charged PDMAEMA surface appeared to lead to degradation.

The CO_2 cleaning effect was studied on surface that had been exposed to albumin in buffer and plasma, respectively. Based on research by Sanjuan [140] and Zhao [138], CO_2-induced desorption was expected to be correlated to polymer layer thickness; these workers found that as the thickness increased from 0 to 40 nm desorption increased, passed through a maximum and then decreased. The experimental data obtained in the present work using surfaces with layers of thickness 15 nm and 20 nm showed that layers of 20 nm thickness lost 30%

adsorbed albumin after 30 min CO_2 treatment, while 15 nm thick layers lost only 8%. Western blots for albumin, C3, vitronectin and prothrombin in the eluates from plasma-exposed surfaces showed that these proteins were desorbed from the PDMAEMA-modified surfaces by CO_2 treatment. The extent of desorption was highest for vitronectin.

5.2 Recommendations for Future Work

5.2.1 Mechanism of the interactions of PDMAEMA-modified surface with vitronectin and prothrombin

PDMAEMA has been considered to be a biocompatible material due to its ability to resist fouling by proteins. However, the results of this research show that while the adsorption of most of the plasma proteins investigated was low, the adsorption of vitronectin and prothrombin from plasma was significant on the PDMAEMA-modified surface. The adsorbed quantity of vitronectin appeared to be higher than on the unmodified silicon and it was degraded on contact with the PDMAEMA surface. Bale et al. reported that vitronectin desorbed from carboxylic acid-containing polymer surfaces after plasma contact was degraded and a fragment of molecular weight 48 kDa was identified [156].

It is clearly of great interest to obtain additional information on vitronectin interactions with the PDMAEMA surfaces. To this end the following is suggested:

(1) Investigate structural changes in vitronectin after surface contact. Since it seems likely that the interactions are charge related, knowledge of the distribution of charges on the

protein surface before and after adsorption may be helpful. Electrophoretic mobility measurement may also be helpful.

(2) Investigate the possibility that proteolysis is due to the activation of clotting in the plasma contact experiments. Thrombin generation and the clotting times of plasma in contact with the surfaces should be measured.

(3) Useful information may be generated studying the interactions of vitronectin with free PDMAEMA in solution.

Similar studies are recommended to elucidate the interactions of prothrombin with the PDMAEMA surfaces. In this case activation of clotting could convert prothrombin to thrombin. Measurement of thrombin generation may be a useful measurement to investigate this possibility.

5.2.2 Protein adsorption from whole blood

Protein adsorption studies in whole blood are recommended to investigate the protein resistance of PDMAEMA-modified surfaces under more biomedically relevant conditions. Such studies would constitute a much more severe test of the ability of these materials to resist protein fouling. Cell adhesion from whole blood should also be studied in this connection, with the expectation that adhesion would be reduced compared to controls.

5.2.3 Adsorption of lysozyme on PDMAEMA surfaces

Given that electrostatic interactions are expected to be important, investigation of the adsorption of lysozyme (and other "positive" proteins) on the PDMAEMA surfaces may be of interest. The isoelectric point of lysozyme is ~11; therefore charge effects in its interactions with PDMAEMA-modified surfaces might be quite different than for albumin and other plasma proteins with pIs < 7.4. Moreover as a small (13 kDa), hard protein its shape is not expected to change with pH. Thus it may show a greater elution response than more acidic proteins on treatment with CO_2.

REFERENCES

[1] K. Nakanishi, T. Sakiyama, and K. Imamura, "On the adsorption of proteins on solid surfaces, a common but very complicated phenomenon.," *J. Biosci. Bioeng.*, vol. 91, no. 3, pp. 233–44, Jan. 2001.

[2] J. D. Andrade, V. Hlady, A. Wei, C. Ho, A. S. Lea, S. I. Jean, and E. Strou, "Proteins at Interfaces : Principles , Multivari Aspects , Protein Resistant Surfaces , and Direct Imaging and Manipulation of Adsorbed Proteins," *Clin. Mater.*, vol. 11, pp. 67–84, 1992.

[3] J. L. Brash, "Behavior of proteins at interfaces," *Curr. Opin. Colloid Interface Sci.*, vol. 1, no. 5, pp. 682–688, Oct. 1996.

[4] J. M. Anderson, "Biological Responses to Materials," *Annu. Rev. Mater. Res*, vol. 31, pp. 81–110, 2001.

[5] B. D. Ratner and S. J. Bryant, "Biomaterials: where we have been and where we are going.," *Annu. Rev. Biomed. Eng.*, vol. 6, no. 1, pp. 41–75, Jan. 2004.

[6] J. M. Courtney, N. M. Lamba, S. Sundaram, and C. D. Forbes, "Biomaterials for blood-contacting applications.," *Biomaterials*, vol. 15, no. 10, pp. 737–44, Aug. 1994.

[7] Y. Efimova, *Proteins at surfaces*. Amsterdam: Press, an imprint of Delft University Press, 2006.

[8] B. D. Ratner, "New ideas in biomaterials science - a path to engineered biomaterials," *J. Biomed. Mater. Res.*, vol. 27, pp. 837–850, 1993.

[9] L. Pauling, R. Corey, and H. Branson, "The structure of proteins; two hydrogen-bonded helical configurations of the polypeptide chain," *Proc Natl Acad Sci USA*, vol. 37, no. 4, pp. 205–211, 1951.

[10] E. Buxbaum, *Fundamentals of Protein Structure and Function*. Boston, MA: Springer US, 2007.

[11] J. Brash and T. Horbett, *Proteins at Interfaces: Physicochemical and Biochemical Studies*. Washington DC: American Chemical Society, 1987.

[12] J. Israelachvili, *Intermolecular and surface forces*, 3rd ed. Burlington, MA: Academic Press, 2011.

[13] F. Fang, J. Satulovsky, and I. Szleifer, “Kinetics of protein adsorption and desorption on surfaces with grafted polymers.,” *Biophys. J.*, vol. 89, no. 3, pp. 1516–1533, Sep. 2005.

[14] W. Norde and J. Lyklema, “Thermodynamics of Protein Adsorption,” *J. Colloid Interface Sci.*, vol. 71, no. 2, pp. 350–366, 1979.

[15] J. J. Ramsden, “From Kinetics to Structure: High Resolution Molecular Microscopy,” in *Proteins at Solid-Liquid Interfaces*, P. Déjardin, Ed. Berlin: Springer Berlin Heidelberg, 2006, pp. 20–49.

[16] W. Norde and J. Lyklema, “Why proteins prefer interfaces.,” *J. Biomater. Sci. Polym. Ed.*, vol. 2, no. 3, pp. 183–202, Jan. 1991.

[17] W. Norde, *Biopolymers at interfaces*, 2nd ed. New York : Marcel Dekker, 2003.

[18] B. R. Young, W. G. Pitt, and S. L. Cooper, “Protein Adsorption on Polymeric Biomaterials. I. Adsorption Isotherms,” *J. Colloid*, vol. 124, no. 1, pp. 28–43, 1988.

[19] I. Lundström, “Models of protein adsorption on solid surfaces,” *Prog. Colloid Polym. Sci.*, vol. 70, pp. 76–82, 1985.

[20] T. a. Horbett, “Chapter 13 Principles underlying the role of adsorbed plasma proteins in blood interactions with foreign materials,” *Cardiovasc. Pathol.*, vol. 2, no. 3, pp. 137–148, Jul. 1993.

[21] S. L. Hirsh, D. R. McKenzie, N. J. Nosworthy, J. a Denman, O. U. Sezerman, and M. M. M. Bilek, “The Vroman effect: competitive protein exchange with dynamic multilayer protein aggregates.,” *Colloids Surf. B. Biointerfaces*, vol. 103, pp. 395–404, Mar. 2013.

[22] L. Vroman, A. L. Adams, G. Fischer, and P. Munoz, “Interaction of High Molecular Weight Kininogen, Factor XII, and Fibrinogen in Plasma at Interfaces,” *Blood*, vol. 55, no. 1, pp. 156–159, 1980.

[23] C. Bamford, L. Cooper, and T. Tsurutta, *The Vroman Effect*. Midsomer Norton: Bookcraft (Bath) Ltd., 1992.

[24] M. C. Corti, J. M. Guralnik, M. E. Salive, and J. D. Sorkin, “Serum albumin level and physical disability as predictors of mortality in older persons.,” *JAMA*, vol. 272, no. 13, pp. 1036–42, Oct. 1994.

[25] X. He and D. Carter, “Atomic Structure and Chemistry of Human Serum Albumin,” *Nature*, vol. 358, pp. 209–215, 1992.

[26] T. Peters Jr., *All about Albumin: Biochemistry, Genetics, and Medical Application*. San Diego, CA: Academic Press, 1995.

[27] P. G. Squire, P. Moser, and C. Konski, “The Hydrodynamic Properties of Bovine Serum Albumin Monomer and Dimer,” *Biochemistry*, vol. 7, no. 12, pp. 4261–4272, 1968.

[28] S. Sugio, a Kashima, S. Mochizuki, M. Noda, and K. Kobayashi, “Crystal structure of human serum albumin at 2.5 A resolution.,” *Protein Eng.*, vol. 12, no. 6, pp. 439–46, Jun. 1999.

[29] L. Longsworth and C. Jacobsen, “An Electrophoretic Study of the Binding of Salt Ions by β-Lactoglobulin and Bovine Serum Albumin,” *J. Phys. Chem. B*, vol. 53, no. 1, pp. 126–134, 1949.

[30] G. Fanali, A. di Masi, V. Trezza, M. Marino, M. Fasano, and P. Ascenzi, “Human serum albumin: from bench to bedside.,” *Mol. Aspects Med.*, vol. 33, no. 3, pp. 209–90, Jun. 2012.

[31] F. Putnam, *The plasma proteins: structure, function, and genetic control*. New York, NY: Academic Press, 1975.

[32] a Sahu and J. D. Lambris, “Structure and biology of complement protein C3, a connecting link between innate and acquired immunity.,” *Immunol. Rev.*, vol. 180, no. 4, pp. 35–48, Apr. 2001.

[33] S. K. Law and a W. Dodds, “The internal thioester and the covalent binding properties of the complement proteins C3 and C4.,” *Protein Sci.*, vol. 6, no. 2, pp. 263–74, Feb. 1997.

[34] D. Male, *Immunology*, 8th ed. Philadephia, PA: Elsevier, 2013.

[35] D. W. Barnes and J. Silnutzer, “Isolation of human serum spreading factor.,” *J. Biol. Chem.*, vol. 258, no. 20, pp. 12548–52, Oct. 1983.

[36] E. G. Hayman, M. D. Pierschbacher, Y. Ohgren, and E. Ruoslahti, “Serum spreading factor (vitronectin) is present at the cell surface and in tissues.,” *Proc. Natl. Acad. Sci. U. S. A.*, vol. 80, no. 13, pp. 4003–7, Jul. 1983.

[37] I. Schvartz, D. Seger, and S. Shaltiel, “Vitronectin.,” *Int. J. Biochem. Cell Biol.*, vol. 31, no. 5, pp. 539–44, May 1999.

[38] S. Suzukis, M. D. Pierschbacherq, G. Hayman, K. Nguyen, and Y. Ohgren, “Domain Structure of Vitronectin,” *J. Biol. Chem.*, vol. 259, no. 24, pp. 15307–15314, 1984.

[39] D. a Waltz, L. R. Natkin, R. M. Fujita, Y. Wei, and H. a Chapman, “Plasmin and plasminogen activator inhibitor type 1 promote cellular motility by regulating the interaction between the urokinase receptor and vitronectin.,” *J. Clin. Invest.*, vol. 100, no. 1, pp. 58–67, Jul. 1997.

[40] C. Kost, W. Stüber, H. J. Ehrlich, H. Pannekoek, and K. T. Preissner, “Mapping of binding sites for heparin, plasminogen activator inhibitor-1, and plasminogen to vitronectin’s heparin-binding region reveals a novel vitronectin-dependent feedback mechanism for the control of plasmin formation.,” *J. Biol. Chem.*, vol. 267, no. 17, pp. 12098–105, Jun. 1992.

[41] D. Seger, Z. Gechtman, and S. Shaltiel, “Phosphorylation of Vitronectin by Casein Kinase II: Identification of the sites and their promotion of cell adhesion and spreading,” *J. Biol. Chem.*, vol. 273, no. 38, pp. 24805–24813, Sep. 1998.

[42] K. T. Preissner, “Structure and biological role of vitronectin,” *Annu. Rev. Cell Dev. Biol.*, vol. 7, pp. 275–310, 1991.

[43] W. Seegers, R. McClaughry, and J. Fahey, “Some properties of purified prothrombin and its activation with sodium citrate,” *Blood*, vol. 5, no. 5, pp. 421–433, 1950.

[44] W. Seegers, *Prothrombin*. Cambridge, Mass: Harvard University Press, 1962.

[45] P. Roach, D. Eglin, K. Rohde, and C. C. Perry, “Modern biomaterials: a review - bulk properties and implications of surface modifications.,” *J. Mater. Sci. Mater. Med.*, vol. 18, no. 7, pp. 1263–77, Jul. 2007.

[46] Y. Ikada, “Surface modification of polymers for medical applications.,” *Biomaterials*, vol. 15, no. 10, pp. 725–36, Aug. 1994.

[47] K. Dee, D. Puleo, and R. Bizios, “Protein–surface interactions,” in *An introduction to tissue-biomaterial interactions*, K. Dee, D. Puleo, and R. Bizios, Eds. Hoboken, NJ: John Wiley and Sons, 2002.

[48] S. Pasche, J. Voros, H. J. Griesser, N. D. Spencer, and M. Textor, “Effects of Ionic Strength and Surface Charge on Protein Adsorption at PEGylated Surfaces,” *J. Phys. Chem. B*, vol. 109, pp. 17545–17552, 2005.

[49] Y. Tran, P. Auroy, L.-T. Lee, and M. Stamm, “Polyelectrolyte brushes: Counterion distribution and complexation properties,” *Phys. Rev. E*, vol. 60, no. 6, pp. 6984–6990, Dec. 1999.

[50] a. Wittemann, B. Haupt, and M. Ballauff, “Adsorption of proteins on spherical polyelectrolyte brushes in aqueous solution,” *Phys. Chem. Chem. Phys.*, vol. 5, no. 8, pp. 1671–1677, Mar. 2003.

[51] D. R. Schmidt, H. Waldeck, and W. J. Kao, “Protein Adsorption to Biomaterials,” in *Biological Interactions on Materials Surfaces*, D. Puleo and R. Bizios, Eds. Springer US, 2009, pp. 1–18.

[52] M. Malrnsten, “Ellipsometry studies of the effects of surface hydrophobicity on protein adsorption,” *Colloids Surfaces B Biointerfaces*, vol. 3, pp. 197–308, 1995.

[53] S. Lan, M. Veiseh, and M. Zhang, “Surface modification of silicon and gold-patterned silicon surfaces for improved biocompatibility and cell patterning selectivity.,” *Biosens. Bioelectron.*, vol. 20, no. 9, pp. 1697–708, Mar. 2005.

[54] Q. Yu, Y. Zhang, H. Wang, J. Brash, and H. Chen, “Anti-fouling bioactive surfaces.,” *Acta Biomater.*, vol. 7, no. 4, pp. 1550–7, Apr. 2011.

[55] A. J. García, “Surface Modification of Biomaterials,” in *Foundations of Regenerative Medicine: Clinical and Therapeutic Applications*, 1st ed., A. Atala, R. Lanza, J. Thomson, and R. Nerem, Eds. San Diego, CA: Academic Press, 2010, pp. 368–377.

[56] I. Banerjee, R. C. Pangule, and R. S. Kane, “Antifouling coatings: recent developments in the design of surfaces that prevent fouling by proteins, bacteria, and marine organisms.,” *Adv. Mater.*, vol. 23, no. 6, pp. 690–718, Feb. 2011.

[57] S. Krishnan, C. J. Weinman, and C. K. Ober, “Advances in polymers for anti-biofouling surfaces,” *J. Mater. Chem.*, vol. 18, no. 29, p. 3405, 2008.

[58] A. Kumar, A. Srivastava, I. Y. Galaev, and B. Mattiasson, “Smart polymers: Physical forms and bioengineering applications,” *Prog. Polym. Sci.*, vol. 32, no. 10, pp. 1205–1237, Oct. 2007.

[59] W. Senaratne, L. Andruzzi, and C. K. Ober, “Self-assembled monolayers and polymer brushes in biotechnology: current applications and future perspectives.,” *Biomacromolecules*, vol. 6, no. 5, pp. 2427–48, 2005.

[60] S. W. Lee and P. E. Laibinis, “Protein-resistant coatings for glass and metal oxide surfaces derived from oligo(ethylene glycol)-terminated alkytrichlorosilanes.,” *Biomaterials*, vol. 19, no. 18, pp. 1669–75, Sep. 1998.

[61] S. Jo and K. Park, “Surface modification using silanated poly (ethylene glycol) s,” *Biomaterials*, vol. 21, pp. 605–616, 2000.

[62] J. H. Lee, J. Kopecek, and J. D. Andrade, “Protein-resistant surfaces prepared by PEO-containing block copolymer surfactants.,” *J. Biomed. Mater. Res.*, vol. 23, no. 3, pp. 351–68, Mar. 1989.

[63] K. M. Hansson, S. Tosatti, J. Isaksson, J. Wetterö, M. Textor, T. L. Lindahl, and P. Tengvall, “Whole blood coagulation on protein adsorption-resistant PEG and peptide functionalised PEG-coated titanium surfaces.,” *Biomaterials*, vol. 26, no. 8, pp. 861–72, Mar. 2005.

[64] J. Blümmel, N. Perschmann, D. Aydin, J. Drinjakovic, T. Surrey, M. Lopez-Garcia, H. Kessler, and J. P. Spatz, "Protein repellent properties of covalently attached PEG coatings on nanostructured SiO(2)-based interfaces.," *Biomaterials*, vol. 28, no. 32, pp. 4739–47, Nov. 2007.

[65] C. Yoshikawa, A. Goto, Y. Tsujii, T. Fukuda, T. Kimura, K. Yamamoto, and A. Kishida, "Protein Repellency of Well-Defined, Concentrated Poly(2-hydroxyethyl methacrylate) Brushes by the Size-Exclusion Effect," *Macromolecules*, vol. 39, no. 6, pp. 2284–2290, Mar. 2006.

[66] E. Hirota, K. Ute, M. Uehara, T. Kitayama, M. Tanaka, and A. Mochizuki, "Study on blood compatibility with poly(2-methoxyethylacrylate)--relationship between surface structure, water structure, and platelet compatibility in 2-methoxyethylacrylate/2-hydroxyethylmethacrylate diblock copolymer.," *J. Biomed. Mater. Res. A*, vol. 76, no. 3, pp. 540–50, Mar. 2006.

[67] M. Tanaka, T. Motomura, M. Kawada, T. Anzai, Y. Kasori, T. Shiroya, K. Shimura, M. Onishi, and a Mochizuki, "Blood compatible aspects of poly(2-methoxyethylacrylate) (PMEA)--relationship between protein adsorption and platelet adhesion on PMEA surface.," *Biomaterials*, vol. 21, no. 14, pp. 1471–81, Jul. 2000.

[68] S. Gunaydin, B. Farsak, M. Kocakulak, and T. Sari, "Clinical Performance and Biocompatibility of Poly (2-Methoxyethylacrylate)– Coated Extracorporeal Circuits," *Ann. Thorac. Surg.*, vol. 74, pp. 819–824, 2002.

[69] S. Robinson and P. A. Williams, "Inhibition of Protein Adsorption onto Silica by Polyvinylpyrrolidone," *Langmuir*, vol. 18, pp. 8743–8748, 2002.

[70] Z. Wu, H. Chen, X. Liu, Y. Zhang, D. Li, and H. Huang, "Protein adsorption on poly(N-vinylpyrrolidone)-modified silicon surfaces prepared by surface-initiated atom transfer radical polymerization.," *Langmuir*, vol. 25, no. 5, pp. 2900–6, Mar. 2009.

[71] W. Feng, S. Zhu, K. Ishihara, and J. L. Brash, "Adsorption of fibrinogen and lysozyme on silicon grafted with poly(2-methacryloyloxyethyl phosphorylcholine) via surface-initiated atom transfer radical polymerization.," *Langmuir*, vol. 21, no. 13, pp. 5980–7, Jun. 2005.

[72] Y. Iwasaki and K. Ishihara, "Phosphorylcholine-containing polymers for biomedical applications.," *Anal. Bioanal. Chem.*, vol. 381, no. 3, pp. 534–46, Feb. 2005.

[73] J. Ladd, Z. Zhang, S. Chen, J. C. Hower, and S. Jiang, "Zwitterionic polymers exhibiting high resistance to nonspecific protein adsorption from human serum and plasma.," *Biomacromolecules*, vol. 9, no. 5, pp. 1357–61, May 2008.

[74] B. Zhao and W. J. Brittain, "Polymer brushes : surface-immobilized macromolecules," *Prog. Polym. Sci.*, vol. 25, pp. 677–710, 2000.

[75] S. G. Boyes, A. M. Granville, M. Baum, B. Akgun, B. K. Mirous, and W. J. Brittain, "Polymer brushes—surface immobilized polymers," *Surf. Sci.*, vol. 570, no. 1–2, pp. 1–12, Oct. 2004.

[76] Y. Tsujii, K. Ohno, S. Yamamoto, and A. Goto, "Structure and Properties of High-Density Polymer Brushes Prepared by Surface-Initiated Living Radical Polymerization," in *Surface-Initiated Polymerization I*, no. January, R. Jordan, Ed. Berlin: Springer Berlin Heidelberg, 2006, pp. 1–45.

[77] R. Bhat, M. Tomlinson, T. Wu, and J. Genzer, "Surface-Grafted Polymer Gradients: Formation, Characterization, and Applications," in *Surface-Initiated Polymerization II*, vol. 198, R. Jordan, Ed. Belin: Springer Berlin Heidelberg, 2006, pp. 51–124.

[78] G. Storm, S. Belliot, T. Daemenb, and D. D. Lasic, "Surface modification of nanoparticles to oppose uptake by the mononuclear phagocyte system," *Adv. Drug Deliv. Rev.*, vol. 17, no. 1, pp. 31–48, 1995.

[79] W. a. Braunecker and K. Matyjaszewski, "Controlled/living radical polymerization: Features, developments, and perspectives," *Prog. Polym. Sci.*, vol. 32, no. 1, pp. 93–146, Jan. 2007.

[80] K. Matyjaszewski and J. Spanswick, "Controlled / living radical polymerization," *Mater. Today*, pp. 26–33, 2005.

[81] J. Chiefari, Y. K. B. Chong, F. Ercole, J. Krstina, J. Jeffery, T. P. T. Le, R. T. A. Mayadunne, G. F. Meijs, C. L. Moad, G. Moad, E. Rizzardo, S. H. Thang, and C. South, "Living Free-Radical Polymerization by Reversible Addition - Fragmentation Chain Transfer : The RAFT Process," *Macromolecules*, vol. 31, pp. 5559–5562, 1998.

[82] M. Destarac, D. Charmot, X. Franck, S. Z. Zard, R. Recherches, H. Coq, and A. Cedex, "Dithiocarbamates as universal reversible addition- fragmentation chain transfer agents," *Macromol. Rapid Commun.*, vol. 21, pp. 1035–1039, 2000.

[83] M. Ejaz, S. Yamamoto, K. Ohno, Y. Tsujii, and T. Fukuda, "Controlled Graft Polymerization of Methyl Methacrylate on Silicon Substrate by the Combined Use of the Langmuir-Blodgett and Atom Transfer Radical Polymerization Techniques," *Macromolecules*, vol. 31, pp. 5934–5936, 1998.

[84] M. Husseman, E. E. Malmstro, M. Mcnamara, M. Mate, D. Mecerreyes, D. G. Benoit, J. L. Hedrick, P. Mansky, E. Huang, T. P. Russell, and C. J. Hawker, "Controlled Synthesis of Polymer Brushes by ' Living ' Free Radical Polymerization Techniques," *Macromolecules*, vol. 32, pp. 1424–1431, 1999.

[85] K. Matyjaszewski, P. J. Miller, N. Shukla, B. Immaraporn, A. Gelman, B. B. Luokala, T. M. Siclovan, G. Kickelbick, T. Vallant, H. Hoffmann, and T. Pakula, "Polymers at Interfaces : Using Atom Transfer Radical Polymerization in the Controlled Growth of

Homopolymers and Block Copolymers from Silicon Surfaces in the Absence of Untethered Sacrificial Initiator," *Macromolecules*, vol. 32, pp. 8716–8724, 1999.

[86] W. H. Yu, E. T. Kang, K. G. Neoh, and S. Zhu, "Controlled Grafting of Well-Defined Polymers on Hydrogen-Terminated Silicon Substrates by Surface-Initiated Atom Transfer Radical Polymerization," *J. Phys. Chem. B*, vol. 107, no. 37, pp. 10198–10205, Sep. 2003.

[87] G. Zheng and H. D. H. Sto, "Grafting of Poly (alkyl (meth) acrylates) from Swellable Poly (DVB80- co -HEMA) Microspheres by Atom Transfer Radical Polymerization," *Macromolecules*, vol. 35, pp. 7612–7619, 2002.

[88] S. H. Lee, D. R. Dreyer, J. An, A. Velamakanni, R. D. Piner, S. Park, Y. Zhu, S. O. Kim, C. W. Bielawski, and R. S. Ruoff, "Polymer Brushes via Controlled, Surface-Initiated Atom Transfer Radical Polymerization (ATRP) from Graphene Oxide.," *Macromol. Rapid Commun.*, vol. 31, no. 3, pp. 281–8, Feb. 2010.

[89] J. Kim, M. L. Bruening, and G. L. Baker, "Surface-Initiated Atom Transfer Radical Polymerization on Gold at Ambient Temperature," *J. Am. Chem. Soc.*, vol. 122, pp. 7616–7617, 2000.

[90] K. Ohno, T. Morinaga, K. Koh, Y. Tsujii, and T. Fukuda, "Synthesis of Monodisperse Silica Particles Coated with Well-Defined, High-Density Polymer Brushes by Surface-Initiated Atom Transfer Radical Polymerization," *Macromolecules*, vol. 38, no. 6, pp. 2137–2142, Mar. 2005.

[91] H. Ma, J. Hyun, P. Stiller, and a. Chilkoti, "'Non-Fouling' Oligo(ethylene glycol)-Functionalized Polymer Brushes Synthesized by Surface-Initiated Atom Transfer Radical Polymerization," *Adv. Mater.*, vol. 16, no. 4, pp. 338–341, Feb. 2004.

[92] C. J. Fristrup, K. Jankova, R. Eskimergen, J. T. Bukrinsky, and S. Hvilsted, "Protein repellent hydrophilic grafts prepared by surface-initiated atom transfer radical polymerization from polypropylene," *Polym. Chem.*, vol. 3, no. 1, p. 198, 2012.

[93] H. Ma, D. Li, X. Sheng, B. Zhao, and A. Chilkoti, "Protein-resistant polymer coatings on silicon oxide by surface-initiated atom transfer radical polymerization.," *Langmuir*, vol. 22, no. 8, pp. 3751–6, Apr. 2006.

[94] Z. Jin, W. Feng, S. Zhu, H. Sheardown, and J. L. Brash, "Protein-resistant materials via surface-initiated atom transfer radical polymerization of 2-methacryloyloxyethyl phosphorylcholine.," *J. Biomater. Sci. Polym. Ed.*, vol. 21, no. 10, pp. 1331–44, Jan. 2010.

[95] D. M. Jones, A. A. Brown, W. T. S. Huck, P. Street, and C. Cb, "Surface-Initiated Polymerizations in Aqueous Media : Effect of Initiator Density," *Langmuir*, vol. 18, pp. 1265–1269, 2002.

[96] J. N. Kizhakkedathu and D. E. Brooks, “Synthesis of Poly (N , N -dimethylacrylamide) Brushes from Charged Polymeric Surfaces by Aqueous ATRP : Effect of Surface Initiator Concentration,” *Macromolecules*, vol. 36, pp. 591–598, 2003.

[97] M. Ejaz, Y. Tsujii, and T. Fukuda, “Controlled grafting of a well-defined polymer on a porous glass filter by surface-initiated atom transfer radical polymerization,” *Polymer (Guildf).*, vol. 42, pp. 6811–6815, 2001.

[98] K. Yamamoto, Y. Miwa, H. Tanaka, M. Sakaguchi, and S. Shimada, “Living radical graft polymerization of methyl methacrylate to polyethylene film with typical and reverse atom transfer radical polymerization,” *J. Polym. Sci. Part A Polym. Chem.*, vol. 40, no. 20, pp. 3350–3359, Oct. 2002.

[99] Y. Tsujii, M. Ejaz, K. Sato, A. Goto, and T. Fukuda, “Mechanism and Kinetics of RAFT-Mediated Graft Polymerization of Styrene on a Solid Surface . 1 . Experimental Evidence of Surface Radical Migration,” *Macromolecules*, vol. 34, no. 26, pp. 8872–8878, 2001.

[100] D. Zhou, X. Gao, W. Wang, and S. Zhu, “Grafting from Flat Surfaces by Addition of Deactivator,” *Macromolecules*, vol. 45, pp. 1198–1207, 2012.

[101] I. Y. Galaev and B. Mattiasson, “‘Smart’ polymers and what they could do in biotechnology and medicine,” *Trends Biotechnol.*, vol. 17, pp. 335–340, 1999.

[102] B. Jeong and A. Gutowska, “Lessons from nature: stimuli-responsive polymers and their biomedical applications.,” *Trends Biotechnol.*, vol. 20, no. 7, pp. 305–11, Jul. 2002.

[103] M. Ebara, Y. Kotsuchibashi, R. Narain, N. Idota, Y.-J. Kim, J. M. Hoffman, K. Uto, and T. Aoyagi, “Smart Surfaces,” in *Smart Biomaterials*, 1st ed., N. Ohashi, Ed. Tokyo: Springer Japan, 2014, pp. 115–188.

[104] M. Ebara et. al., “Introductory Guide to Smart Biomaterials,” in *Smart Biomaterials*, 1st ed., N. et. a. Ohashi, Ed. Tokyo: Springer Japan, 2014, pp. 1–7.

[105] D. Roy, J. N. Cambre, and B. S. Sumerlin, “Future perspectives and recent advances in stimuli-responsive materials,” *Prog. Polym. Sci.*, vol. 35, no. 1–2, pp. 278–301, Jan. 2010.

[106] S. Kumar, X. Tong, Y. L. Dory, M. Lepage, and Y. Zhao, “A CO2-switchable polymer brush for reversible capture and release of proteins.,” *Chem. Commun. (Camb).*, vol. 49, no. 1, pp. 90–2, Jan. 2013.

[107] Q. Yu, Y. Zhang, H. Chen, F. Zhou, Z. Wu, H. Huang, and J. L. Brash, “Protein adsorption and cell adhesion/detachment behavior on dual-responsive silicon surfaces modified with poly(N-isopropylacrylamide)-block-polystyrene copolymer.,” *Langmuir*, vol. 26, no. 11, pp. 8582–8, Jun. 2010.

[108] a. K. Bajpai, S. K. Shukla, S. Bhanu, and S. Kankane, "Responsive polymers in controlled drug delivery," *Prog. Polym. Sci.*, vol. 33, no. 11, pp. 1088–1118, Nov. 2008.

[109] M. Motornov, R. Sheparovych, E. Katz, and S. Minko, "Chemical gating with nanostructured responsive polymer brushes: mixed brush versus homopolymer brush.," *ACS Nano*, vol. 2, no. 1, pp. 41–52, Jan. 2008.

[110] L. a. Fielding, S. Edmondson, and S. P. Armes, "Synthesis of pH-responsive tertiary amine methacrylate polymer brushes and their response to acidic vapour," *J. Mater. Chem.*, vol. 21, no. 32, p. 11773, 2011.

[111] S. Lin and P. Theato, "CO2 -Responsive polymers.," *Macromol. Rapid Commun.*, vol. 34, no. 14, pp. 1118–33, Jul. 2013.

[112] Q. Yan and Y. Zhao, "Recent Aavances of CO2-Responsive Polymers and Their Applications," *Polym. Mater. Sci. Egineering*, vol. 30, no. 2, pp. 170–178, 2014.

[113] T. Endo, D. Nagai, T. Monma, H. Yamaguchi, and B. Ochiai, "A Novel Construction of a Reversible Fixation - Release System of Carbon Dioxide by Amidines and Their Polymers," *Macromolecules*, vol. 37, pp. 2007–2009, 2004.

[114] Q. Yan, R. Zhou, C. Fu, H. Zhang, Y. Yin, and J. Yuan, "CO2-responsive polymeric vesicles that breathe.," *Angew. Chem. Int. Ed. Engl.*, vol. 50, no. 21, pp. 4923–7, May 2011.

[115] Q. Zhang, G. Yu, W.-J. Wang, H. Yuan, B.-G. Li, and S. Zhu, "Preparation of N2/CO2 triggered reversibly coagulatable and redispersible latexes by emulsion polymerization of styrene with a reactive switchable surfactant.," *Langmuir*, vol. 28, no. 14, pp. 5940–6, Apr. 2012.

[116] Q. Yan and Y. Zhao, "CO2-stimulated diversiform deformations of polymer assemblies.," *J. Am. Chem. Soc.*, vol. 135, no. 44, pp. 16300–3, Nov. 2013.

[117] B. Yan, D. Han, O. Boissière, P. Ayotte, and Y. Zhao, "Manipulation of block copolymer vesicles using CO2: dissociation or 'breathing,'" *Soft Matter*, vol. 9, no. 6, p. 2011, 2013.

[118] D. Han, O. Boissiere, S. Kumar, X. Tong, L. Tremblay, and Y. Zhao, "Two-Way CO 2 - Switchable Triblock Copolymer Hydrogels," *Macromolecules*, vol. 45, no. 18, pp. 7440–7445, Sep. 2012.

[119] Y. Hoshino, K. Imamura, M. Yue, G. Inoue, and Y. Miura, "Reversible absorption of CO2 triggered by phase transition of amine-containing micro- and nanogel particles.," *J. Am. Chem. Soc.*, vol. 134, no. 44, pp. 18177–80, Nov. 2012.

[120] D. Nagai, A. Suzuki, Y. Maki, and H. Takeno, "Reversible chain association/dissociation via a CO2 responsive crosslinking/decrosslinking system.," *Chem. Commun. (Camb).*, vol. 47, no. 31, pp. 8856–8, Aug. 2011.

[121] H. Wang, P. G. Jessop, and G. Liu, "Support-Free Porous Polyamine Particles for CO 2 Capture," *ACS Macro Lett.*, vol. 1, pp. 944–948, 2012.

[122] S. U. N. H. Cho, M. U. S. Jhon, S. H. Yuk, and H. A. I. B. Lee, "Temperature-Induced Phase Transition of Poly (N , N- dimethylaminoethyl methacrylate-co-acrylamide)," *J. Polym. Sci. Part B Polym. Phys.*, vol. 35, no. 4, pp. 595–598, 1997.

[123] F. A. Plamper, M. Ruppel, A. Schmalz, O. Borisov, M. Ballauff, and A. H. E. Mu, "Tuning the Thermoresponsive Properties of Weak Polyelectrolytes : Aqueous Solutions of Star-Shaped and Linear Poly (N , N -dimethylaminoethyl Methacrylate)," *Macromolecules*, vol. 40, pp. 8361–8366, 2007.

[124] Z. Dong, H. Wei, J. Mao, D. Wang, M. Yang, S. Bo, and X. Ji, "Synthesis and responsive behavior of poly(N,N-dimethylaminoethylmethacrylate) brushes grafted on silica nanoparticles and their quaternized derivatives," *Polymer (Guildf).*, vol. 53, pp. 2074–2084, 2012.

[125] O. Schepelina and I. Zharov, "Poly(2-(dimethylamino)ethyl methacrylate)-modified nanoporous Colloidal films with pH and ion response.," *Langmuir*, vol. 24, no. 24, pp. 14188–94, Dec. 2008.

[126] V. Bütün, S. P. Armes, and N. Billingham, "Synthesis and aqueous solution properties of near-monodisperse tertiary amine methacrylate homopolymers and diblock copolymers," *Polymer (Guildf).*, vol. 42, pp. 5993–6008, 2001.

[127] K. Nagase, J. Kobayashi, A. Kikuchi, Y. Akiyama, H. Kanazawa, and T. Okano, "Preparation of thermoresponsive cationic copolymer brush surfaces and application of the surface to separation of biomolecules.," *Biomacromolecules*, vol. 9, no. 4, pp. 1340–7, Apr. 2008.

[128] F. Cao, Z. Luo, D. Zhou, R. Zeng, and Y. Wang, "Hydroxyethylcellulose-graft-poly(2-(dimethylamino)ethyl methacrylate) as physically adsorbed coating for protein separation by CE.," *Electrophoresis*, vol. 32, no. 10, pp. 1148–55, May 2011.

[129] S. B. Lee, R. R. Koepsel, S. W. Morley, K. Matyjaszewski, Y. Sun, and A. J. Russell, "Permanent, nonleaching antibacterial surfaces. 1. Synthesis by atom transfer radical polymerization," *Biomacromolecules*, vol. 5, no. 3, pp. 877–82, 2004.

[130] S. J. Yuan, F. J. Xu, S. O. Pehkonen, Y. P. Ting, K. G. Neoh, and E. T. Kang, "Grafting of antibacterial polymers on stainless steel via surface-initiated atom transfer radical polymerization for inhibiting biocorrosion by Desulfovibrio desulfuricans.," *Biotechnol. Bioeng.*, vol. 103, no. 2, pp. 268–81, Jun. 2009.

[131] J. Huang, R. R. Koepsel, H. Murata, W. Wu, S. B. Lee, T. Kowalewski, A. J. Russell, and K. Matyjaszewski, "Nonleaching antibacterial glass surfaces via 'Grafting Onto': the effect of the number of quaternary ammonium groups on biocidal activity.," *Langmuir*, vol. 24, no. 13, pp. 6785–95, Jun. 2008.

[132] J. P. H. Pérez, E. López-Cabarcos, and B. López-Ruiz, "The application of methacrylate-based polymers to enzyme biosensors.," *Biomol. Eng.*, vol. 23, no. 5, pp. 233–45, Oct. 2006.

[133] S. Agarwal, Y. Zhang, S. Maji, and A. Greiner, "PDMAEMA based gene delivery materials," *Mater. Today*, vol. 15, no. 9, pp. 388–393, Sep. 2012.

[134] A. Mathew, H. Cao, E. Collin, W. Wang, and A. Pandit, "Hyperbranched PEGmethacrylate linear pDMAEMA block copolymer as an efficient non-viral gene delivery vector.," *Int. J. Pharm.*, vol. 434, no. 1–2, pp. 99–105, Sep. 2012.

[135] Z. H. Wang, W. B. Li, J. Ma, G. P. Tang, W. T. Yang, and F. J. Xu, "Functionalized Nonionic Dextran Backbones by Atom Transfer Radical Polymerization for Efficient Gene Delivery," *Macromolecules*, vol. 44, no. 2, pp. 230–239, Jan. 2011.

[136] A. Kusumo, L. Bombalski, Q. Lin, K. Matyjaszewski, J. W. Schneider, and R. D. Tilton, "High capacity, charge-selective protein uptake by polyelectrolyte brushes.," *Langmuir*, vol. 23, no. 8, pp. 4448–54, Apr. 2007.

[137] Y. Chen, D. Liu, Q. Deng, X. He, and X. Wang, "Atom Transfer Radical Polymerization Directly from Poly (vinylidene fluoride): Surface and Antifouling Properties," *J. Polym. Sci. Part A Polym. Chem.*, vol. 44, pp. 3434–3443, 2006.

[138] D. Han, X. Tong, and Y. Zhao, "General Strategy for Making CO 2 -Switchable Polymers," *ACS Macro Lett.*, vol. 1, pp. 57–61, 2012.

[139] Y.-L. Su and C. Li, "The reorientation of poly(2-dimethylamino ethyl methacrylate) after environment stimuli improves hydrophilicity and resistance of protein adsorption.," *J. Colloid Interface Sci.*, vol. 316, no. 2, pp. 344–9, Dec. 2007.

[140] S. Sanjuan, P. Perrin, N. Pantoustier, and Y. Tran, "Synthesis and swelling behavior of pH-responsive polybase brushes.," *Langmuir*, vol. 23, no. 10, pp. 5769–78, May 2007.

[141]P. Frantz and S. Granick, "Surface Preparation of Silicon for Polymer Adsorption Studies," *Langmuir*, vol. 8, pp. 1176–1182, 1992.

[142] A. Ramakrishnan, R. Dhamodharan, and J. Rühe, "Controlled Growth of PMMA Brushes on Silicon Surfaces at Room Temperature," *Macromol. Rapid Commun.*, vol. 23, pp. 612–616, 2002.

[143] J.-S. Wang and K. Matyjaszewski, "Controlled/'Living' Radical Polymerization. Halogen Atom Transfer Radical Polymerization Promoted by a Cu(I)/Cu(II) Redox Process," *Macromolecules*, vol. 28, no. 23, pp. 7901–7910, Nov. 1995.

[144] K. Matyjaszewski and J. Xia, "Atom Transfer Radical Polymerization," *Chem. Rev.*, vol. 101, no. 9, pp. 2921–2990, Sep. 2001.

[145] J. M. Walker, *The Protein Protocols Handbook*, 2nd ed. Totowa, NJ: Humana Press, 2002.

[146] J.-K. Chen and B.-J. Bai, "pH-Switchable Optical Properties of the One-Dimensional Periodic Grating of Tethered Poly(2-dimethylaminoethyl methacrylate) Brushes on a Silicon Surface," *J. Phys. Chem. C*, vol. 115, pp. 21341–21350, Nov. 2011.

[147] W. Feng, J. Brash, and S. Zhu, "Atom-transfer radical grafting polymerization of 2-methacryloyloxyethyl phosphorylcholine from silicon wafer surfaces," *J. Polym. Sci. Part A Polym. Chem.*, vol. 42, no. 12, pp. 2931–2942, Jun. 2004.

[148] Z. Bao, M. L. Bruening, G. L. Baker, R. V January, V. Re, M. Recei, and V. May, "Control of the Density of Polymer Brushes Prepared by Surface-Initiated Atom Transfer Radical Polymerization," *Macromolecules*, vol. 39, pp. 5251–5258, 2006.

[149] M. S. Kim, G. Khang, and H. B. Lee, "Gradient polymer surfaces for biomedical applications," *Prog. Polym. Sci.*, vol. 33, no. 1, pp. 138–164, Jan. 2008.

[150] K. Kato, E. Uchida, E. Kang, Y. Uyama, and Y. Ikada, "Polymer surface with graft chains," *Prog. Polym. Sci.*, vol. 28, pp. 209–259, 2003.

[151] J. H. Lee, B. J. Jeong, and H. B. Lee, "Plasma protein adsorption and platelet adhesion onto comb-like PEO gradient surfaces.," *J. Biomed. Mater. Res.*, vol. 34, no. 1, pp. 105–14, Jan. 1997.

[152] K. Fujimoto, H. Inoue, and Y. Ikada, "Protein adsorption and platelet adhesion onto polyurethane grafted with methoxy-poly(ethylene glycol) methacrylate by plasma technique.," *J. Biomed. Mater. Res.*, vol. 27, no. 12, pp. 1559–67, Dec. 1993.

[153] P. Wang, K. L. Tan, and E. T. Kang, "Surface modification of poly(tetrafluoroethylene) films via grafting of poly(ethylene glycol) for reduction in protein adsorption," *J. Biomater. Sci. Polym. Ed.*, vol. 11, no. 2, pp. 169–186, Jan. 2000.

[154] W. Feng, J. L. Brash, and S. Zhu, "Non-biofouling materials prepared by atom transfer radical polymerization grafting of 2-methacryloloxyethyl phosphorylcholine: separate effects of graft density and chain length on protein repulsion.," *Biomaterials*, vol. 27, no. 6, pp. 847–55, Feb. 2006.

[155] J. Tan and J. L. Brash, "Nonfouling biomaterials based on polyethylene oxide-containing amphiphilic triblock copolymers as surface modifying additives: adsorption of proteins

from human plasma to copolymer/polyurethane blends.," *J. Biomed. Mater. Res. A*, vol. 90, no. 1, pp. 196–204, Jul. 2009.

[156] L. A. Wohlfahrt, D. F. Mosher, B. Tomasini, R. C. Sutton, L. A. Wohlfahrt, and C. Sutton, "Identification of Vitronectin as a Major Plasma Protein Adsorbed on Polymer Surfaces of Different Copolymer Composition.," *Blood*, vol. 74, no. 8, pp. 2698–2706, 1989.